PHYSICAL AND MECHANICAL BEHAVIOR OF A TWO COMPONENT CEMENT-BASED GROUT FOR MECHANIZED TUNNELING APPLICATION

Alfredo Quiroga Flores

Dissertação de Mestrado apresentada ao Programa de Pós-graduação em Engenharia Civil, COPPE, da Universidade Federal do Rio de Janeiro, como parte dos requisitos necessários à obtenção do título de Mestre em Engenharia Civil.

Orientadores: Romildo Dias Toledo Filho
Flávio de Andrade Silva

Rio de Janeiro
Outubro de 2015

PHYSICAL AND MECHANICAL BEHAVIOR OF A TWO COMPONENT CEMENT-BASED GROUT FOR MECHANIZED TUNNELING APPLICATION

Alfredo Quiroga Flores

DISSERTAÇÃO SUBMETIDA AO CORPO DOCENTE DO INSTITUTO ALBERTO LUIZ COIMBRA DE PÓS-GRADUAÇÃO E PESQUISA DE ENGENHARIA (COPPE) DA UNIVERSIDADE FEDERAL DO RIO DE JANEIRO COMO PARTE DOS REQUISITOS NECESSÁRIOS PARA A OBTENÇÃO DO GRAU DE MESTRE EM CIÊNCIAS EM ENGENHARIA CIVIL.

Examinada por:

Prof. Romildo Dias Toledo Filho, D.Sc.

Prof. Flávio de Andrade Silva, D. Sc.

Profª. Michéle Dal Toé Casagrande, D.Sc.

Prof. Alex Neves Junior, D. Sc.

RIO DE JANEIRO, RJ-BRASIL

OUTUBRO DE 2015

Quiroga Flores, Alfredo

Physical and mechanical behavior of a two component cement-based grout for mechanized tunneling application/ Alfredo Quiroga Flores. – Rio de Janeiro: UFRJ/COPPE, 2015.

XX, 131 p.: il.; 29,7 cm

Orientadores: Romildo Dias Toledo Filho

Flávio de Andrade Silva

Dissertação (mestrado) – UFRJ/COPPE/Programa de Engenharia Civil, 2015.

Referências Bibliográficas: p. 92-94

1. Graute Cimento-Bentonita. 2. Efeito da cinza volante. 3. Graute bi-componente. I. Toledo Filho, Romildo Dias *et al.* II. Universidade Federal do Rio de Janeiro, COPPE, Programa de Engenharia Civil. III. Título.

A mis queridos padres, Alfredo y Eva.
A mis queridos hermanos, Roxana y Luis Enrique.

ACKNOWLEDGEMENTS

I deeply thank God for allowing me to be alive and healthy and guiding me through life.

Tive a honra e privilégio de ser orientado pelos professores Romildo Dias Toledo Filho e Flávio de Andrade Silva. Agradeço-lhes muito pela oportunidade de aprofundar meus conhecimentos, pelo suporte, sugestões e discussões em momentos importantes no mestrado e pela confiança para realizar o presente trabalho. Graças aos senhores, ingressei no mundo da pesquisa acadêmica e foi uma experiência totalmente gratificante, admirável e interessante. Ficarei sempre grato.

Siempre faltarán palabras para agradecer la incansable e invaluable labor de dos personas a las que amo y admiro mucho, mi papá y mamá, Alfredo y Eva. A ustedes les debo todo lo que soy y lo que pueda llegar a ser. Gracias por el alto grado de confianza depositado en mi, el estímulo que generan, la educación impartida, el amor incondicional y por estar junto a mi aunque la distancia temporalmente nos separe. A mis hermanos. Roxana y Luis Enrique, la unión y apoyo sin condiciones van más allá de nuestros rasgos consanguíneos. Les tengo uma profunda admiración, respeto y son modelos a seguir para mi. Al resto de mi família, que siempre me apoyó y expresó sus mejores deseos de superación, muchas gracias.

A mis amigos en Bolivia, gracias por la amistad, los buenos deseos y hermandad brindada. En especial para Juan José y Patricia, amigos de toda la vida.

Também quero agradecer aos meus irmãos e irmãs do Brasil, Renato, Nelson, Karyne, Mariane, Rafaela, Erica, William, Rodrigo, e Vinicius. Vocês me acolheram e me mostraram o melhor da amizade brasileira, com cada um de vocês aprendi e cresci todos os dias. À Karyne, por ser uma pessoa valiosa de grandes qualidades, agradeço a sorte de conhecer pessoas como você. À Lívia, por sua amizade, bondade e interesse no desenvolvimento das pessoas ao seu redor. Ao Dimas, meu irmão brasileiro, que me mostrou a importância do otimismo e perseverança. Nossas conversas nunca serão esquecidas. Em todos vocês encontrei objetivos e valores comuns que fizeram que nossa amizade ficasse muito mais forte.

Aos amigos e colegas do laboratório NUMATS, Tamara, Carol, Mayara, Aline, Daniele, Adriana, Clarice, Kathelyn, Tina, Samantha, Renata, Natália, Bartosz, Mostafa, Otávio, Yassin, Saulo e Fabricio pela convivência e conversas no dia a dia.

À equipe do NUMATS e LABEST da UFRJ, em especial à Luzidelle, Sandra e ao Paulinho (*in memoriam*), por sua orientação e auxilio. À Rosângela, pelo apoio nos ensaios químicos. Aos técnicos do laboratório Adailton, Márcio, Anderson, Hidekel, Jean e Alessandro, obrigado pelo suporte.

Ao CNPq, Programa Estudantes-Convênio de Pós-Graduação PEC-PG, pelo apoio financeiro que fez possível meu mestrado no Brasil..

Resumo da Dissertação apresentada à COPPE/UFRJ como parte dos requisitos necessários para a obtenção do grau de Mestre em Ciências (M.Sc.)

COMPORTAMENTO FÍSICO E MECÂNICO DE UM GRAUTE BICOMPONENTE À BASE DE CIMENTO PARA USO EM TUNELAMENTO MECANIZADO

Alfredo Quiroga Flores

Outubro/2015

Orientadores: Romildo Dias Toledo Filho
Flávio de Andrade Silva

Programa: Engenharia Civil

O presente trabalho reporta os resultados de uma pesquisa experimental feita em um graute bicomponente para uso em tunelamento mecanizado. No processo de tunelamento, um espaço anular é formado entre o solo e a estrutura principal do túnel. Para que as tensões sejam transmitidas entre o solo e a estrutura um graute cimentício é utilizado. No presente trabalho foi desenvolvido um graute cimentício composto por bentonita, cimento, cinza volante e um acelerador de silicato de sódio. Foram investigados os procedimentos de mistura, a reologia, a cinética de hidratação, a retração e o comportamento mecânico dos grautes cimentícios. A bentonita sódio-ativada controlou a segregação da água, a distribuiu uniformemente para hidratar o cimento e manteve as partículas cimentícias em suspensão. O patamar de percolação não teve mudanças significativas com diferentes teores de bentonita mas foi retrasado pela cinza volante. Na etapa fluida, viscosidades aparentes altas corresponderam a taxas cisalhantes menores. A tixotropia das suspensões bentoníticas prevaleceram depois de misturadas com materiais cimentícios e dependem do conteúdo de bentonita, características da mistura e tempo de hidratação. As altas relações água/cimento resultaram em uma retração autógena baixa e fissuração na retração por secagem. A cinza volante contribuiu com propriedades pozolânicas e melhoras na reologia. O acelerador não só causou um imediato enrijecimento do graute, porém, redução dos produtos de hidratação e, consequentemente, a resistência à compressão a idades posteriores foi afetada.

Abstract of Dissertation presented to COPPE/UFRJ as a partial fulfillment of the requirements for the degree of Master of Science (M.Sc.)

PHYSICAL AND MECHANICAL BEHAVIOR OF A TWO COMPONENT CEMENT-BASED GROUT FOR MECHANIZED TUNNELING APPLICATION

Alfredo Quiroga Flores

October/2015

Advisors: Romildo Dias Toledo Filho
Flávio de Andrade Silva

Department: Civil Engineering

The present work reports the results of an experimental research on a two component cement-based grout for mechanized tunneling application. During a Tunnel-Boring-Machine-based excavation an annulus gap is formed between the surrounding ground and the tunnel main structure. The gap is filled with cementitious grout in order to distribute the stresses to the tunnel structure. In the present research a grout formed by Portland cement, bentonite, fly ash and a sodium-silicate-based accelerator was developed. The mixing protocols, hydration kinetics, shrinkage and mechanical behavior were studied. It was observed that sodium-activated bentonite controls bleeding, providing sufficient water for cement hydration maintaining the cement particles in suspension. The percolation threshold did not change among the bentonite content variants and was delayed because of fly ash additions. At the fluid stage, high apparent viscosities were obtained at low shear rates and much less apparent viscosities at higher shear rates. Thyxotropy of bentonite suspensions prevailed after mixing with binders and depended on the bentonite content, mixing protocols and hydration time. High water/cement ratios resulted in low autogenous shrinkage and cracking in drying shrinkage. In addition fly ash resulted in pozzolanic reactions and improved rheology as well. The accelerator admixture not only caused an immediate stiffening but reduction in hydration products, consequently, may affect the compressive strengths at later ages.

TABLE OF CONTENTS

Page

LIST OF FIGURES

Page

LIST OF TABLES

Page

LIST OF SYMBOLS AND ABBREVIATIONS

A	Accelerator, chemical admixture
ABNT	Associação Brasileira de Normas Técnicas
Accel/cement	Accelerator/cement ratio
AFm	Monosulphate
ASTM	American Society for Testing and Materials
B	Bentonite
C or PC	Portland cement
C_2S	Dicalcium silicate
C_3A	Tricalcium aluminate
C_3S	Tricalcium silicate
$CaCO_3$	Calcium carbonate
$CaSO_4$	Calcium sulphate
CH	Calcium hydroxide
C-S-H	Calcium silicate hydrate
D(0.1)	Diameter which stands for 10% of total material has lesser size
D(0.5)	Diameter which stands for 50% of total material has lesser size
D(0.9)	Diameter which stands for 90% of total material has lesser size
DTG	Derivative thermogravimetry
E	Modulus of Young or Elasticity
EFNARC	European Federation of Producers and Contractors of Specialist Products for Structures
$\varepsilon_{rupture}$	Strain at rupture
FA	Fly ash
F_{max}	Maximum force
HB	Herschel Bulkley
K	Consistency factor, rheological parameter
L	Length
LABEST	Laboratory of Structures and Materials of COPPE/UFRJ
LVDT	Linear variable differential transformer
n	Flow behavior index
q	Heat
Q	Total or cumulative heat

SD	Standard deviation
σ_{max}	Maximum stress
T1	Type 1 of mixing protocol
T2	Type 2 of mixing protocol
T3	Type 3 of mixing protocol
TBM	Tunnel Boring Machine
TG	Thermogravimetry
UCA	Ultrasonic Cement Analyzer
UNFPA	United Nations Populationm Fund
w/b	Water-binder ratio
w/c	Water-cement ratio
y	Shear stress
$y_{0\ app}$	Apparent yield stress, rheological parameter
y_0	Yield stress, rheological parameter

1 INTRODUCTION

1.1 MOTIVATION AND OBJECTIVES

Currently it is estimated that world population exceeded more than 7 billion people (UNFPA, 2011) and (WORLDOMETERS, 2015), hence, infrastructure projects across the globe are continuously needed and should gather high engineering standards of efficiency and durability. The fact that many countries are experiencing densely populated areas stresses the current infrastructure systems of every city. One aspect of this pressure is highly focused on transportation systems which the daily activities depend on. Consequently infrastructure projects seek for attending these needs such as shortening distances by constructing tunnels, bridges, and so on.

So far tunnels have been constructed by using various methods and for different purposes. One way depends on the use of a tunnel boring machine (TBM) consisting of a circular cross section machine which excavates the ground by pressuring a cutter head against the ground in order to produce a cylindrical-shape tunnel. A ring-shape structure to support the tunnel, also known as tunnel lining, is placed accordingly the tunnel excavation advancement and it is considered the main structure of the tunnel. However the annulus gap formed between the ground and the tunnel lining needs to be filled with a grout to transmit stresses between the tunnel structure and soil. Therefore understanding this grout behavior acquires great importance because of the functions it must carry out: avoid ground settlement, water-tightness, durability for the tunnel, pumpability, workability to fill the void, limited shrinkage, stiffen quickly, resist segregation, bleeding and wash-out.

A two-component grout can be used for this task. This kind of grout can be formed by a component A, a cement-bentonite mixture, and the component B, a hardener or activator admixture in order to stiffen the mix quickly. Although its current use, there is lack of research on different aspects of this grout such as the cement-bentonite interaction, influence of the bentonite and dimensional changes (JEFFERIS, 2012).

Therefore, this thesis has the following main objective:

- Study the hydration, rheology, shrinkage and mechanical behavior of the cement-based grout used for filling the annulus gap between the tunnel lining and the surrounding ground in a tunnel excavated with a tunnel boring machine.

In order to achieve the main objective, specific objectives are established because it is mandatory to previously define various variables influencing the two-component grout, such as bentonite rheological behavior, mixing protocols, low and high shear mixing, influence of bentonite, fly ash and the accelerator chemical admixture. After satisfying every objective, a variable will be defined based on results. Thus, they follow below:

- Determine the effects of bentonite concentration and hydration time on rheology of bentonite suspensions prepared under high shear mixing by employing viscometry tests. Thus, define bentonite concentrations for the subsequent stages.

- Evaluate the outcome of two mixing protocols used for grout production by mechanical compression tests and consequently select the better protocol.

- Establish the influence of low and high shear mixing in cement-bentonite grouts, with different bentonite contents, through bleeding and mechanical compression tests. Then select the better one based on results.

- Determine the influence of different bentonite contents on cement-bentonite systems by studying the rheology, hydration kinetics and shrinkage behavior through viscometry, thermal analyses, isothermal calorimetry, ultrasonic cement analyzer and autogenous and drying shrinkage tests. As a result, establish the best cement-bentonite composition among them for next stages.

- Determine the influence of fly ash additions as partial replacements of Portland cement on cement-bentonite grouts by studying the rheology, hydration kinetics, mechanics and shrinkage through viscometry, mud balance, thermal analyses, isothermal calorimetry, ultrasonic cement analyzer, mechanical compression and autogenous and drying shrinkage tests. As a result, establish the best fly ash addition among them for the last stage of the thesis.

- Determine the influence of an accelerating admixture on cement-bentonite-fly-ash grouts by studying the hydration kinetics, mechanics and shrinkage behavior through thermal analyses, isothermal calorimetry, ultrasonic cement analyzer, mechanical compression and autogenous shrinkage tests. As a result, establish the best accelerator content addition as part of a two-component grout.

1.2 SCOPE OF THE THESIS

The present work is divided in the following chapters:

- Chapter 1. Introduction. Overview of the problem and establishment of objectives
- Chapter 2. Literature review. State of the current research on the field.
- Chapter 3. Materials.
- Chapter 4. Experimental plan and methods for experiments.
- Chapter 5. The cement bentonite system: rheology, mixing protocol, mechanics and hydration kinetics
- Chapter 6. The effect of fly ash inclusion on the cement bentonite system
- Chapter 7. The effect of an accelerator admixture on the cement bentonite system
- Chapter 8. Conclusions and suggestions.

2 LITERATURE REVIEW

2.1 GROUTS

According to the American Society for Testing and Materials (ASTM C125-13a, 2013), grout is defined as a mixture of cementitious material and water, with or without aggregate or admixtures, that is used primarily to fill voids. Grouts are widely used in different civil engineering fields such as masonry walls, ceramic tile, toppings, underlayments, bonding and repair grout, flowable fill, post-tensioning ducts, column baseplates, machine bases, ground anchors, preplaced aggregate concrete, stone masonry restoration, foundation jacking, rock and soil grouting, slurry trenches, railroad track stabilization, demolition grouting, oil well grouting, slabjacking, and subsealing.

There are two kinds of grouts which are widely used in the construction industry: cement-based and epoxy grouts. For the particular interest of the present study, the former acquires importance because its use in the annular grout of mechanized tunneling. Cement-based grouts can be composed of different components. First, Portland cement and water are important constituents because of the hydration reactions. Second, fine aggregates can be added depending on the project specification. Third, chemical admixtures may also be added such as: superplasticizers, accelerators, retarders, air entraing, foaming, consistency control stabilisers, non-shrink agents and others depending on the technical properties to be acquired. Fourth, fly ash, silica fume, blast furnace slag and nanometric silica can be included as mineral admixtures. Fifth, additions classified as non-hydraulic (EFNARC, 2005) can be part of the grout, among them: limestone powder, finely divide quarts flour and bentonite.

On the other hand, epoxy grouts have a different formulation. Epoxy grouts are formed by three parts: a resin, the curing agent or hardener and the aggregate system. The epoxy resin is a product of a chemical reaction and nowadays common resins are obtained from the reaction between epichlorohydrin and bisphenol A. Common curing agents are the amines, especially aliphatic and aromatic amines (HARRISON, 2013). During the mixing process chemical reactions happen between the epoxy resins and the curing agent. This process is known as polymerization in which the epoxy grows in size

and interlinking among molecules produces a strong grout structure. The construction industry still carries out the product selection mainly on cost criteria and they started to be used in the 1950s because its properties such as good adhesion to concrete, high bond strength, long-term resistance to harsh environments, easy application, and minimal shrinkage during curing. This thesis is not focused on this grout type nevertheless.

2.2 MATERIALS

2.2.1 CEMENT

Portland cement must comply with apropos standards. In the current study the Brazilian standard has been used as reference (ABNT NBR 11578, 1991). Previous work showed that characteristics such as its specific surface, granulometry and particle size can influence on workability and on ulterior grout properties (MIRZA *et al*., 2013).

2.2.2 BENTONITE

It is an aluminum phyllosilicate widely known because of its absorbent properties. It is an impure clay which essentially consists of montmorrillonite. It also possesses secondary mineral components such as quartz, calcite and micas. Its name was given by Wilbur C. Knight in 1898 as a consequence of the Cretaceous Benton Shale close to Rock River in Wyoming, USA. The different types of bentonite are classified according to its dominant element, for example, sodium, potassium, calcium and aluminum. This material is formed as a result of the weathering of volcanic ash under the presence of water and also comes from mica, feldspar, FeMg silicates, silification of detrital phylis and also direct precipitation of solution. All this process occur in different environments, i.e., marine, lacustrine, soil and hydrothermal.

It is common that bentonites are treated for industrial applications, treatment can consist of salt or polymer addition (BESQ *et al*., 2003). For example, calcium and sodium bentonites are used for industrial purposes. Sodium bentonites have expansive properties under wetting conditions and are used in cement-bentonite slurries. On the

other hand, the calcium bentonite is used for adsorbing ions in solutions such as oils and fats and is known as one of the earliest industrial cleaning agents. It can be converted to sodium bentonite by following an 'ion exchange" process as will be explained. In order to obtain sodium activated calcium bentonite the following reaction can be followed:

$$CaB + Na_2CO_3 \rightarrow NaB + CaCO_3 \qquad \text{Equation 2-1}$$

Where B stands for bentonite. This chemical reaction is reversible under acid and alkaline conditions. As a matter of fact, the sodium activated bentonite can be reversed to its previous condition if it is exposed to more soluble calcium species such calcium hydroxide or calcium sulphate. For this reason, it is of great interest its behavior as part of the alkaline cementitous system (JEFFERIS, 2012) .

Its structure is composed of platelike particles and is part of the phylosilicate 2:1 family. It consists on a octahedral layer covered along the sides by tetrahedral layers Silicon, Si^{4+}, belongs to the tetrahedral sheets and aluminum, Al^{3+}, to the octahedral one (BEKKOUR, et al., 2005). The structure according to Hofmann and co workers (HOFMANN, et al., 1933) can be seen in Figure 2.1. There are negative charges in theses layers and calcium and sodium cations compensate these charges. Bentonite has an important characteristic which is the sensitiveness to hydration. It consists on the insertion of water particles between its expanding clay lattices (LUCKHAM *et al*., 1999). This process is known as swelling. The expansibility of particles changes the rheology of suspensions and elastic behavior was noticed in previous research (RAMOS-TEJADA *et al*., 2001).

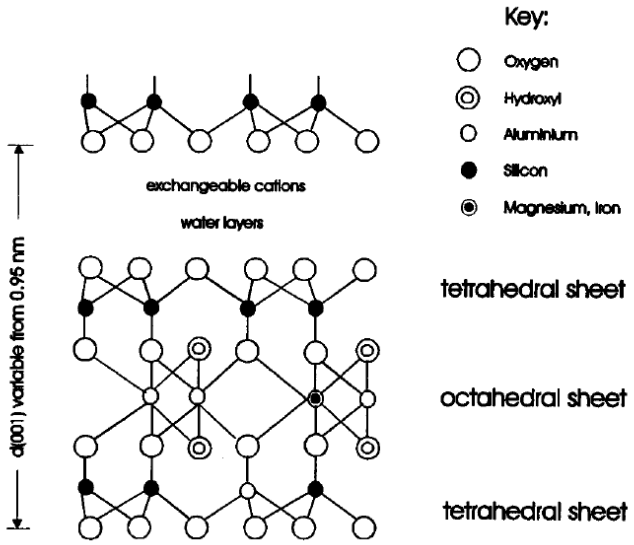

Figure 2.1 The structure of montmorrillonite according to Hofmann, Wilm, Marshal, Maegdefra7u and Hendricks (HOFMANN *et al*., 1933). Figure extracted of Luckham *et al*. (1999)

2.2.3 CHEMICAL ADMIXTURE

2.2.3.1 SODIUM-SILICATE-BASED ACCELERATOR

Sodium silicates, $nNa_2O \cdot SiO_2$ $n{\sim}3.3$, is part of the alkaline silicate accelerators also known as water glass. Its use covers not only shotcrete but also backfilling grout as part of the two component grout of a tunnel boring machine system. Sodium silicate is presented in liquid form and its mechanism consists on offering quick set based on precipitation of soluble silicates as calcium silicates (PRUDÊNCIO, 1998). Drying shrinkage increment and both bond and strength decrease have been found when large amounts of admixture have been used. This admixture can cause 40-60% compressive strength decrease and waterproof concrete reduction as well. It has also presented, diminution of the elastic modulus with time, and the admixture presents high viscosity at low temperature (MAILVAGANAM, et al., 1999):

2.2.4 MINERAL ADMIXTURES

2.2.4.1 FLY ASH

It is a supplementary cementing material which modifies the hydration rates of the clinker phases, the calcium hydroxide content and there are additional hydration

products due to the reaction of fly ash. It possesses pozzolanic properties since fly ash reacts with lime. Its action is perceived by: retardation of alite reaction at early ages, acceleration at middle stage due to the nucleation sites on fly ash particles. As a consequence, aluminate and ferrite phases' hydration is quicker and also modification on belite phase reaction occurs.

2.3 GROUTING IN A TUNNEL BORING MACHINE TUNNEL

2.3.1 TUNNEL BORING MACHINE

There are different types of excavation used in the construction of underground infrastructures such as hand mining, drilling & blasting, tunnel-boring-machine excavation and so on. Excavation by using a tunnel boring machine (TBM) is an interesting alternative because of its limited disturbance to the surrounding ground. A TBM essentially consists of a rotating cutter head, at the front and is followed by a main bearing, a thrust system and trailing support mechanisms, Figure 2.2 a and b.

a

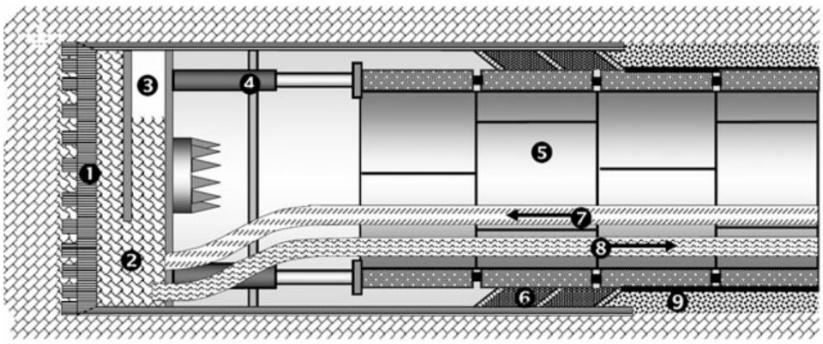

b

1, cutterhead; 2, bentonite slurry/soil; 3, air bubble; 4, thrust arms; 5, segments; 6, tail sealant; 7 bentonite slurry feed; 8, bentonite slurry/soil return; 9, annulus grout.

Figure 2.2 A Tunnel Boring Machine.

a) Overview of a TBM under a densely populated area (HERRENKNECHT, 2015) and b) Frontal part of a TBM (EFNARC, 2005).

The excavation process consists of removing the soil and rock by exerting pressure through cutter head against the strata and, consequently, this material needs to be removed from the front of the machine. This method is the main advantage of a TBM since it produces limited disturbances to the ground and is advised to be used in densely urbanized areas.

2.3.2 TBM TUNNEL STRUCTURE

The main structure, also known as tunnel lining, is composed of structural rings made of prefabricated concrete or steel segments. In many projects concrete segments are cast in specialized precise forms in near concrete plant. These segment possess conventional steel bar reinforcement and fibers are also being used nowadays because of its tenacity properties and crack reduction potential (CHIAIA *et al*., 2009), (BURATTI *et al*., 2013), (TIBERTI, et al., 2014). Figure 2.3 shows the tunnel lining characteristics:

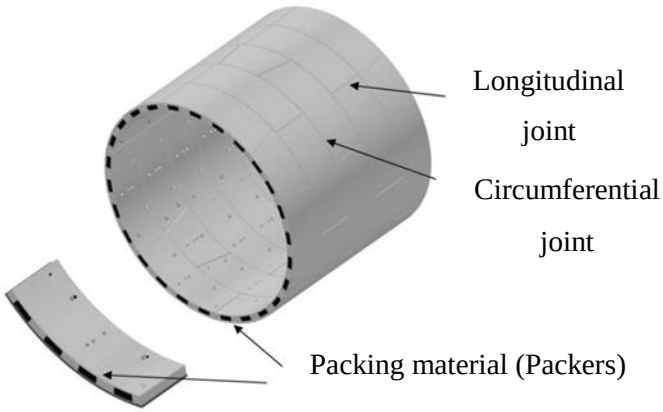

Figure 2.3 Segmental tunnel lining (ORNAU *et al*., 2012).

2.3.3 GROUTING THE ANNULUS VOID

A circular annular gap is left after tunneling with a shielded TBM. The width of the gap is limited on the interior side by the lining segments and on the exterior side by

the surrounding ground. This gap occurs because of overcut, conicity of the shield skin and design of the seal as can be seen in

Figure 2.4. The gap width ranges between 13 and 18 cm (THEWES *et al*., 2009) and must be filled with grout in order to minimize settlements and to ensure good embedment of the tunnel lining. Therefore, grouting occurs continuously during the tunneling and it shall be able to transmit forces and homogenize the contact surface between the tunnel lining and the ground.

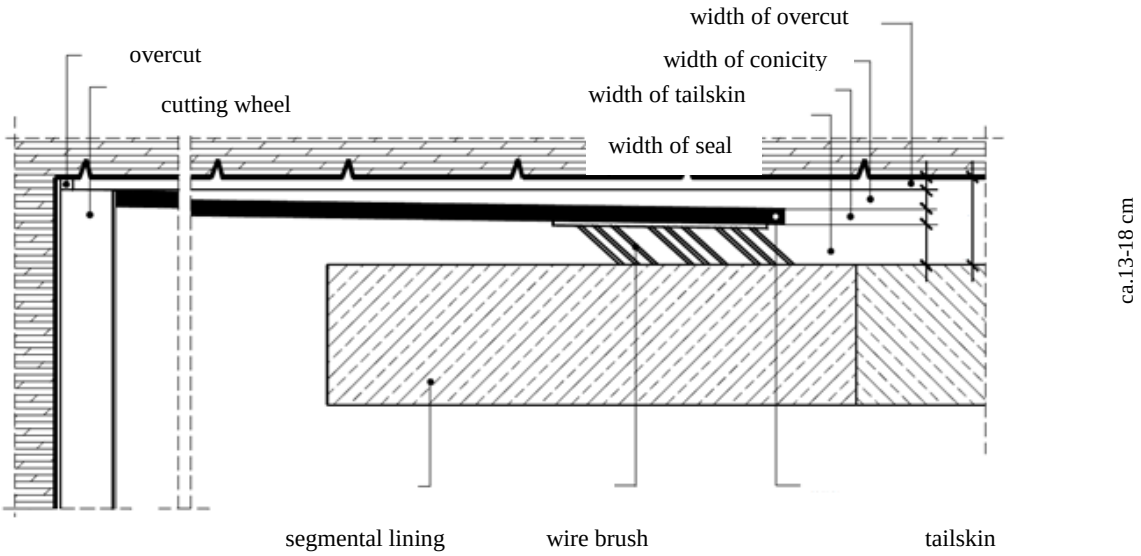

Figure 2.4 Influencing factors on the width of the annular gap (THEWES *et al*., 2009).

Hydraulically setting mortar and two-component grout are the grout types generally used for grouting tunnels and pea gravel is used especially for hard rocks. The first one consists of material binders mixed with sand and bentonite. They should attend requirements such as embedment of the segment lining, minimization of settlements, sealing against ground water and leakage water, workability, pumpability, high stability, erosion stability and temporary behavior with respect to compression and shear strength. These mortars are divided according to the quantity of cement material: active systems (over 200 kg/m3), reduced active systems (50-200 kg/m3) and inert systems (no cement) (THEWES *et al*., 2009). Table 2.1 shows examples and materials used.

]

Table 2.1 Grout Mixtures with an active system, reduced active and inert systems of a major traffic tunnel (THEWES *et al*., 2009).

Grout	Cement	Sand 0-1 (mm)	Sand 0-2 (mm)	Sand 2-8 (mm)	Bentonite-slurry (concentration 6%)	Fly Ash	Water
	(kg)	(kg)	(kg)	(kg)	(kg)	(kg)	(kg)
Active system	194	169	674	454	153	194	207
Reduced active system	120	169	674	454	183	268	177
Reduced active system	60	169	674	454	166	328	164
Inert system	0	169	674	454	183	420	135

The two-component grout is focused in achieving good pumpability, workability and a quick setting. The first component, A, is composed of cement and bentonite and the second, B, is a hardener or activator admixture. Both of them must have a slurry consistency and are mixed and pumped close to the annular gap.

Table 2.2 expresses the common material quantities for this type of grout:

Table 2.2 Grout mixture of two component mortar (BÄPPLER, 2008).

	Component A				Component B	
	Cement	Bentonite	Stabilisator	Water	Activator	Water
Grout	(kg)	(kg)	(kg)	(kg)	(kg)	(kg)
Two-component grout (Bäppler, 2008)	482	46	4	742	89	7

PEILA et al. (2011) gathered examples of two-component systems used in various projects in the world, they are presented in Table 2.3 through Table 2.6.

Table 2.3 Two component grout used in Metro C Line in Rome, Italy. Mix for 1 m^3 of hardened grout (PEILA *et al*., 2011)

Water	770-820 kg
Bentonite	30-60 kg
Cement	310-350 kg
Retarding agent by Mapel	3-7 l
Accelerator admixture by Mapel	50-100 l

Table 2.4 Two component grout used in Oraki Main Sewer Hobson Diversion in Auckland, New Zealand. Mix for 1 m^3 of hardened grout (PEILA *et al*., 2011)

Water	730 kg
Bentonite	30 kg
Cement	480 kg
Retarding agent by Mapel	1 l
Superplasticizer by Mapel	5 l
Accelerator admixture by Mapel	50 l

Table 2.5 Two component grout used in Metro Line in Sofia, Bulgaria. Mix for 1 m^3 of hardened grout (PEILA *et al*., 2011)

Water	795 kg
Bentonite	25 kg
Cement	290 kg
Retarding agent by Mapel	2.5 l
Accelerator admixture by Mapel	74 l

Table 2.6 Two component grout used in Metro Line 1 in Brescia, Italy. Mix for 1 m^3 of hardened grout (PEILA *et al*., 2011)

Water	816 kg
Bentonite	42 kg
Cement	315 kg
Retarding agent	3 l
Accelerator admixture	60 l

In hard rocks the penetration of mortar into the excavation chamber might occur and cause damage when shield machines are used without pressure at the working face. So pea gravel is used with sizes between 8 and 12 mm and can be broken or rounded.

In Table 2.7, it is gathered some characteristics of the three ways to fill the annular gap.

Table 2.7 Overview of application range and backfilling system for certain grouts (THEWES *et al*., 2009).

	Application range		Backfilling system		Required equipment				
Material	Hard Rock	Soil	Grouting through grout holes in the lining segments	Grouting through the tailskin	Piston pump	Peristaltic pump	Progressive cavity pump	Pressurised air	Specifics / remarks
Mortar - active system	x	x	x	x	x				Conventional mortar, stiffness behaviour depends on using of additives
Mortar- reduced active system	x	x		x	x				Stiffness behaviour depends on using of additives
Mortar - inert system		x		x	x				Stiffness behaviour depends on using of additives
Two-component grout		x	x	x		(X)	x		Stiffness behaviour just after mixing
Deforming mortar	x		x	x			x		Only usable in hard rock (material under development)
Pea gravel	x		x					x	Often used in hard rock, increasing of bedding by using mortar at the bottom, normally lower modulus of deformation and lower properties of embedment than for an active mortar

x = applicable
(x) = limited applicability

2.3.4 GROUT REQUIREMENTS AND CHARACTERISTICS

The European Federation of Producers and Contractors of Specialist Products for Structures (EFNARC, 2005) has published The Specification and Guidelines for the use of specialist products for Mechanized Tunneling (TBM) in Soft Ground and Hard Rock in which requirements and characteristics are established for grouts.

The general characteristics of the grout shall satisfy the following requirements:

- In the short term the grouting procedure shall prevent settlement prejudicial to the safety of the environment.
- In the long term the grout shall be a factor for water-tightness and durability of the tunnel.

Similarly the following characteristics are included:

- have minimum water content sufficient to allow pumping but resist segregation;
- be of a suitable consistency and workability to fill the void created during shield advancing;
- have limited shrinkage during and after hardening;
- set or stiffen quickly, where required to avoid settlement;
- resist segregation and bleeding in order not to block lines, pumps and tail seals (less than 1%);
- resist wash-out from water entering the void from the surrounding soil;
- provide a long term homogenous, stable and low permeability ring around the tunnel lining.

2.4 RHEOLOGICAL PROPERTIES

Pumping and placement are important characteristics for grouts. However, those areas have little research despite the considerable amount of publications about rheology of concrete, mortar and cement pastes. Moreover publications on the oil well industry cannot be used as reference because the testing conditions of pressure and temperature are different (ANNETT, 1994). In addition, there are many variables which influence the rheological parameters. First, the mixing method influence on the rheological properties. Low shear mixes and high shear mixes cause different behavior on the grouts as can be seen in the following table. For this reason, it is advised to choose the mixing method corresponding to the actual project, see Table 2.8.

Table 2.8 Different properties of high and low shear mixed grouts. (ANNETT, 1994).

Property	Mixer	
	Low shear	High shear
Bleed	High	Low
Yield stress	Low	High
Plastic vicosity	High	Low
Internal cohesion	Low	High

2.5 DIMENSIONAL STABILITY

2.5.1 CHEMICAL SHRINKAGE

According to BENTUR (2002), chemical shrinkage is the internal-microscopic volume reduction which is the result of the fact that the absolute volume of the hydration products is smaller than that of the reacting constituents. It is a volume balance at the molecular scale and creates autogenous shrinkage at a larger scale (BARCELO, 2002). Figure 2.5 shows the behavior of C_3S phase.

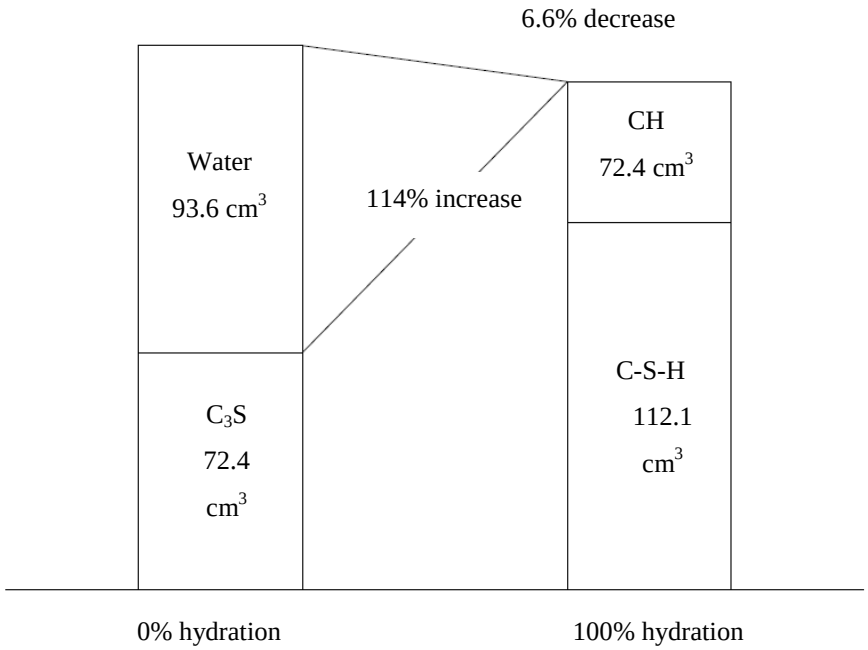

$$C_3S + 5.2H \rightarrow C_{1.7}SH_{3.9} + 1.3CH$$

Figure 2.5 Volume balance for C_3S phase. (BARCELO, 2002).

The decrease in absolute volume varies according to the authors; it forms 7 to 10% of the initial volume. Neville shows the variations, see Figure 2.6.

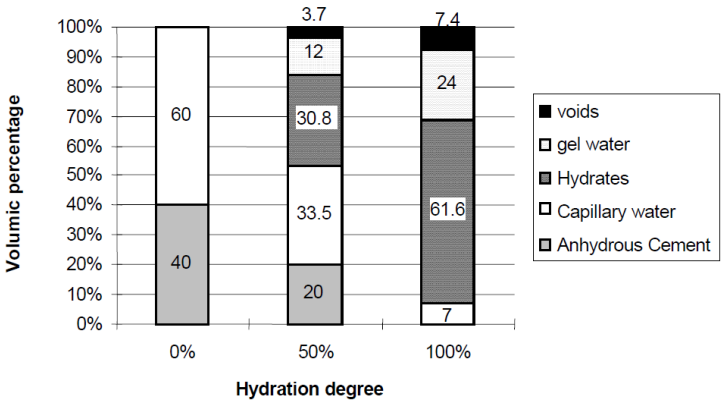

Figure 2.6 Volumetric balance (NEVILLE , 1995).

2.5.2 AUTOGENOUS SHRINKAGE

Autogenous shrinkage is circumscribed as the macroscopic volume reduction of a cementitious material. It does not take into account moisture transfer, temperature variation and application of external restraints and forces (JCI, 1999). Bentonite has been proven to reduce linear shrinkage in high-strength concrete (AFZAL *et al*., 2014). In addition, fly ash substitutions affect autogenous shrinkage at later ages (TERMKHAJORNKIT *et al*., 2005).

2.5.3 DRYING SHRINKAGE

Drying shrinkage is defined as the time dependent deformation due to loss of water at constant temperature and relative humidity (HANSEN, 1987). Drying shrinkage has been studied for ordinary Portland cement pastes and concretes but the basic nanoscale mechanisms of drying shrinkage have so far not been precisely established. For OPC four mechanisms have been proposed: surface free energy, capillary tension, movement of interlayer water and disjoining pressure.

3 MATERIALS

3.1 INTRODUCTION

Portland cement, bentonite, fly ash and a chemical admixture have been utilized in this thesis. The next sections describe these materials and its particular properties, such as chemical composition, loss on ignition, granulometry and so on.

3.1.1 CEMENT

The Portland cement (PC) to be used corresponds to Type II of the current Brazilian standard, (ABNT NBR 11578, 1991), under the code CP II F-32. It was chosen because its availability in the local market. Manufacturer: Lafarge.

3.1.2 BENTONITE

A Brazilian bentonite used in the construction industry will be part of the mixture. It is a sodium activated bentonite fabricated by Bentonit União Nordeste Ind. and Com. Ltda under the product name Permagel.

3.1.3 MINERAL ADMIXTURES

It is prompted to be used fly ash because of both pozzolanic and rheological properties. Fly ash was bought from Pozo Fly company. The three materials are shown in Figure 3.1.

Figure 3.1 CPII F-32 Portland cement, sodium activated bentonite and fly ash

3.2 PROPERTIES OF RAW MATERIALS

3.2.1 CHEMICAL COMPOSITION

The chemical compositions for cement (PC), fly ash (FA) and Bentonite (B) are shown in Table 3.1:

Table 3.1 Chemical Compositon of raw materials.

Basic Oxide	PC	FA	B
CaO	63.00	1.90	1.20
SiO2	18.30	52.74	59.70
Fe2O3	3.30	4.74	7.70
SO3	1.10	1.89	<0.10
Al2O3	4.70	33.64	15.80
K2O	0.37	3.46	0.28
SrO	0.21	0.02	<0.10
TiO2	0.23	1.31	0.72
MnO		0.04	
ZnO		0.04	
ZrO2		0.101	
Cr2O3		0.02	
Rb2O		0.025	
Y2O3		0.014	
NbO		0.005	
V2O5		0.065	
Na2O	0.52		2.40
MgO	1.80		2.70
Cl	<0.10		0.15
LOI	6.10	1.29	9.10

3.2.2 GRANULOMETRY

Granulometry is presented of all materials in Figure 3.2

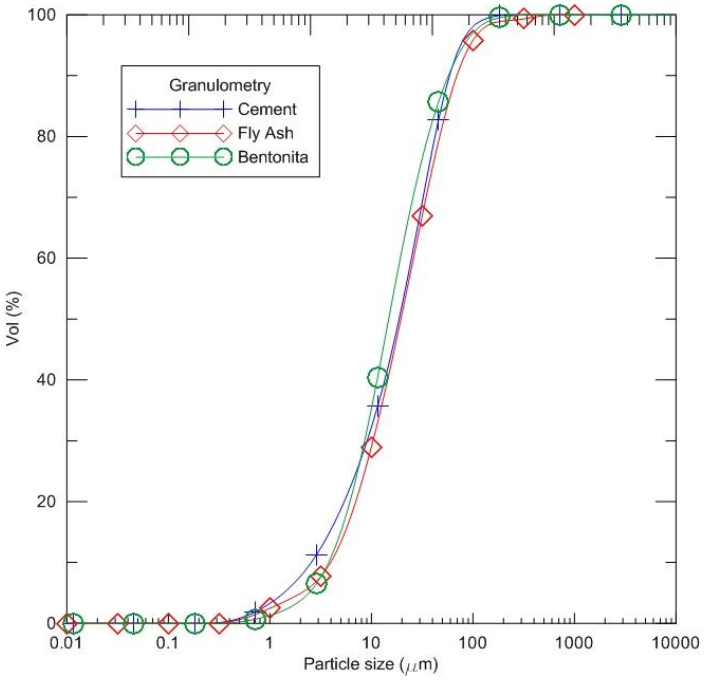

Figure 3.2 Granulometry

The materials present similar particle size distribution. Table 3.2 summarizes characteristic points which show bentonite as the material with particles slightly smaller than the others, d(0,5) and d(0,9).

Table 3.2 Size distribution of raw material particles.

Particle size dispersion	Diameters (μm)		
	CP II F 32	Bentonite	Fly Ash
d (0.1)	2.55	3.80	3.97
d (0.5)	18.73	14.77	19.87
d (0.9)	58.68	57.20	70.46

3.2.3 DENSITY

Density of the three materials is presented in Table 3.3.

Table 3.3 Density

Material	Density(g/cm^3)
Cement	3150
Fly Ash	2350
Bentonite	2491

3.2.4 SOLID CONTENT OF CHEMICAL ADMIXTURE

It was used an accelerator admixture for backfilling grout. Some characteristics have been extracted from the manufacturer´s technical specifications:

- Density 1.4±0.03 kg/l
- pH: 11 approx.
- Chemical base: Sodium silicate solution

Sodium silicate accelerators are also known as water glass (PRUDÊNCIO, 1998). Solid content was obtained based on the proper Brazilian standard procedure (ABNT NBR 10908, 1990). See Table 3.4 and Figure 3.3.

Table 3.4 Solid content of chemical admixture.

Chemical Admixture	Sigunit L65 BR	
	1	2
Free Capsule	159.9	157.3
Cap+admixture	209.2	209.1
Cap+admixture, after evaporation	183.8	183.1
Solid residue,%	48.4	49.8
Average Solid Residue, %	49.1	

Figure 3.3 Accelerator admixture before and after drying process

4 EXPERIMENTAL PLAN AND METHODS FOR EXPERIMENTS

4.1 EXPERIMENTAL PLAN

4.1.1 BASIC GROUTS FOR MECHANIZED TUNNELING

Based on grout proportioning in different tunneling projects across the world (PEILA *et al*., 2011) (COPPETEC-PEC, 2014), three material proportioning have been chosen (Table 4.1) by using the specific characteristics of cement and bentonite characterized in the previous chapter as a starting point. They vary in bentonite content and slightly in water/cement ratio in order to produce 1 cubic meter of grout.

Table 4.1 Basic grouts for mechanized tunneling, 1 m^3.

Material/Code	CB20	CB40	CB60
Cement	350	350	350
Water/binder	2.518	2.495	2.472
Bentonite	20	40	60
Total water	881.43	873.40	865.37
Bentonite/water	0.0227	0.0458	0.069

4.1.2 RESEARCH STRUCTURE THROUGH A GENERAL OVERVIEW CHART

The grout proportions in Table 4.1served as starting point for the experimental plan and the variables to be studied in the following chapters are the influence of bentonite, fly ash and accelerator content. However it was necessary to carry out preliminary research in rheology of bentonite, mixing protocols and high and low shear mixing effects.

In order to show the thesis structure, a chart was built and presented in Figure 4.1.

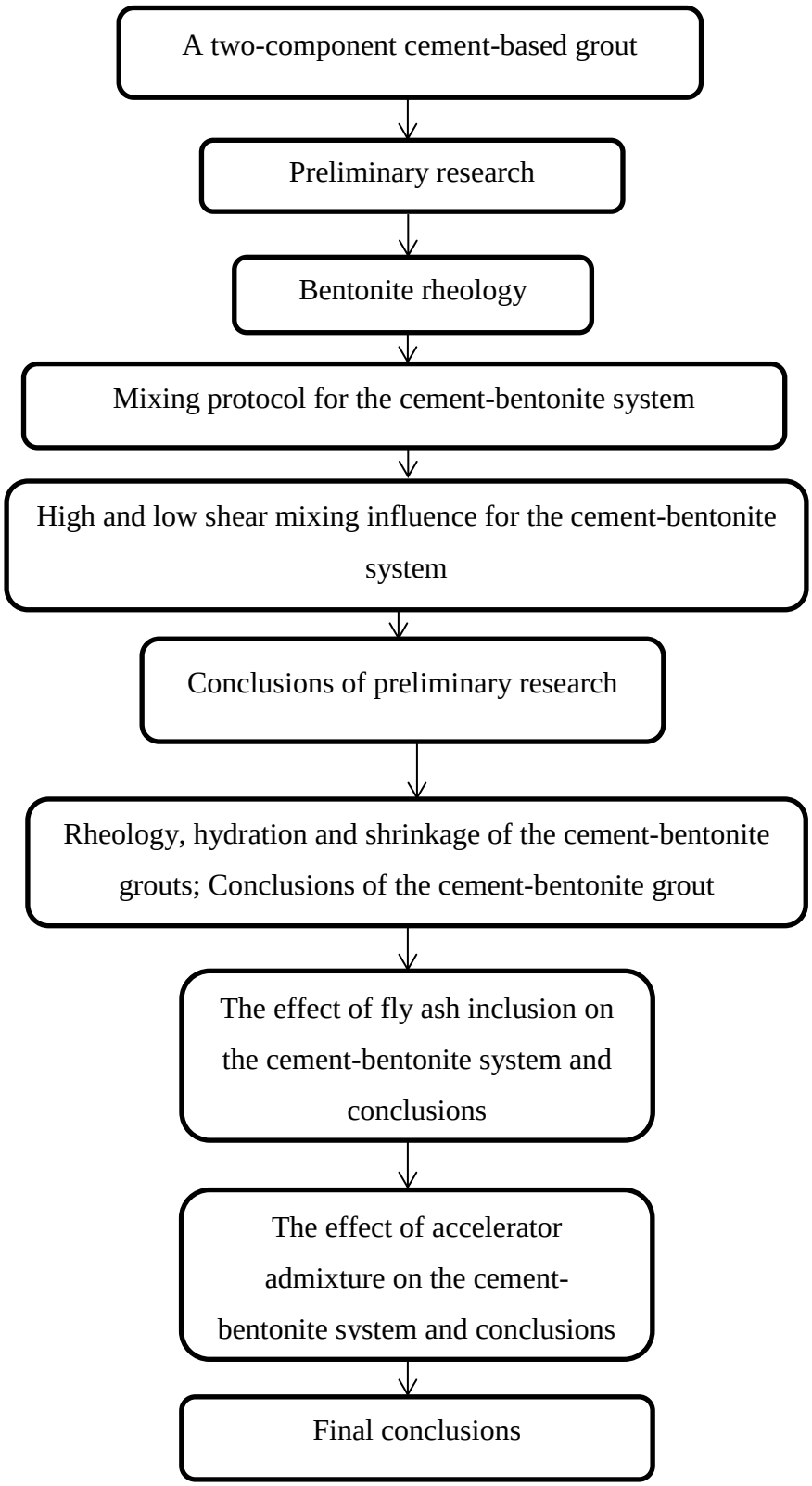

Figure 4.1 A general overview chart

4.1.3 PRELIMINARY RESEARCH OF THE CEMENT-BENTONITE SYSTEM

In order to understand the cement-bentonite mix, it is necessary to previously comprehend the various parameters which determine final grout behavior. Therefore, it is imperative to know the independent behavior of the materials being used such as bentonite. Its properties can vary among natural deposits and industrial processes executed upon it. Hence, experiments were done on bentonite and its rheology behavior was studied as a first stage. Second, it is also thought the order on which materials are poured during mixing has later effects on grouts, so the result of two different batching procedures was the next focus. Third, the outcome of high and low shear energy mixing was also determined.

4.1.3.1 BENTONITE RHEOLOGICAL BEHAVIOR

Development of rheological properties of bentonite suspensions was studied. First, the experiments were focused on the bentonite concentration effect (2.27%, 4.58% and 10%) on rheology and, second, attention was given to the evolution of rheological properties as a function of time. For the latter, a unique bentonite concentration was used 4,58% since the main purpose is to study the dependency of bentonite rheology on time

Therefore, 2.27%, 4.58% and 10% bentonite contents correspond to 2.27 g, 4.58 g and 10 g in 100 g of distilled water, respectively. They belong to the bentonite contents of CB20 (2,27%) and CB40 (4,58%) of Table 4.1, Additionally, the 10% concentration was selected because it was necessary to establish the rheological behavior at higher amounts.

Figure 4.2 gathers the objectives, variables and tests to be done:

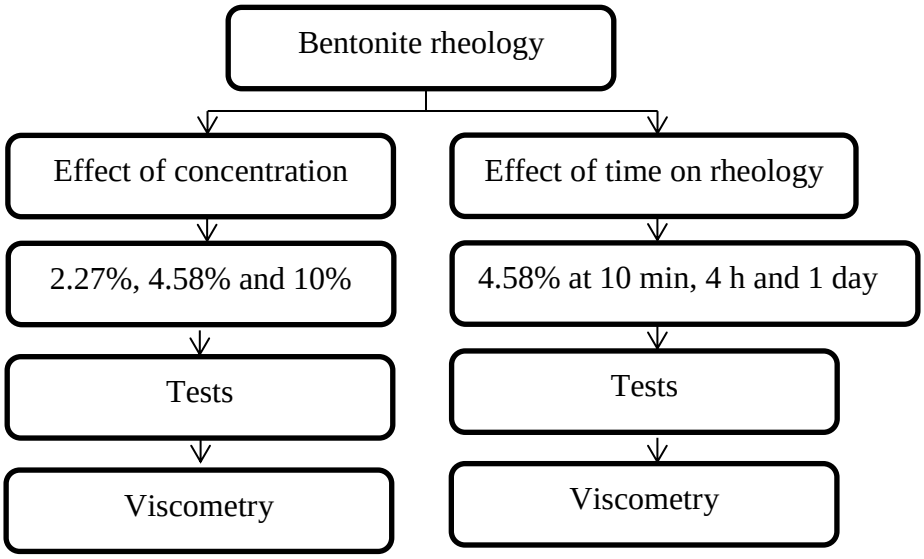

Figure 4.2 Bentonite rheological behavior

First, bentonite was dried in an oven at 100 ±5 °C for 8 hours in order to remove humidity. Previous research indicates the importance of high shear energy employed during mixing (JEFFERIS, 1982) in order to simulate a good site mixing in a centrifugal pump time mixer. For this reason, JEFFERIS (1982) suggests a 10000 rpm high shear for 5 minutes in order to guarantee a good mix and also indicates a 2000 rpm mix resembles a poor site mixer. In addition, other researchers also used a different mixing procedure, intensive mixing for short times (BESQ *et al*., 2003) at the beginning and then 24 hour slow mixing (BEKKOUR *et al*., 2005). Consequently, a two-step mixing process was adopted:

- First, water was poured in a Chandler Engineering mixer.
- Then bentonite was placed in small amounts during 4000-rpm mixing for 4 minutes, this stage has clay dispersion purposes.
- Immediately, 12000 rpm high shear mixing was imposed for 5 minutes for breaking floculization of bentonite. Both angular velocities were chosen because they are pre-set constant velocities available in the mixer and stand for high shear mixing.

A Fann viscometer was used to establish the rheological behavior of the suspensions. Shear rates were executed accordingly to section 4.7.1. Increasing and

decreasing shear rates were imposed and experiments were done at 23±1°C laboratory temperature. Experiments on suspensions with different bentonite contents were studied after a short-period. The material was cooled down, when needed, until the suspension reached room temperature. On the other hand, 4.58% suspension was studied at different ages, 10 minutes, 4 hours and 1 day. It is labeled as B40 on rheograms because it is part of the CB40 grout as stated before.

4.1.3.2 MIXING PROTOCOL FOR THE CEMENT BENTONITE SYSTEM

Cement-bentonite grouts require additional attention because of bentonite behavior. According to JEFFERIS (1982) there are three different procedures for mixing this grout: dry mixing (T1), dry cement addition to prehydrated bentonite (T2) and pre-dispersion of cement (T3). For dry mixing, both dry materials are added together to water previously poured in the mixer. In this case, calcium ions from water-cement reactions forbid the dispersion of bentonite particles. So bleeding would not be contained and this procedure is recommended for low water cement ratios. On the second procedure, a bentonite suspension is previously prepared similarly to section 5.2 and dry cement is added before finishing mixing. The third procedure consists on preparing a cement slurry and mixing together with bentonite previously prehydrated. It is believed based on the available literature that the last two procedures produce more homogenous grouts.

In this section it will be evaluated the efficiency of the last two procedures, T2 and T3, see Table 4.2. Mechanical compression tests will help evaluate the performance of the order on which materials are mixed.

Table 4.2 Mixing types to be used

Mixing Characteristics	Type (label)
Addition of dry cement to pre-hydrated bentonite	T2
Predispersion of the cement	T3

Therefore, the procedure is the following for T2 batching:

- Prehydrate bentonite. Use 4000 rpm for 2 min mixing for dispersion and 12000 rpm for 2 min for avoiding floculization. Hydrate bentonite suspension for 24-72 hours.
- Pour prehydrated bentonite in the Chandler Engineering mixer. Then pour dry cement and mix for two minutes at 12 000 rpm.

Similarly, the procedure is the following for T3 batching:

- Prehydrate bentonite with the same characteristics stated before. However, the total amount of water was split, so use Water 2, see Table 4.6. Hydration time of the suspension remains the same.
- A cement slurry is prepared by using a w/c 0,5. Water 1 was used, see Table 4.6. Use 4000 rpm mixing for two minutes.
- Pour the previously hydrated bentonite and mix them together for 2 minutes at 12000 rpm. Chandler Engineering mixer was used in all the steps.

Both protocols are summarized in Table 4.3 and Table 4.4 for quick comparison.

Table 4.3 Mixing procedure for T2 mixing protocol

Stage	Order	Description	Mixing type	Shearing characteristics (RPM)	
				Speed (RPM)	Time
Bentonite hydration	1	Dispersion	T2	4000	2 min
	2	Avoid Floculization		12000	2 min
	3	Water absortion		24-72 hours	
Grout production	4	Cement pre-hydration		Step does not apply	
	5	Cement - bentonite		12000	2 min

Table 4.4 Mixing procedure for T3 protocol

Stage	Order	Description	Mixing type	Shearing characteristics (RPM)	
				Speed (RPM)	Time
Bentonite hydration	1	Dispersion	T3	4000	2 min
	2	Avoid Floculization		12000	2 min
	3	Water absortion		24-72 hours	
Grout production	4	Cement pre-hydration		4000	2 min
	5	Cement - bentonite		12000	2 min

Portland cement type II F-32, sodium activated bentonite and distilled water were used. Their specific characteristics can be found in chapter 3. CB40 will be used for compression tests for evaluation of protocols.

Table 4.5 Grout composition for T2 grout, $1m^3$.

Material	Quantity (kg)
Cement	350
W/b	2.495
bentonite	40
water	873.40

Table 4.6 Grout composition and distribution of materials for T3 grout, $1m^3$.

Material		Quantity (kg)
Cement		350
W/b		2.495
Bentonite		40
Total water		873.40
Cement slurry	w1/c =	0.5
Water 1		175
Bentonite slurry		
Water 2		698.40

The following path has been used for establishing codes for the different mixes:

CB40TxHV2y

Where:

C: Cement

B: Bentonite, 40 kg/m^3

Tx: Type, 2 or 3

H: high shear mixing

V: speed type 2 (combined 4000 RPM for dispersion and high shear mix 12000 RPM)

y: specimen number

Curing was done in humid chamber until age of testing, see section 4.5.

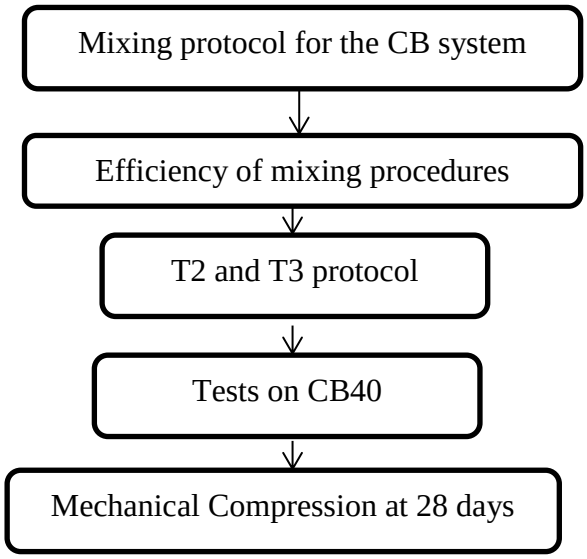

Figure 4.3 Mixing protocol chart

4.1.3.3 HIGH AND LOW SHEAR MIXING INFLUENCE FOR THE CEMENT-BENTONITE SYSTEM

So far high shear energy was used for mixing in the present study; however, it is the intent of to evaluate both the possibility of using low shear mixing and other mixer's efficiency.. A Hobart planetary mixer was used for low shear mixing (136 rpm) and the Chandler engineering one for high shear (4000 and 12000 rpm combination).

Bleeding was evaluated for all mixes. Depending on these results, stress-strain compression behavior is presented for the high shear mix with the lowest bleeding. For the low shear case, compression behavior was determined for the three bentonite contents.

Portland cement type II F-32, bentonite and distilled water were used. Grouts were produced by using 20, 40 and 60 kg/m3 of dry bentonite.(refer to Table 4.7).

Table 4.7 Grout compositions used

	Quantity (kg)			1 m3
Material/Code	CBRef	CB20	CB40	CB60
Cement	350	350	350	350
W/b	2.541	2.518	2.495	2.472
bentonite	0	20	40	60
Total water	889.46	881.43	873.40	865.37

It is important to state that mixing protocol depends on results and conclusions of previous research see section 4.1.3.2 and Figure 4.1. If T3 mixing were chosen, division of total water is needed for prehydration of both bentonite and cement, Table 4.8.

Table 4.8 Division of total water for the T3 mixing protocol

	Quantity (kg)			1 m3
Material/Code	CBRef	CB20	CB40	CB60
Cement slurry		w1/c =0.5		
Water 1	175	175	175	175
Bentonite slurry				
Water 2	714.46	706.43	698.40	690.37

Where:

Water 1 + water 2 = total water Equation 4-1

Mixing time is presented in Table 4.9 : Mixing times seek for guarantee effective and sufficient mixing when grouts with high bentonite content are prepared or low shear mixing is employed. In case of T2 mixing were chosen after results and conclusion, step 4 is left out.

Table 4.9 Mixing energy and procedure for mixes

Stage	Order	Description	Mixing type	Shearing characteristics (RPM)			
				Speed (RPM)		Time	
				Low	High	Low	High
Bentonite hydration	1	Dispersion	T3	136	4000	2 min	2 min
	2	Avoid Floculization		136	12000	2 min	2 min
	3	Water absorption		24-72 hours			
Grout production	4	Cement pre-hydration		136	4000	2 min	2 min
	5	Cement - bentonite		136	12000	5 min	5 min

The codes for the mixes are:

CBxTySVzHw

Where:

C: Cement

Bx: Bentonite content, where x stands for the amount used: Ref, for reference grout.

Ty: Type of mixing 2 or 3.

S: shearing characteristics: low (L) or high (H) shear.

Vz: speed type V1 (136 RPM) and V2 (combined 4000 RPM for dispersion and high shear mix 12000 RPM)

Hw: hydration time of bentonite, where z indicates hydration time in hours.

Curing was done in humid chamber until age of testing, see section 4.5. A chart summarizes the research,

Figure 4.4.

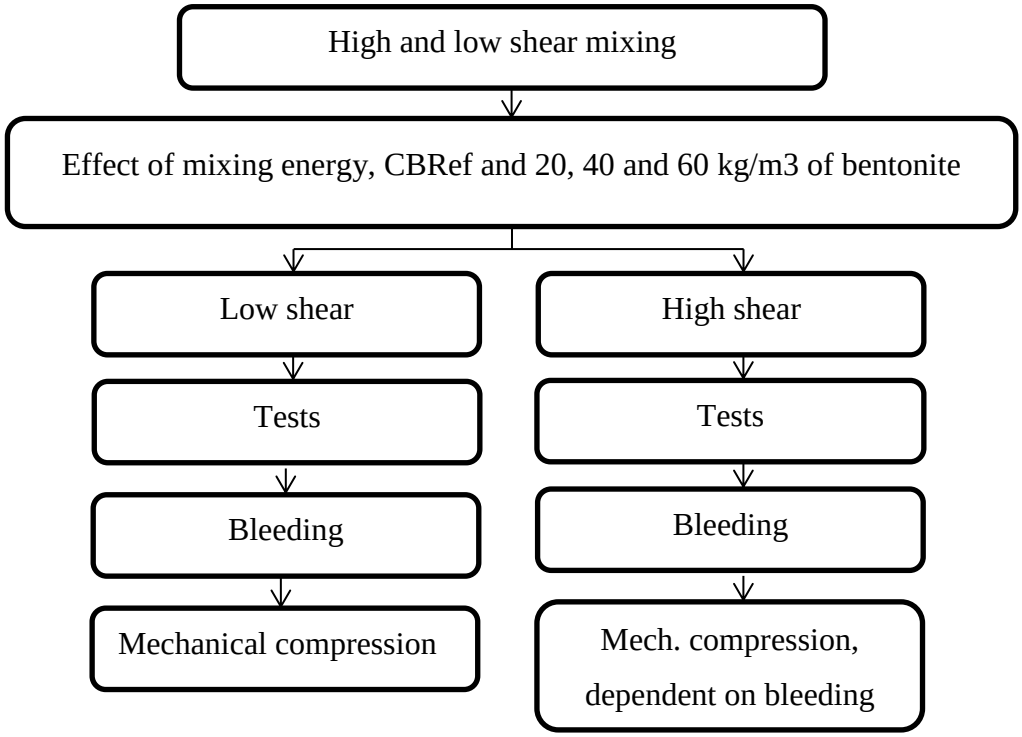

Figure 4.4 High and low shear mixing chart

4.1.4 THE CEMENT BENTONITE SYSTEM

After accomplishing the aforementioned studies, the bentonite effects on hydration, rheology and shrinkage are studied. A reference with no bentonite and three bentonite contents were used: 20, 40 and 60 kg/m3 of dry bentonite. Grout proportions accord with Table 4.7. Figure 4.5 details the tests and mixtures.

Mixing protocol and mixing time depend on results of preliminary researches. They will be indicated in the opportune section.

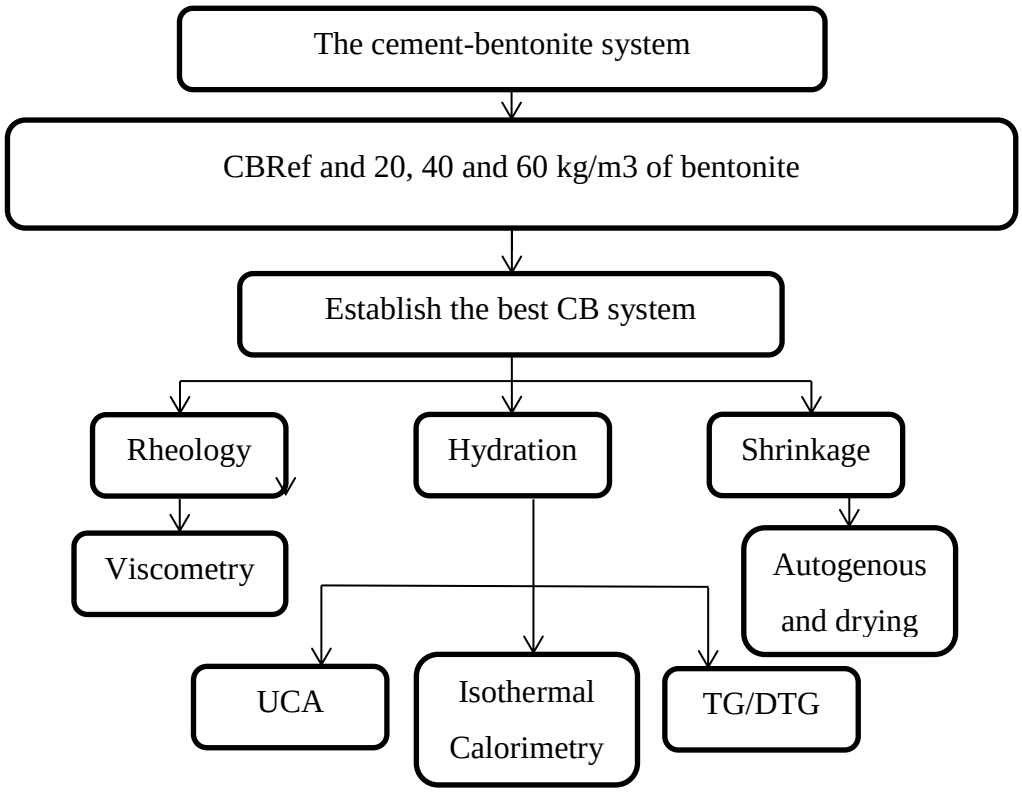

Figure 4.5 CB system chart

4.1.5 THE EFFECT OF FLY ASH INCLUSION ON THE CEMENT BENTONITE SYSTEM

By analyzing results of cement-bentonite grouts, a grout with the best behavior is to be chosen as reference. Then three fly ash contents are added as partial replacements of cement, see Table 4.10.

Table 4.10 Percentage of cement replacement by Fly ash for 1 m^3.

% FA replacement	0	10	30	50
Fly ash (kg)	0	35	105	175
Remaining cement (kg)	350	315	245	175

The following codes were employed for the different mixes and will be used in the next sections:

CBxFAyTz

Where:

C: Cement

Bx: Bentonite content, x mass in kilograms per cubic meter of grout

FAy: Fly ash as cement partial replacement, y fly ash percentage

Tz: Type of mixing to be adopted.

Mixing protocol and time are the same of section 4.1.4. Experimental results in rheology, hydration, shrinkage and mechanical compression will determine the best fly ash addition. See

Figure 4.6.

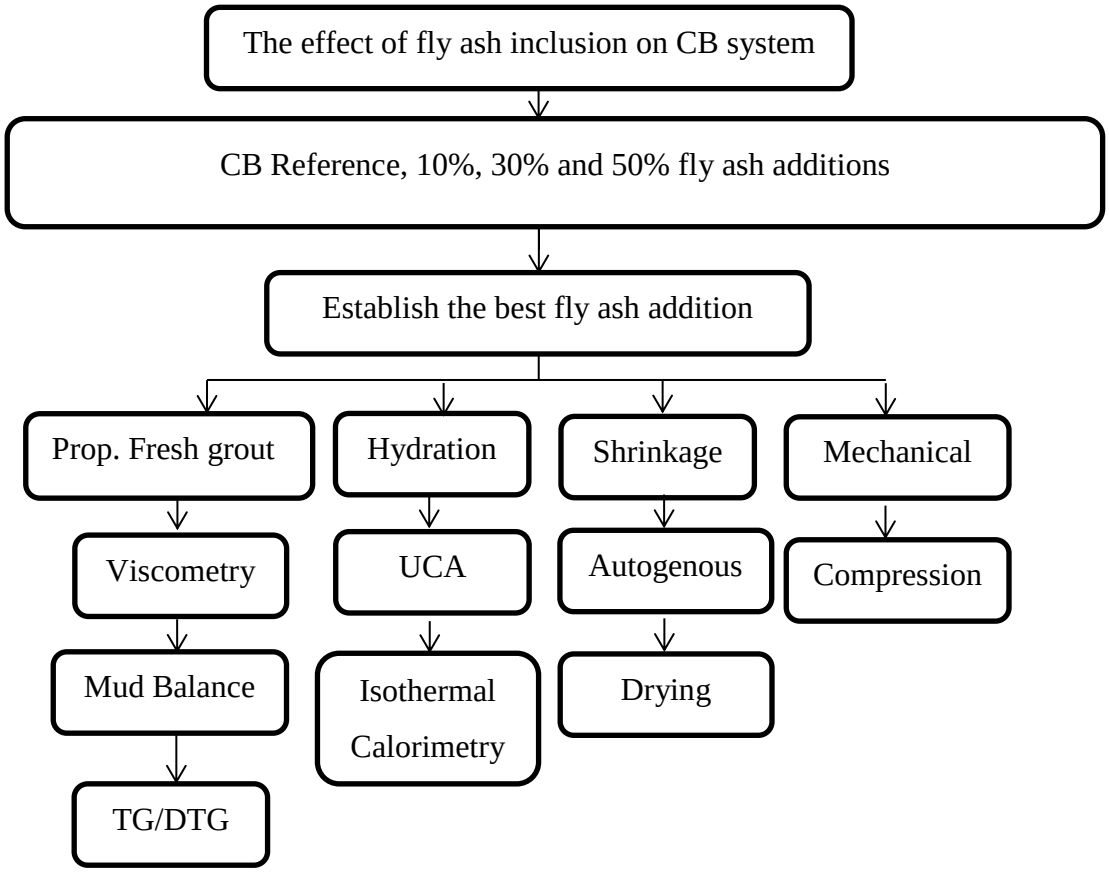

Figure 4.6 The effect of fly ash inclusion on CB system

4.1.6 THE EFFECT OF AN ACCELERATOR ADMIXTURE ON THE CEMENT BENTONITE SYSTEM

After studying the CBFA grouts and choosing its best grout as reference because of its performance, it is time to study the two-component grout. It is formed by component A, CBFA grout, and component B, an accelerator chemical admixture. Various dosages of component B were used. In spite of the use in the tunneling industry, and to the author´s knowledge, there is lack of technical documents or scientific publications which study deep enough this type of grout on hydration, mechanical and shrinkage terms.

The accelerator dosages are gathered in Table 4.11. They correspond to 5%, 15%, 30% and 45% of cement weight. Specimen Codes are in accordance to the ones used across the thesis.

Table 4.11 Two-component grouts studied.

Material/Code: CBxFAyAz	FA10A0	FA10A5	FA10A15	FA10A30
Cement	315			
W/b ratio	2.495			
bentonite	To be defined by results			
Fly Ash, % replacement	To be defined by results			
Fly Ash weight	To be defined by results			
water	873.40			
Cement slurry , w/c	0.5			
Water 1	175			
Bentonite slurry				
Water 2	698.40			
Accelerator				
Accel/cement ratio	0	0.05	0.15	0.3
Admixture weight	0	15.75	47.25	94.5

Mixing procedure is the same for producing the cement-bentonite-fly ash grout, component A. Accelerator admixture, component B, was mixed with component A just seconds before pouring in the molds.

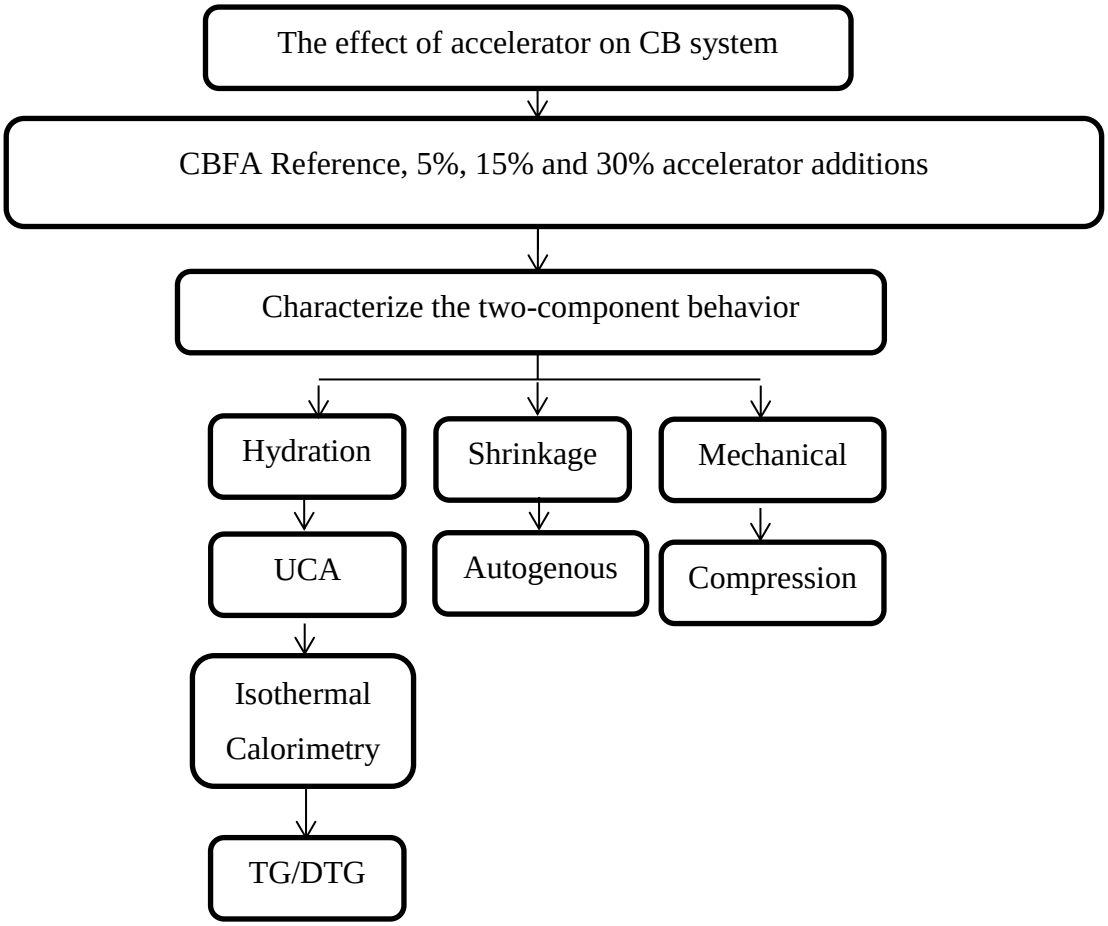

Figure 4.7 The effect of an accelerator admixture on CB system

4.2 TEST METHODS

The study needed the following experimental tests ordered by categories, see Figure 4.8. In the next chapters, they are mentioned and follow the procedures and details established in the current chapter. Particular test details depending on some material behavior will be stated in the corresponding section across the thesis. Bleeding and Mud Balance were included in the rheology category since they are performed when the grout is still fluid.

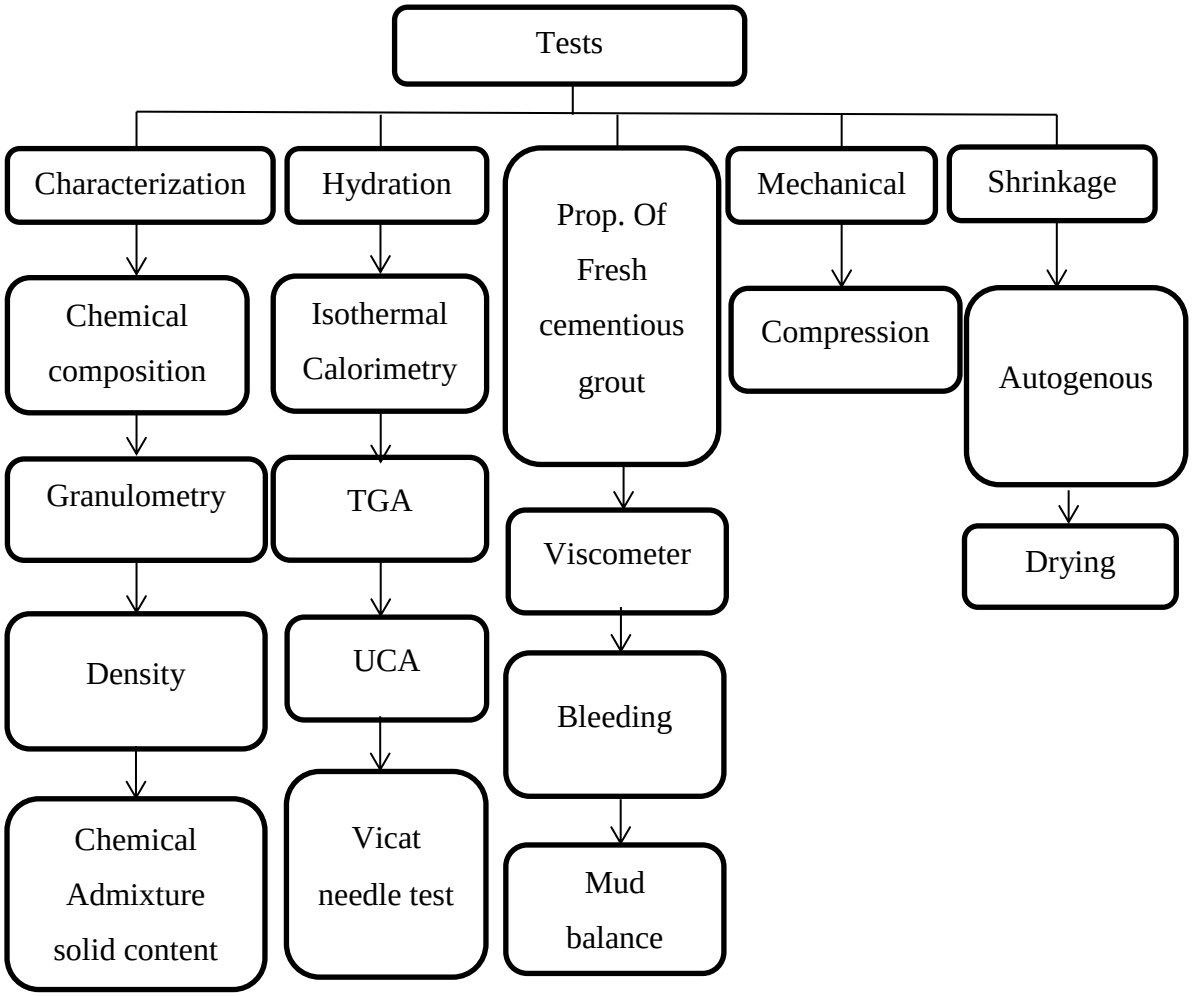

Figure 4.8 Tests employed in the thesis

4.3 CHARACTERIZATION OF MATERIALS

4.3.1 CHEMICAL COMPOSITION

Chemical composition tests were done at two places, Laboratório de Estruturas e Materiais (LABEST) and Centro de Tecnologia Mineral (CETEM). LABEST depends on COPPE/UFRJ at Ilha do Fundão, Rio de Janeiro and Centro de Tecnologia Mineral is a research center depending on the Science, Technology and Innovation Ministry of Brazil at Ilha do Fundão in Rio de Janeiro as well. At LABEST, chemical composition of fly ash was carried out by fluorescence spectroscopy of X-ray dispersive energy with the Shimadzu DX 800, Figure 4.9. At CETEM, bentonite and Portland cement chemical components were obtained by semiquantitative analysis of X-ray fluorescence

spectrometer –wavelength dispersive spectroscopy (WDS), model AXIOS (Panalytical). Sulfur content was obtained by elementar analyzer of Carbone and Sulfur, LECO SC632.

Since the LABEST equipment had limitations to obtain the sodium oxide content in bentonite. Cement sample was also sent to be analyzed at CETEM facility for comparison purposes. Because there were no significant changes in content, cement composition obtained at CETEM is presented in the proper section.

Figure 4.9 Shimadzu DX 800 equipment, LABEST/COPPE/UFRJ

4.3.2 GRANULOMETRY

Particle size analysis via laser diffraction is carried out by using Malvern Mastersizer 2000 equipment at LABEST, see Figure 4.10. Ethylic alcohol must be used as dispersant when cement is under test and distilled water for the other two materials: bentonite and fly ash. It is important to mention ultrasound dispersion was used for bentonite for 5 minutes.

Figure 4.10 Malvern Mastersizer 2000 equipment, LABEST/COPPE/UFRJ

4.3.3 DENSITY

A gas pycnometer is the equipment used for this test, see Figure 4.11. It was used 2-4 g samples in order to determine its density. Before inserting the sample in the equipment, it is necessary to establish its weight. The equipment consists of a gas pycnometer of Micromeritics, model AccuPyc 1340. It functions based on gas displacement and Boyle´s law. The procedure consists on:

- Drying sample at 40°C oven for two hours
- Pouring a 2-4 g sample in the cylindrical recipient of equipment. Insert it vertically and lock the black seal.
- Register readings done by equipment and obtain the sample density.

Figure 4.11 Gas pycnometer used for experiments

4.3.4 CHEMICAL ADMIXTURE SOLID CONTENT

This test allows obtaining the solid content of a chemical admixture by following the Brazilian standard procedure (ABNT NBR 10908, 1990). The steps are:

- Weigh 50 g approx. of sample in a porcelain capsule
- Evaporate the content until dryness.
- Place the capsule in an oven at 105±5 °C for 24 hours
- Cool the capsule in a desiccator for 30 min and weigh
- Place it again in an oven at 105±5 °C for 1.5 hours. Cool down again for 30 minutes and weigh
- If the weight remains constant, obtain the solid content percentage. Repeat last steps if necessary.

4.4 MIXING EQUIPMENT

Two mixers were employed in the present study: a Hobart planetary mixer which parts can be seen in Figure 4.12 and a Chandler Engineering mixer. The Hobart mixer is a N50 model, HP 1/6, 115 Volts and was made by The Hobart MFG CO., Ohio, USA. It consists of a gear-driven transmission with B flat beater, see Figure 4.12. The agitator disposes of three speeds: low, intermediate and high, 136, 281 and 580 rpm respectively (HOBART, 2015).

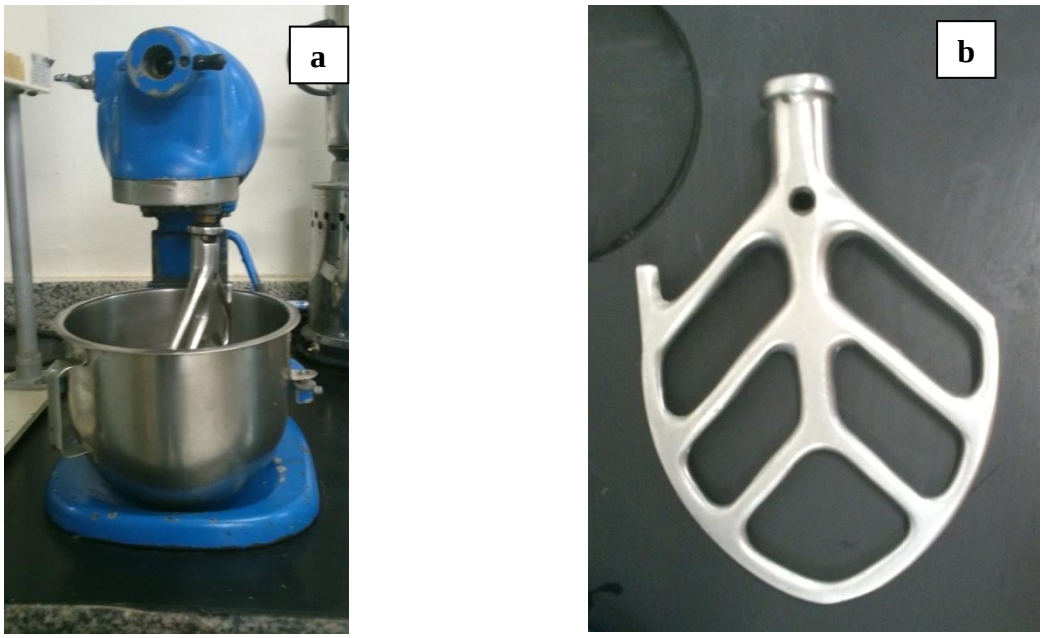

Figure 4.12 Hobart planetary mixer: a) whole view; b) “B” flat beater

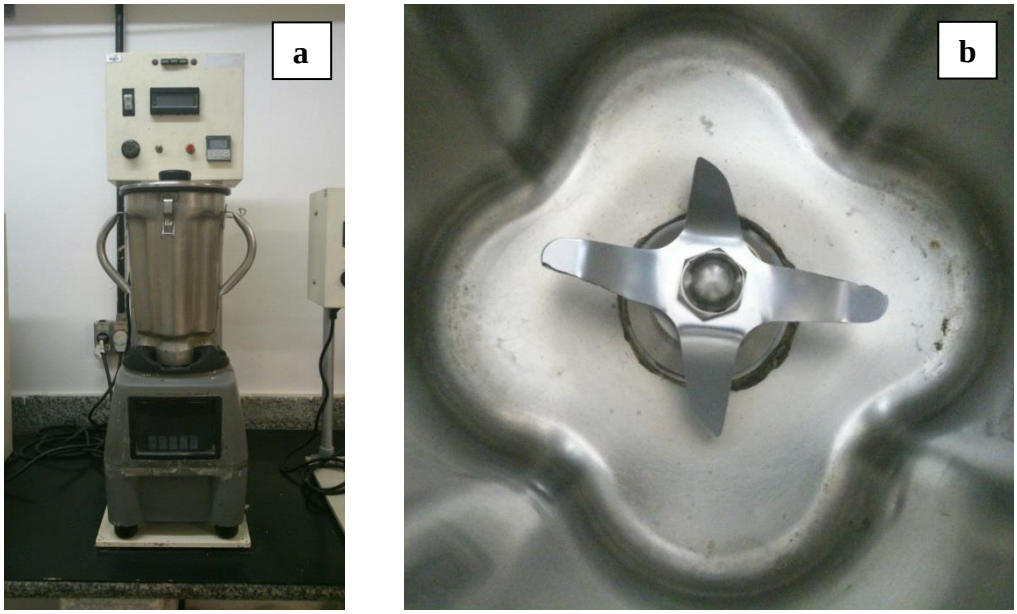

Figure 4.13 Chandler Engineering mixers a a) whole view; b) propeller

4.5 CURING METHOD

Curing for all grouts was carried out in a humid chamber at LABEST/COPPE/UFRJ.

4.6 HYDRATION KINETICS

4.6.1 ISOTHERMAL CALORIMETRY

It is carried out by measuring the heat produced in the sample in order to evaluate chemical reactions. The preparation of samples complies with the instructions below:

- Weigh a determined amount of material into an empty glass ampoule.
- Seal the ampoule with an aluminum cap, press both cap and ampoule together with the proper tool in order to guarantee the seal.
- Mark the center in the cap and place an eyelet on it. See Figure 4.14.
- Place the ampoule in a calorimeter channel.

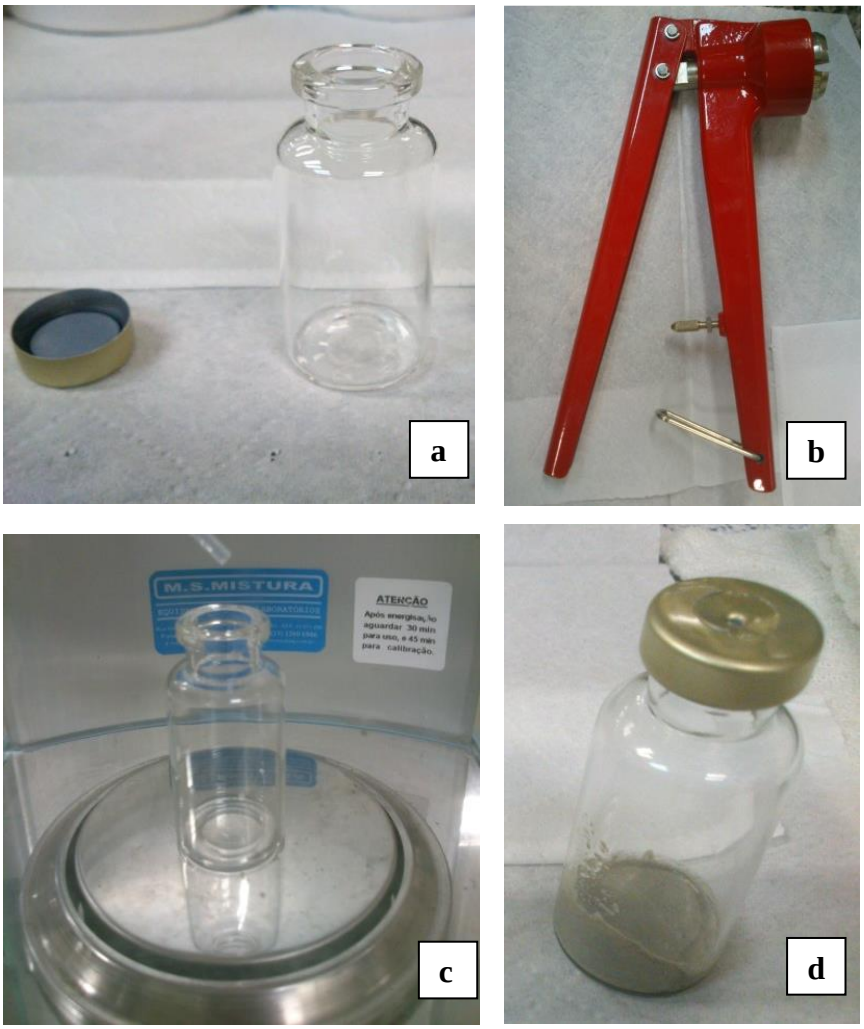

Figure 4.14 Sample for Isothermal Calorimetry.

a) and b) Ampoule, cap and tool needed, c) Weighing the sample, d) Ampoule with grout after test

Tests were executed under 23°C calorimeter temperature and a 7-day time.

4.6.2 THERMOGRAVIMETRIC ANALYSIS

It is a method in which changes in chemical properties of materials are measured as a function of increasing temperature (with constant heating rate), or as a function of time with constant temperature and/or constant mass loss (COATS *et al*., 1963). The equipment is shown below in Figure 4.15 and corresponds to a SDT Q600 Simultaneuous TGA/DTA/DSC from TA instruments

Figure 4.15 Thermogravimetric equipment, LABEST/COPPE/UFRJ.

The analyses were carried under the next characteristics (NEVES JUNIOR, et al., 2012): The procedure allows to obtain separated peaks in different temperature ranges.

- Drying of samples, at 1°C/min from 30 to 35°C.
- Isothermal step at 35°C for 1 hour.
- Heating step, from 35 to 1000 °C by using 100 mL/min of nitrogen flow.

Samples of less than 20 mg are used for thermal analyses.

By analyzing cementitious materials, mass losses occur at different temperature ranges and correspond to the following equations (DWECK, et al., 2000) (DWECK, et al., 2002), (NEVES JUNIOR, et al., 2012):

- Ettringite, theoretical mass loss 45.14%:

$$3CaO \cdot Al_2O_3 \cdot 3CaSO_4 \cdot 31H_2O \rightarrow 3CaO \cdot Al_2O_3 \cdot 3CaSO_4 + 31H_2O \quad \text{Equation 4-2}$$

- Dehydration of dihydrated calcium sulphate, theoretical mass loss 20,93%.

$$CaSO_4 \cdot 2H_2O \rightarrow CaSO_4 + 2H_2O \quad \text{Equation 4-3}$$

- Dehydration of calcium hydroxide, theoretical mass loss 24.32%.

$$3Ca(OH)_2 \rightarrow CaO + H_2O \quad \text{Equation 4-4}$$

- Decomposition of calcium carbonate, theoretical mass loss 44%.

$$CaCO_3 \rightarrow CaO + CO_2 \quad \text{Equation 4-5}$$

- Tobermorite, theoretical mass loss depends on hydration evolution.

4.6.3 ULTRASONIC CEMENT ANALYZER

The speed of sound is sensitive to the viscoelastic properties of the materials and in this way ultrasound may be utilized to monitor the setting and process of hardening. The tests can be conducted under a pressure exceeding 1000 psi (6.90 MPa) in an equipment shown in Figure 4.16, the Ultrasonic Cement Analyzer (UCA).

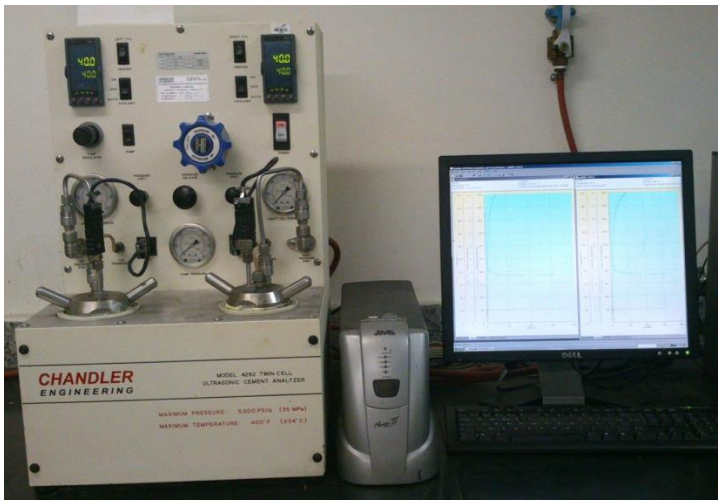

Figure 4.16 UCA equipment of Chandler Enginnering, LABEST/COPPE/UFRJ

Figure 4.17 Cylindrical cell where the grout specimen is poured

The placement of grout samples in the equipment was performed in accordance to Petrobras test manual for batching petroleum wells (PETROBRAS, 2005). The experiments were done under atmospheric pressure and laboratory ambient temperature and the next procedure summarize the steps:

- Prepare the samples by following a required mixing protocol
- Pour the sample into the UCA cell, fill until a marked level.
- Close the cell and insert vertically in the equipment
- Plug the transducer for wave pass through and set the temperature and pressure to normal conditions.
- Start reading when the first transit time is detected.

4.6.4 VICAT NEEDLE TEST

This test allows evaluating the hydration evolution of cementitous materials. As a result, it establishes two time points, initial and final time of setting of the material. The equipment needed consists of: a Vicat apparatus, plane non-adsorptive plate, a flat trowel and a conical ring, see Figure 4.18

Figure 4.18 Vicat needle test equipment

The tests were done by following the ASTM procedure (ASTM C191-13, 2013).

4.7 RHEOLOGICAL TESTS

4.7.1 VISCOMETRY

In order to evaluate the fluid behavior, different shear rates are imposed on the fluid and thus corresponding shear tensions are generated. The rheological response of a cementitious material can be obtained by using a viscometer as shown below in Figure 4.19. The equipement is a Fann viscometer. The principle is the following: a shear rate is imposed in a grout previously filled in the equipment cup and a bob rotation is correlated to shear stresses according to that deformation.

Figure 4.19 Fann Viscometer.

The methodology was based on Petrobras test manual for batching petroleum wells (PETROBRAS, 2005). The tests were carried out at 23°C ambient temperature, no heating was used for the grout sample and strain rates proportional to 3, 6, 30, 60, 100, 200, 300 rpm were employed in the viscometer.

4.7.2 MUD BALANCE

The apparent density is acquired through the balance mud use. It is also used for determining drilling fluid density and consists of a beam formed by a cup in one extreme, a weight slider and a bubble level. The methodology is summarized below (PETROBRAS, 2005):

- Prepare the grout and pour it on the balance cup until the latter is filled. Check if air bubbles are trapped in the cup.
- Place the lid, grout rises of the top hole. Clean the exterior surface of the cup as necessary. Avoid water getting inside the cup during the cleaning process.
- Place the beam on the support and search for equilibrium. Move the weight slider accordingly. Achieve a horizontal position.
- Density is measured on the place the weight slider remains.

The equipment is presented in Figure 4.20

Figure 4.20 Mud balance apparatus, superior and lateral sides

4.7.3 BLEEDING TEST

Expansion and accumulation of bleed water at the surface can be determined by a proper ASTM procedure (ASTM C940-10a, 2010) which was followed in this thesis. Room temperature and all dry materials temperature were at 23°C. The materials consist of glass graduates of 25 and 1000 mL and a thermometer. They can be seen in Figure 4.21

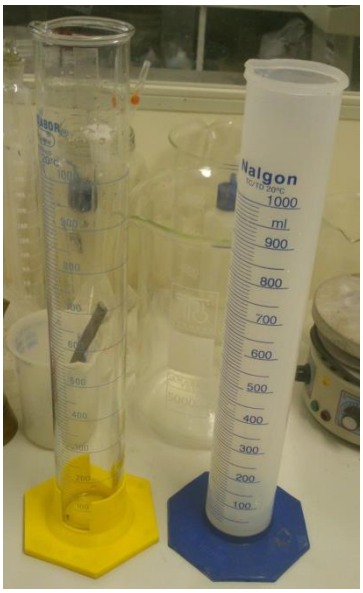

Figure 4.21 Apparatus used for the Expansion and Bleeding test for Grouts

4.8 MECHANICAL TESTS – COMPRESSION

Mechanical behavior plays a key role on the final performance of the grout, so compression tests were done to evaluate the strength and modulus of elasticity.

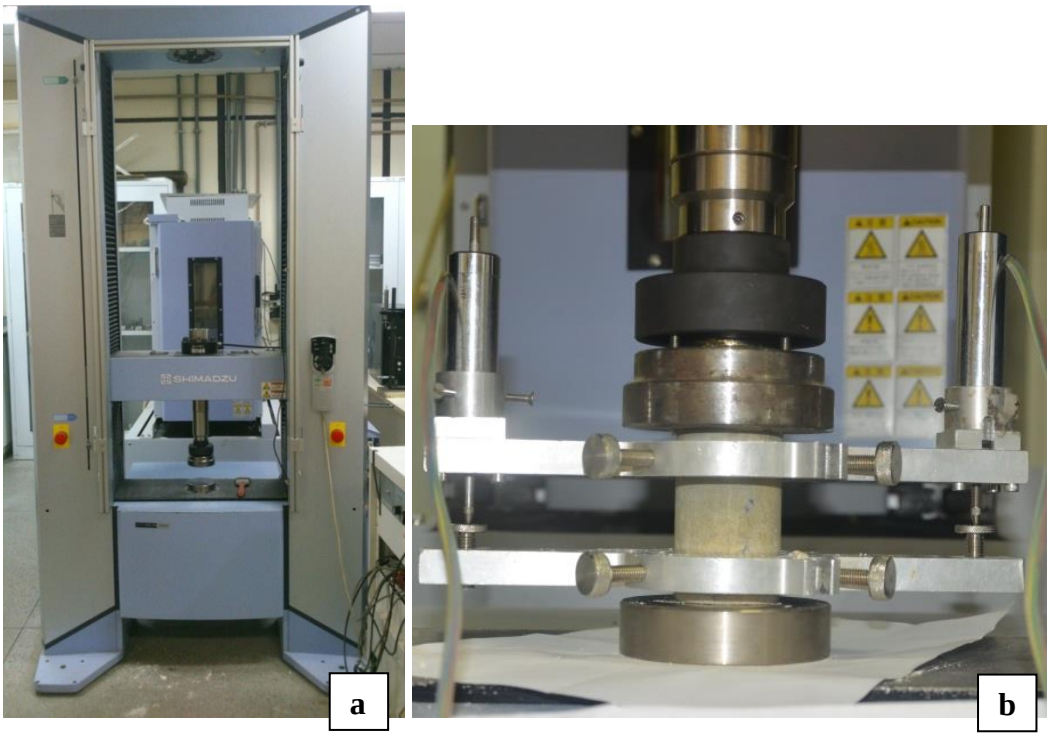

Figure 4.22 Compression test equipment
a) Shimadzu AGX-100 kN testing machine, b) LVDTs arrangement
b)

The Brazilian standard has been used as reference to achieve results (ABNT NBR 5739, 2007). Thus the following characteristics have been adopted:

- 50x100 mm cylinder specimens.
- Displacement control at the rate of, 0.3 mm/min.
- Use of LVDTs for measuring the deformation of the medium half of the specimen (Figure 4.22).
- In order to avoid imperfections on the top and bottom surfaces of the cylinders, either a lathe or a sulfur layer were employed to improve the surfaces aforementioned.
- A Shimadzu AGX-100 kN testing machine was used for the tests, Figure 4.22

4.9 SHRINKAGE TESTS

4.9.1 FREE AUTOGENOUS SHRINKAGE

Specimens were batched in 75x75x285 mm molds and test room conditions were 23±1 °C and 50% relative humidity at LABEST in COPPE/UFRJ. The dimensional changes of the specimens are focused in the longitudinal direction and they follow the next steps:

- Prepare the cuboid molds by gluing Teflon plates in order to provide a nonstick surface between the molds and the specimens. Place the bolts at the opposite ends in the longitudinal direction and secure them properly by using stainless nuts. The former will allow measuring the longitudinal axial length of every specimen along time. Establish a separation distance between the bolts inside the molds. Figure 4.23 a.
- Pour the grout until completely filling the mold. Use an extra Teflon plate for the upper side. Then isolate the specimen by using a plastic film for covering

the whole mold. Next, insert a type K thermocouple until middle height of the mold. Figure 4.23 b and c

- When percolation threshold occurs, axial bolts can be released by removing the nuts and set the LVDTs to measure the longitudinal deformations. After first days, specimens can be unmolded and isolated by employing plastic film layers and Aluminum tape. LVDTs shall continue being used until end of the test. Figure 4.23 d-f.

Figure 4.23 Autogenous Shrinkage test procedure

a)Preparation of molds, b)Batching, c) isolation and thermocouple setup, d) Release of restraints, e) LVDT setup and f) Specimen isolation

4.9.2 FREE DRYING SHRINKAGE

The free drying shrinkage was carried out in body specimens of the same size as section 4.9.1. The specimens were cured in a moist chamber and unmolded after 48 hours, depending on the mixture hydration rate. The essay is similar to autogenous shrinkage test, however, neither thermocouple nor specimen isolation were needed. Ambien conditions were controlled in the laboratory T = 23.0 ± 1.0 ° C and RH = 50 ± 2 %).

•

Shrinkage measurements were made by using both digital retraction frame and LVDT setup. By using the frame, measurements of lengths of specimens are carried out by comparison to the length of a bar reference.

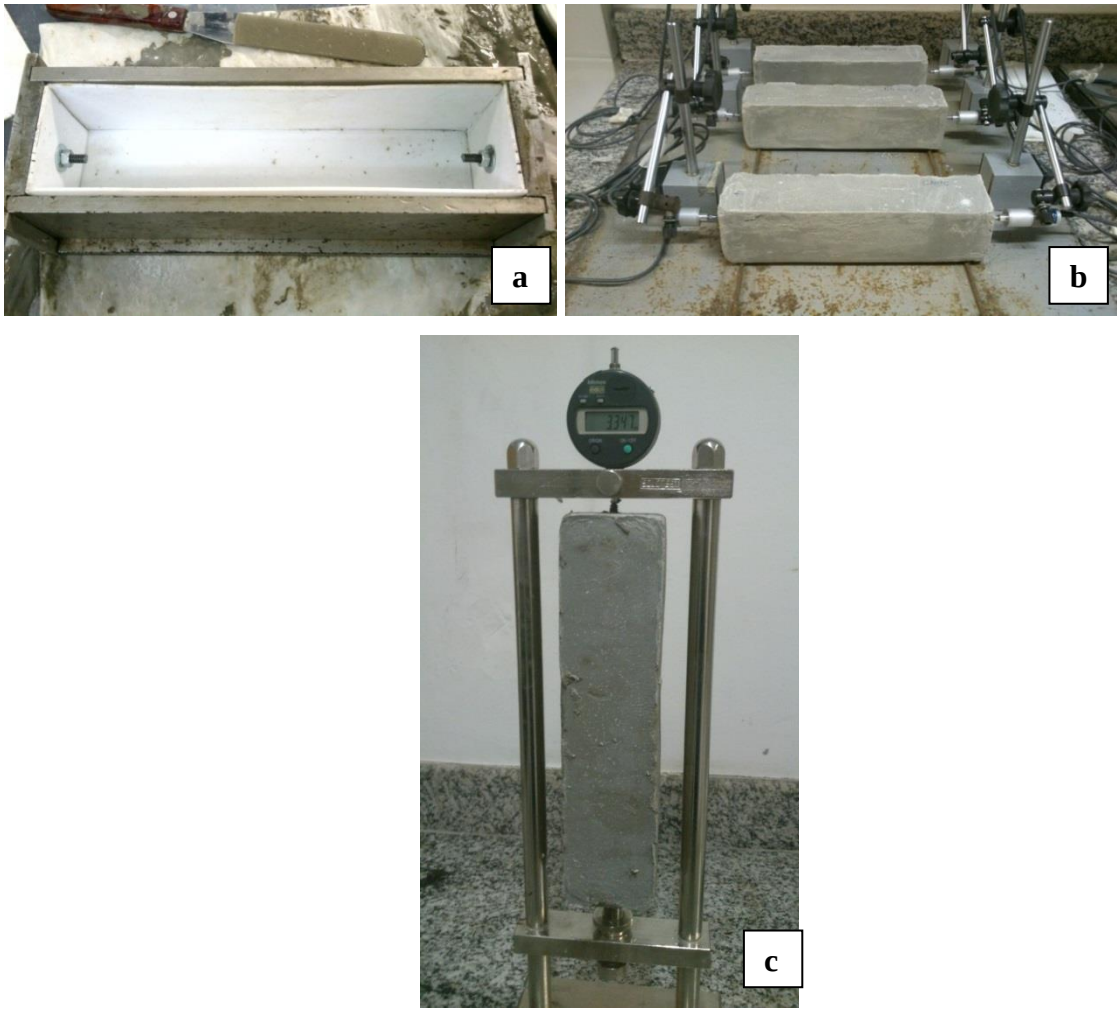

Figure 4.24 Drying shrinkage measurement.
a) Molds and bolt disposition, b) LVDT use and/or c) frame for dimensional changes

5 THE CEMENT BENTONITE SYSTEM: RHEOLOGY, MIXING PROTOCOL, MECHANICS, HYDRATION KINETICS

5.1 INTRODUCTION

This chapter presents results and conclusions of the three preliminary researches, bentonite rheological behavior, mixing protocol and high and low shears mixing for cement bentonite system

5.2 BENTONITE RHEOLOGICAL BEHAVIOR

5.2.1 RESULTS AND DISCUSSION

As shown in Figure 5.1, bentonite does not disperse easily and tends to create flocs as soon as it gets contact with water.

Figure 5.1 Importance of proper dispersion of bentonite.

Influence of bentonite content on the rheological behavior was first studied and the corresponding rheograms are presented in Figure 5.4 and Figure 5.5. In order to evaluate quantitatively the flow behavior, Herschel-Bulkley coefficients were found by employing the method proposed by Glen Mullineux (MULLINEUX, 2008) which consists on the following procedure:

Given the Herschel-Bulkley model:

$$y = y_0 + Kx^n \qquad \text{Equation 5-1}$$

Where:

y_0, yield stress,
K, Consistency factor
n, flow behavior index

By applying linear squares criteria:

$$S = \sum_{i=1}^{m}(y_0 + Kx_i^n - y_i)^2 \qquad \text{Equation 5-2}$$

$$\frac{\partial S}{\partial y_0} = \frac{\partial S}{\partial K} = \frac{\partial S}{\partial n} = 0 \qquad \text{Equation 5-3}$$

Thus a linear equation system is formed and relies on a non-trivial solution. Therefore the following equation needs to be solved:

$$F(n) = \begin{vmatrix} m & \sum x^n & \sum x^n \ln x \\ \sum x^n & \sum x^{2n} & \sum x^{2n} \ln x \\ \sum y & \sum x^n y & \sum x^n y \ln x \end{vmatrix} = 0 \qquad \text{Equation 5-4}$$

After applying the method successively, Herschel-Bulkley parameters were found for the three bentonite suspensions as can be observed in Table 5.1.

Table 5.1 Herschel-Bulkley parameters obtained by the Mullineux approach and Apparent yield stress by Besq for three Bentonite concentrations.

Content, %	2.27		4.58		10	
Shear rate	Increasing	Decreasing	Increasing	Decreasing	Increasing	Decreasing
n	2.11	2.71	0.49	0.59	0.48	1.79
y_0	0.97	0.61	9.34	7.57	13.74	79.83
k	0.000002	0.000000065	0.167232	0.120979	2.072100	-0.000277
$y_{0\ app}$	0.86	0.49	8.44	7.77	14.76	69.50
Experimental Shear stress at 3 rpm	0.7665	0.511	8.687	8.176	16.352	72.562

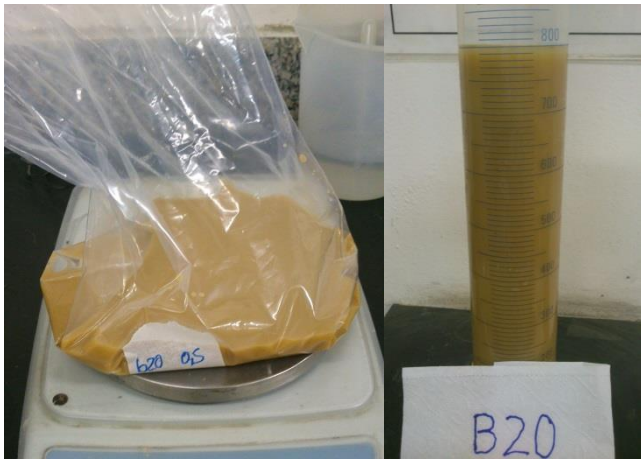

Figure 5.2 B20 or 2,27% bentonite suspension

By analyzing the results, bentonite content highly influences the flow properties such as yield stress, apparent viscosity and hysteresis, see Figure 5.2, Figure 5.3 and Figure 5.4. Yield stress of 4.58% and 10% suspensions increases 9.6 and 14.1 times respectively, when we compare them with a 2.27% bentonite content in increasing-shear-rate curves. Decreasing shear rates prove similar comparison. In addition, yield stresses,

y_0, obtained by the numerical approach (MULLINEUX, 2008) are higher than shear stress at 3 rpm obtained experimentally. On the other hand, the apparent yield stress (BESQ *et al*., 2003) obtained by following the tendency line of the low shear stresses in bentonite suspensions emphasizes the variability on determination of this rheological parameter. Additionally, it is evident apparent viscosity increases with bentonite content as can be observed in the corresponding figures. It occurs due to a stronger structuration of the plate-like bentonite particles and the water attracted between its layers. Moreover,

hysteresis loops show an interesting behavior. At 2.27% content, the area between curves is smaller compared to the others. The internal structuration does not change considerably after imposing shear rates because of the low bentonite content. By using a 4.58% suspension, the area increases which shows the water-bentonite structuration is modified after shearing and small stresses are obtained in the decreasing shear rates. A stronger structuration is seen in 10% suspension and thyxotropy is highly evident. After imposing increasing shear rates, this suspension recovered its solid-like appearance and forbade the viscometer bob of recovering its no-shearing position. Decreasing shear rate caused breaking of the 10% bentonite structures immediately next to the concentrical cylinders and the shear stress readings tended to increase. In accordance with its thyxotropic behavior, after imposing a 510.7 s^{-1} (300 rpm), 10% suspensions attempted to recover its steady-state behavior and exerted torsion on bob.

Figure 5.3 B40 or 4.58% bentonite suspension

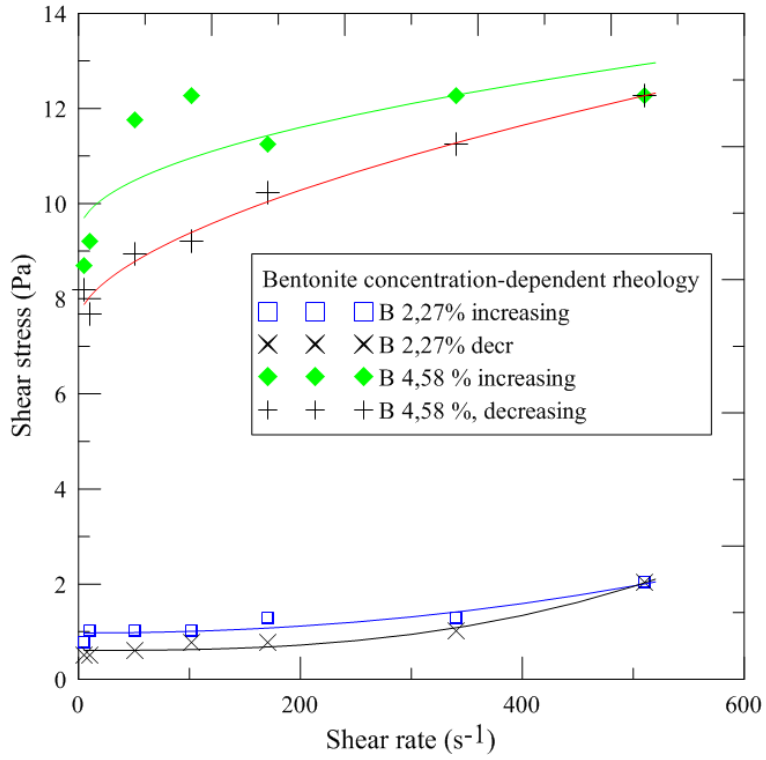

Figure 5.4 Rheogram of 2.27% and 4.58 % bentonite suspensions. Herschel-Bulkley models

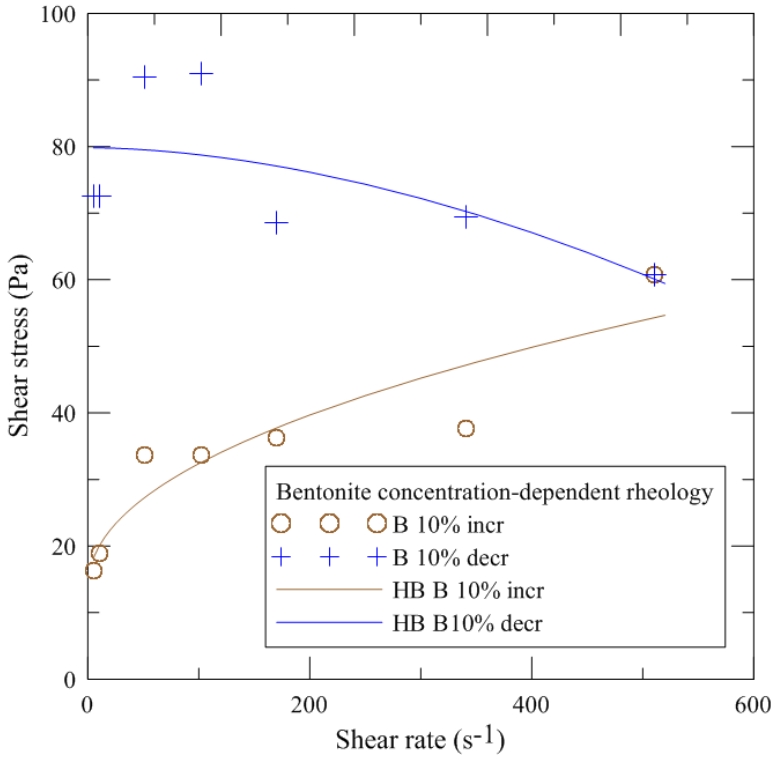

Figure 5.5 Rheogram of 10 % bentonite suspensions. Herschel-Bulkley models

Figure 5.6 Highly thixotropic behavior of 10% bentonite suspension

Rheological evolution across time is shown in Figure 5.7. Apparent viscosity increases and is time-dependent because internal structuration increases during hydration time. At the same time positive hysteresis loops are presented in the three curves. Likewise thixotropic behavior is more evident at 1 day since the insertion of water between the plate-like particles of bentonite achieved a higher stage in accordance to a higher stage of the bentonite swelling process. Additionally, there seems to be two regions in the curves. For shear rates less than 100 s^{-1}, a Bingham model seems to fit better than a Herschel-Bulkley one. At higher shear rates, the suspensions behave more fluidly. Similar results were found by previous research (BESQ *et al*., 2003). Polymer or soluble salts may influence the hysteresis shown (BESQ *et al*., 2002), as a matter of fact, the present bentonite received industrial treatment for turning it a sodium activated bentonite. To the author knowledge, there are no natural sodium bentonite deposits in Brazil.

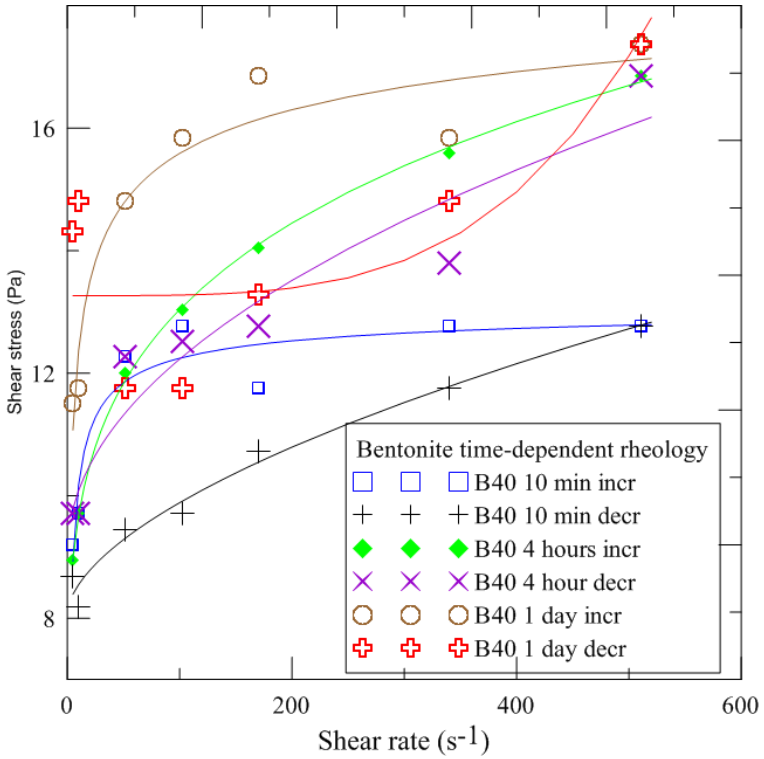

Figure 5.7 Bentonite time-dependent rheology. Herschel-Bulkley models

Corresponding parameters of effect of time on suspensions can be seen in Table 5.2:

Table 5.2 Herschel-Bulkley parameters obtained by the Mullineux approach and Apparent yield stress by Besq. Time-dependent behavior

Age	10 min		4 hours		1 day	
Shear rate	Increasing	Decreasing	Increasing	Decreasing	Increasing	Decreasing
n	-0.49	0.59	0.23	0.49	-0.20	3.76
y_0	13.23	8.08	4.83	9.06	21.10	13.27
k	-9.49	0.12	2.86	0.33	-13.83	2.87E-10
$y_{0\ app}$	8.95	8.28	8.83	9.27	11.07	15.02
Experimental Shear stress at 3 rpm	9.20	8.69	8.94	9.71	11.50	14.31

Herschel-Bulkley parameters were also obtained by the aforementioned numerical approach (MULLINEUX, 2008). Obtained yield stresses of increasing shear rates seem to be higher than expected at 10 minutes and 1 day ages. This is evident when we compare them with the experimental shear stresses at low shear rates, 5.1 s^{-1} (3 rpm). Likewise, the flow behavior index for both ages is negative in both curves. Despite these particular characteristics, those curves seem to fit well the dispersion points.

Particular attention needs to be paid for comparison purposes and because of this fact, the apparent yield stress was also obtained by taking into account the flow behavior at low shear rates as done by BESQ *et al*. (2003). Corresponding apparent yield stresses seem to be more coherent than the ones obtained by the numerical approach.

It is necessary to report the appearance of bubbles after mixing. It might be a result of cavitation during the mixing process (JEFFERIS, 2014) as can be seen in Figure 5.8.

Figure 5.8 Appearance of bubbles after mixing.

5.2.2 CONCLUSIONS

Finally, it has been noticed not only concentration is directly related to viscosity of suspensions but also bentonite suspension rheology is time-dependent. It is concluded b10% lacks of fluid behavior. Therefore less clay contents than 10% are recommended . After mixing and saving the suspensions, it was found a bentonite-water structuration process occurs, i.e., the swelling process happens and water is inserted between the clay particles. At the same time, it was observed the second step of 12000 rpm for 5 minutes increased viscosity. Thus mixing times can be modified in the next sections if necessary. Air bubbles were found, it might be due to cavitation.

5.3 MIXING PROTOCOL FOR THE CEMENT BENTONITE SYSTEM

5.3.1 RESULTS AND DISCUSSION

The uniaxial compressive behavior of both mixes is presented below in Figure 5.9 and Figure 5.10 and Table 5.3 and Table 5.4. Stress-strain curves of all specimens tested are shown in order to carry out the analysis. Comparison of curves is found in Figure 5.11. The pictures of tested specimens are presented in Figure 5.12.

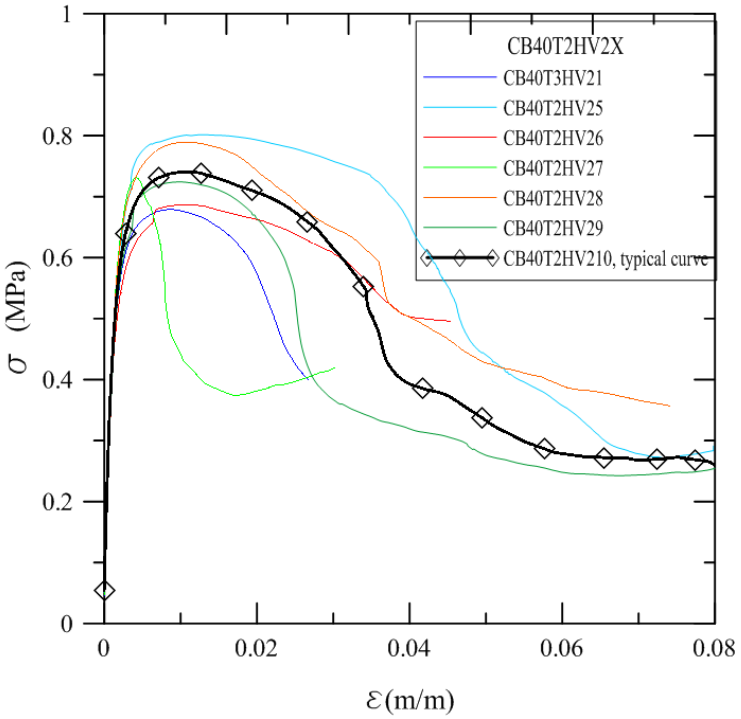

Figure 5.9 Type 2 behavior

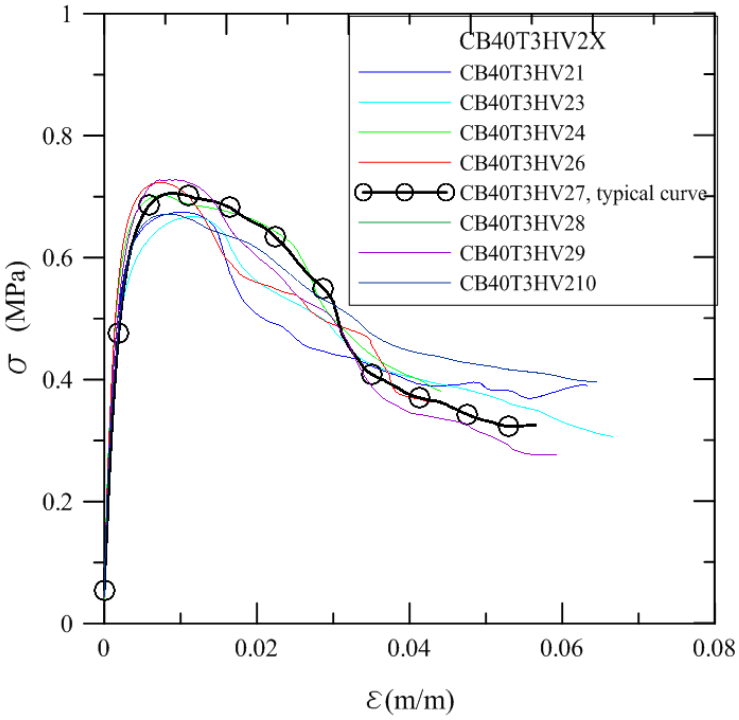

Figure 5.10 Type 3 behavior

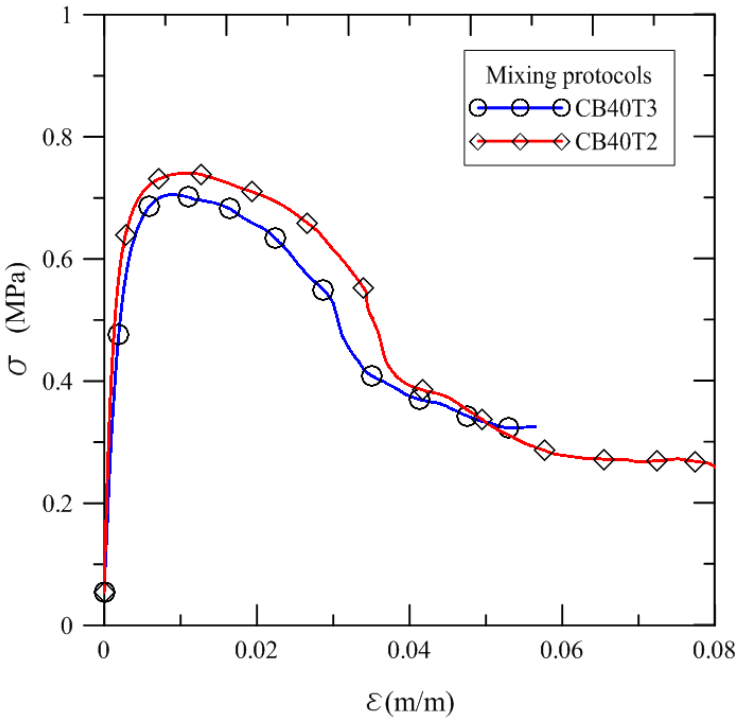

Figure 5.11 Comparison of protocols

T2 presented a less homogenous grout than T3 and slightly higher strength, modulus of elasticity and strain at failure. T2 grout pattern is non-homogenous as observed in the dispersion of curves obtained (see Figure 5.9). This behavior can

explained due to the fact that the cement cannot be totally dispersed. As a consequence, cement nodules covered by bentonite may appear (JEFFERIS, 1982) although high shear mixing seems to have helped diminish the latter (REJEB, 1995). As a result, strength and modulus of elasticity were, respectivlely, 5.6% and 10.1% higher than T3 properties (refer to Table 5.5). On the other hand, and this is important, T2-grout strain at the highest stress is 13.2% higher than the T3 one which might prove that the cement nodules causes a higher propagation of cracks (JEFFERIS, 1982). Because it is more homogenous and might result in less crack propagation, T3 offers a less permeable grout.

Table 5.3 T2 grout mechanical response.

Grout	Fmax (kN)	σ max (MPa)	ε rupture (m/m)	E (MPa)
CB40T2HV21	1.36	0.68	0.008520	413
CB40T2HV25	1.57	0.80	0.012725	412
CB40T2HV26	1.35	0.69	0.011540	337
CB40T2HV27	1.43	0.73	0.004251	396
CB40T2HV28	1.55	0.79	0.010710	421
CB40T2HV29	1.42	0.72	0.009913	385
CB40T2HV210	1.45	0.74	0.010596	410
Average	1.45	0.74	0.009751	397
SD	0.09	0.05	0.002753	29

Table 5.4 T3 grout mechanical response

Grout	Fmax (kN)	σ max (MPa)	ε rupture (m/m)	E (MPa)
CB40T3HV21	1.32	0.67	0.010130	360
CB40T3HV23	1.31	0.67	0.011535	331
CB40T3HV24	1.38	0.70	0.007751	413
CB40T3HV26	1.42	0.72	0.007316	390
CB40T3HV27	1.38	0.71	0.009000	267
CB40T3HV28	1.43	0.73	0.007235	348
CB40T3HV29	1.38	0.70	0.007441	420
CB40T3HV210	1.32	0.67	0.008495	350
Average	1.37	0.70	0.008613	360
SD	0.05	0.02	0.001545	49

Table 5.5 Comparison of T2 and T3 grouts performance

Grout		Fmax (kN)	σ max (MPa)	ε rupture (m/m)	E (MPa)
CB40T2HV2	Average	1.45	0.74	0.009751	397
	SD	0.09	0.05	0.002753	29
CB40T3HV2	Average	1.37	0.70	0.008613	360
	SD	0.05	0.02	0.001545	49
Comparison, T2/T3		1.059	1.056	1.132	1.101

T2 grout

T3 grout

Figure 5.12 Specimens tested at 28 days.

5.3.2 CONCLUSIONS

T3 mixing protocol offered a more homogenous grout with less dispersion on stress-strain curves of the same type of mixing after maximum stress. T2 produced slightly higher strength 5,9%.. However it is shown it achieves higher strains than T3 at the same stress after peak. The latter can prove T2 might produce propagation cracks due to less dispersed cement particles and creation of cement aggrupation. High shear mixing might have helped in the control of cement nodules, though. Therefore, T3 mixing protocol is selected as the best procedure and will be employed in next sections.

5.4 HIGH AND LOW SHEAR MIXING INFLUENCE

5.4.1 PREVIOUS CONSIDERATIONS

- T3 mixing protocol was selected based on conclusions in section 5.3.2.
- Section 4.1.3.3 establishes materials and procedures and mixing time

5.4.2 RESULTS AND DISCUSSION

Low shear mixing could not disperse bentonite properly and agglomerations were presented during bentonite hydration stage. Figure 5.13 shows these results, the picture was taken immediately after mixing. Clumps were presented in the low shear case and water could not be inserted homogenously between the bentonite laminar particles. It was expected that water could permeate inside the agglomerations after the water absorption step, which is the third step of the mixing process, however, it did not occur or could not be observed during the tests. Therefore, not all of the bentonite mass used could help cope with the high amounts of water and the material contribution is diminished.

Low Shear High shear

Figure 5.13 Results after mixing bentonite

Progressively, bleeding results for all grouts are presented in Figure 5.14. The reference grout quantitatively expresses the important bentonite properties of harnessing high amounts of water by comparison with the rest of the grouts which possess a different-than-zero bentonite content. First, there is an inverse proportion between

bentonite content and bleeding for both low and high shear mixing. It is evident in all results except for high- shear-mixed CB60 grout due to other causes. The latter can occur possibly due to its rheological characteristics and the mixing process. Its bentonite suspension has a higher viscosity because of 60 kg/m^3 bentonite content and higher gel strength. So cement-bentonite grout gets more difficult to be mixed. After the mixing process, it was observed that the mix was not completely homogenous.

Therefore, the effect of bentonite can be traced back to bleeding reduction, i.e., cement particles get suspended during hydration process until they can form a solid structure. In addition, high-shear-mixed CB40 grout presented the most efficient combination of materials and mixing characteristics between the six grouts in bleeding terms, 1.178%.

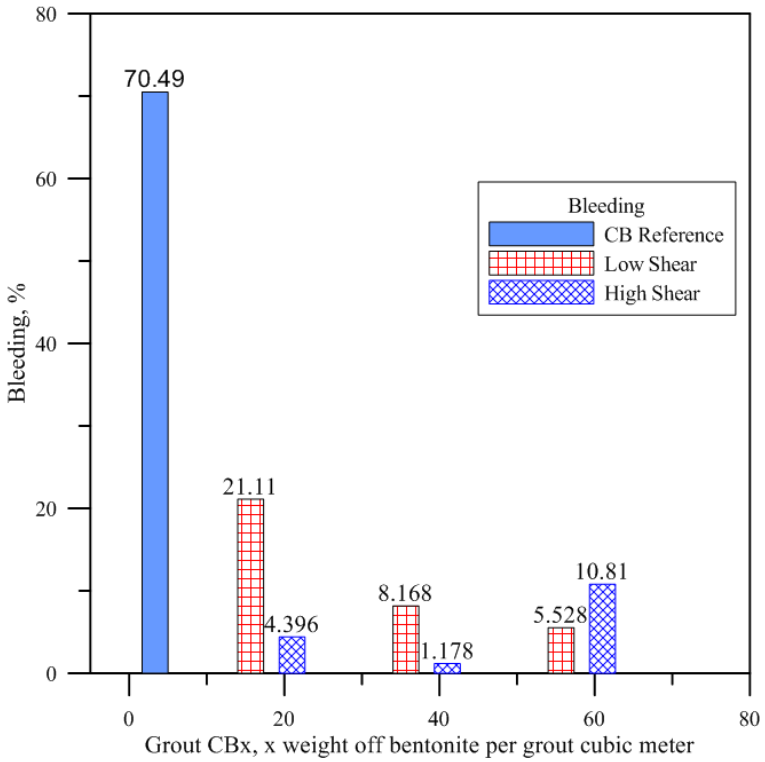

Figure 5.14 Bleeding of cement-bentonite grouts under low and high shear mixing

CB20 CB40 CB60

Figure 5.15 Bleeding process at low shear mixing

CB20 CB60

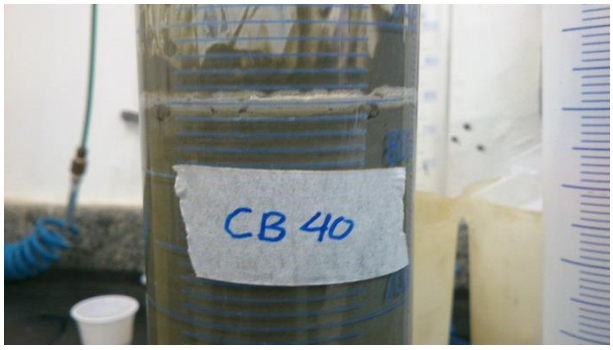

CB40

Figure 5.16 Bleeding process at high shear mixing

Likewise mechanical compression behavior was employed as an additional variable for evaluation. Despite considerable bleeding in low-shear mixing grouts, all of them were studied for comparison purposes. However, specimen lengths were registered and will serve for analysis. In the high shear mixing case, the mixCB60 presents: high viscosity due to the bentonite content effect, difficulty for obtaining homogeneous grouts and bleeding 9.17 times higher than the high shear CB40 case. CB60 at high shear mixing was not studied under compression loading. Similarly, since the high-shear CB20 grout has bleeding 3.73 times higher than the CB40 one, it will not be studied under this term. Table 5.6 and Figure 5.17 summarize the behavior of low shear specimens.

Table 5.6 Mechanical behavior of low shear mixing grouts.

Code	L (mm)	Fmax (kN)	σ max (MPa)	ε rupture (m/m)	E (MPa)
CB20T3LV1H241	72.22	1.37	0.70	0.001583	814
CB20T3LV1H242	71.94	1.76	0.90	0.001862	860
CB20T3LV1H243	75.74	1.48	0.76	0.001668	918
CB20T3LV1H244	73.61	1.87	0.95	0.001652	1035
CB20T3LV1H245	-	1.45	0.74	0.001097	903
Average	73.38	1.59	0.81	0.001572	906
SD	1.74	0.21	0.11	0.000285	83
CB40T3LV1H244	82.90	1.09	0.55	0.001880	724
CB40T3LV1H245	80.27	1.05	0.53	0.002077	569
CB40T3LV1H246	81.66	0.97	0.49	0.001552	377
CB40T3LV1H247	79.37	1.04	0.53	0.001997	510
CB40T3LV1H249	76.73	1.44	0.73	0.002184	741
CB40T3LV1H2410	81.33	1.03	0.52	0.001938	508
Average	80.38	1.10	0.56	0.001938	571
SD	2.16	0.17	0.09	0.000217	140
CB60T3LV1H242	86.69	1.50	0.77	0.003794	495
CB60T3LV1H243	86.94	0.98	0.50	0.002066	451
CB60T3LV1H245	81.48	1.65	0.84	0.004668	630
CB60T3LV1H2410	-	1.15	0.58	0.001778	609
Average	85.04	1.32	0.67	0.003076	546
SD	3.08	0.31	0.16	0.001385	87

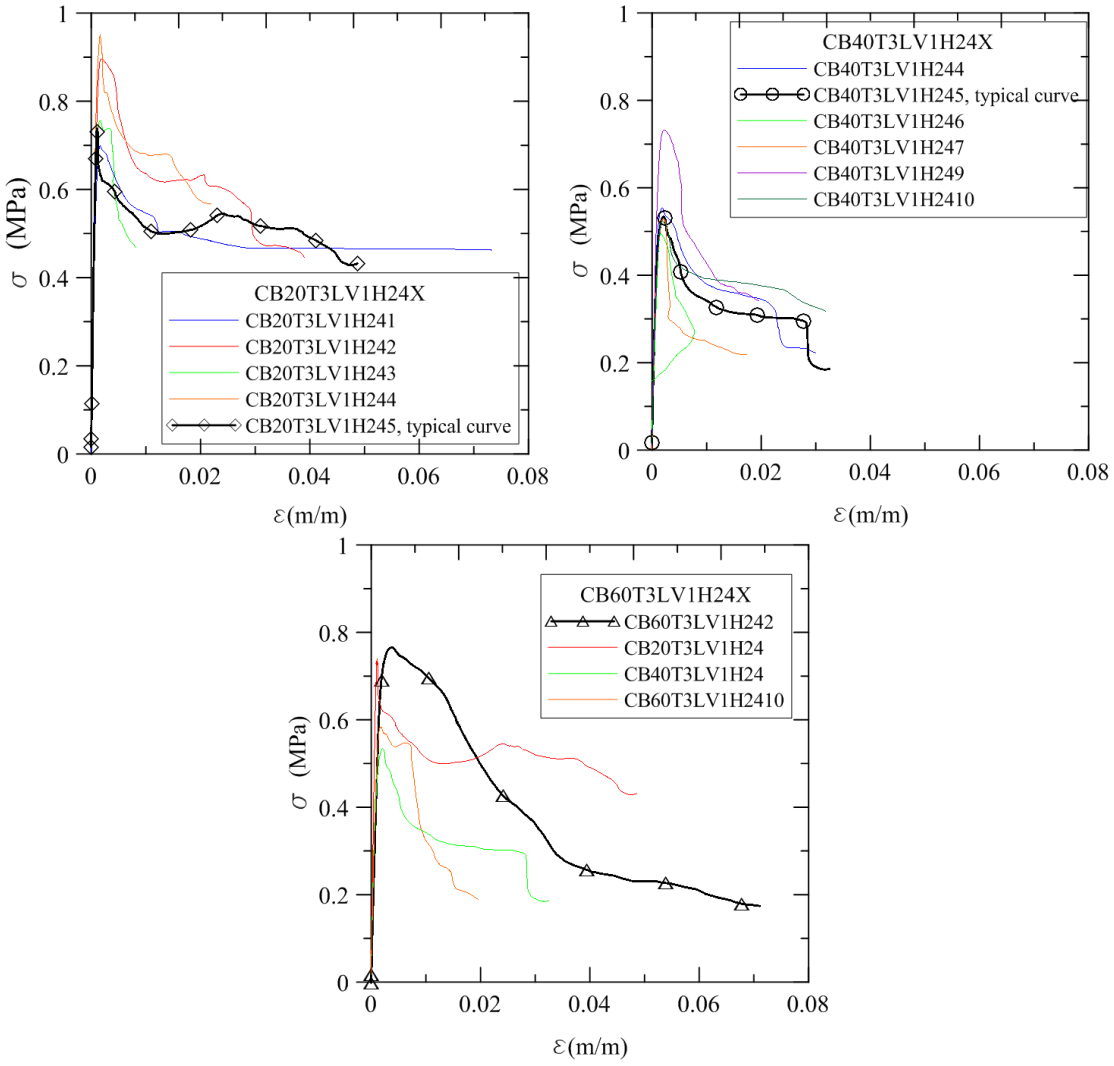

Figure 5.17 Low shear mixing effect, 20, 40 and 60 kg/m^3 of bentonite.

In Figure 5.17 the effects of the mixing characteristics are shown: dispersion of results belonging to the same grout type and the height/diameter ratio effect. Sedimentation process begun during pouring the grout in the cylindrical molds, standards deviation also confirms these results.

.

In order to analyze the reduction in specimen lengths (due to bleeding), compression strength, strain at rupture and modulus of elasticity, Figure 5.18 and Figure 5.19 can be consulted. On these results high-shear CB40 parameters are also presented for comparison. CB20 has higher strength than CB40 and CB60, all of them under low shear mixing. Although it had less solid particles in its matrix, a lesser height/diameter ratio played a key role for results. The height or length of CB20 specimens were less than the others due to a 21.11% bleeding. The average height/diameter ratios are 1.48,

1.61 and 1.70 for CB20, CB40 and CB60 low shear grouts, respectively. If we analyze the cylindrical specimens as columns, slenderness is important when columns are loaded under compression. Moreover, high-shear CB40 grout has a 24.20% higher strength than its corresponding low-shear case.

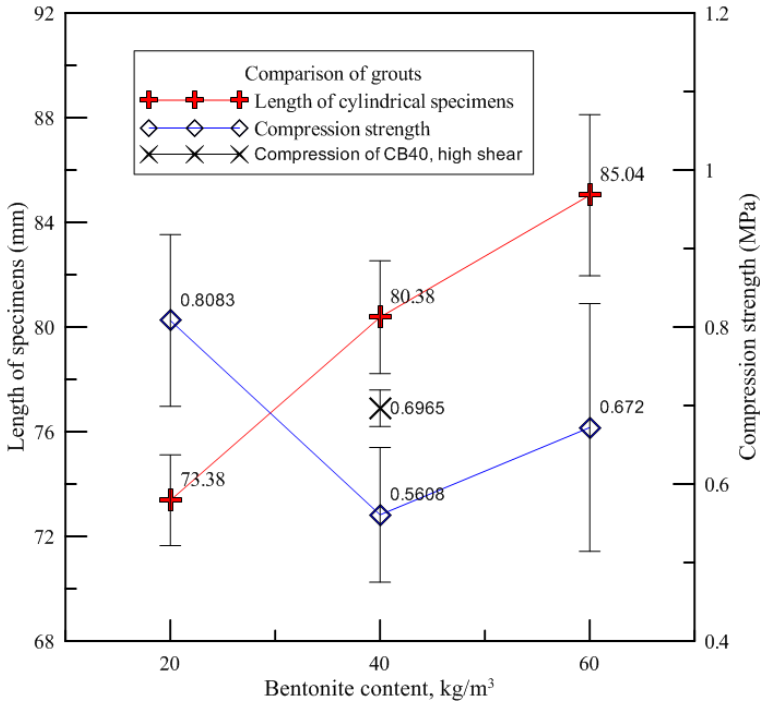

Figure 5.18 Compression strength and length of specimens of low shear mixes.

A less slender CB20 specimens produced higher modulus of elasticity results than the other grouts and more brittle as well (Figure 5.19). By comparing the high shear and low shear mixing of CB40 grouts, it is shown that a high-shear mixing produced a less brittle grout and with less axial stiffness. Strain at rupture is 4,44 times higher at high shear mixing and its modulus of elasticity just stands for 63% of the low shear case. In addition, specimens after being tested are shown in Figure 5.20. Because of the exposed results, low shear mixing was no longer used in the following sections.

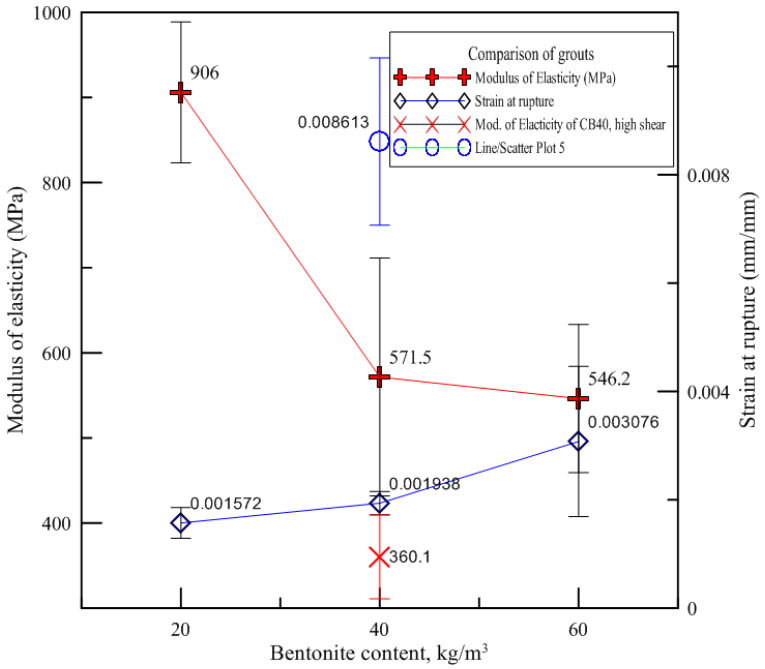

Figure 5.19 Modulus of elasticity and strain at rupture of low shear mixes

CB20 CB40

CB60

Figure 5.20 Specimens prepare at low shear mixing, age 28 days.

5.4.3 CONCLUSIONS

First, bleeding occurs in all grouts but they are higher in the low shear case. About this fact, increasing bentonite content until 60 kg per cubic meter of grout cannot control bleeding due to all clay particles are not used efficiently. Bad dispersion occurs. In the high shear case, it reduces bleeding significantly until 1,178% for CB40. However, higher content of bentonite in CB60 seems to prevent a good mixing. This grouts is less workable and reported higher bleeding than CB40 at high shear case.

The 5^{th} step in mixing which mixtures cement and bentonite was 5 minutes. It represents 150% higher than the 2 minute in the previous research. It is deduced, this step cannot produce a better mixing and does not reduce bad dispersion of previous steps, especially in low shear case. Therefore, it is more important the dispersion of bentonite than the last one. It is recommended to maintain 2 minutes for fifth step since it was already used in the mixing protocol at high shear. By comparing CB40 at low and high shear compression results and the bleeding responses, it is chosen high shear mixing to be used in further sections.

5.5 RHEOLOGY, HYDRATION KINETICS AND SHRINKAGE OF THE CEMENT-BENTONITE SYSTEM BEHAVIOR

5.5.1 PREVIOUS CONSIDERATIONS

- T3 mixing protocol, mixing time and high shear mixing have been selected and correspond to section 4.1.3.2.
- Section 4.1.4 establishes materials and procedures.

5.5.2 RESULTS AND DISCUSSION

Influence of bentonite use was divided in the next four areas, hydration, rheology, shrinkage along the next sections.

5.5.2.1 RHEOLOGY

Figure 5.21 and Table 5.7 gather all rheological data. Grouts present: thyxotropic behavior, two regimes during imposing shear rate and CB60 grout presents a particular rheogram. Thyxotropy is present in the three grouts with higher hysteresis loops for CB40 and CB60 grouts. Additionally, the three curves seem to divide in two regimes depending on the shear rate. At shear rates less than 100 s^{-1}, high apparent viscosities are presented and can fit well for a Bingham model. Then at shear rates higher than 100 s^{-1}, small increases in shear stresses are found.. By observing the CB60 rheogram, this grout shows less yield stress and apparent viscosity than CB 40. This occurs due to the fact that the CB60 grout has the consistency of a gel with a stronger structuration, so the rotor of the viscometer breaks the structure really close to its surface. Therefore, the CB60 rheogram can show a different behavior since it can be observed by visual inspection that it is less fluid than the CB40 grout. In order to CB60 grout flow completely, high shear rate or shear stresses are needed.

On the other hand, the numerical approach to obtain the rheological parameters presented negative yield stresses. Because of this, apparent yield stress was obtained for comparison purposes (BESQ *et al*., 2003).

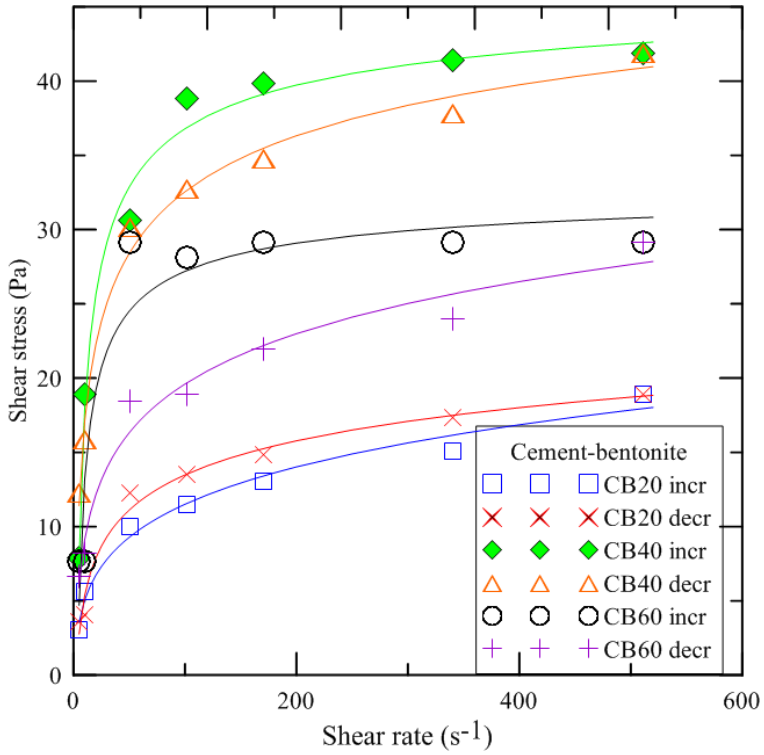

Figure 5.21 Cement- bentonite rheogram

Table 5.7 Herschel-Bulkley parameters obtained by the Mullineux approach and Apparent yield stress by Besq. Cement-bentonite behavior.

Grout	CB20		CB40		CB60	
Shear rate	Incr	Decr	Incr	Decr	Incr	Decr
n	0.18	-0.04	-0.42	-0.14	-0.50	0.05
y_0	-7.86	95.50	48.56	74.21	33.67	-80.59
k	8.61	-99.06	-79.55	-78.29	-64.78	80.32
$y_{0\ app}$	3.27	2.37	9.97	11.14	3.99	5.46
Experimental Shear stress at 3 rpm	3.07	3.58	7.92	12.26	7.66	6.64

5.5.2.2 HYDRATION KINETICS

5.5.2.2.1 Ultrasonic Cement Analyzer

By analyzing Figure 5.22 and Table 5.8, bentonite content variants did not change the percolation threshold among them. A representative curve of the reference grout

could not be obtained successfully. Since the equipment was highly requested for other studies, repetitive tests could not be carried out.

To the author understanding, cement particles are maintained in suspension during hydration and are well provided with water by hydrated bentonite however dispersed in the grout volume. So the construction of an internal solid frame occurs. Based on results, CB60 achieves percolation threshold slightly earlier than the others cement-bentonite grouts do, it might occur due to a higher solid content of bentonite. However, more tests are needed to confirm these results.

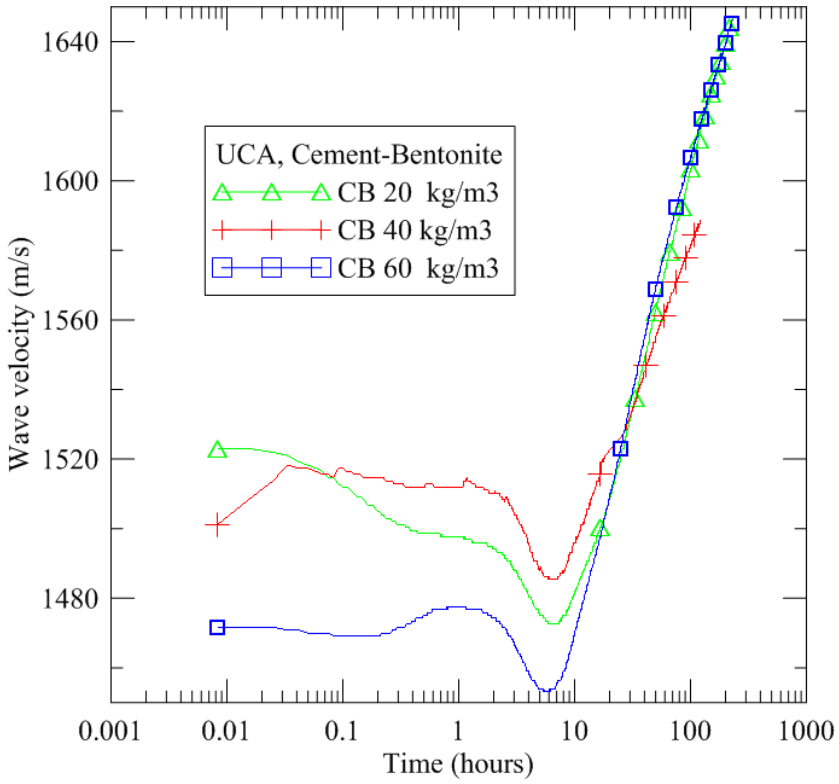

Figure 5.22 UCA tests of cement bentonite grout.

Table 5.8 Time at which wave velocity abruptly starts increasing

Grout	Set point	Minimum wave velocity (m/s)
CB20T3HV2	5h54'00"	1472,46
CB40T3HV2	5h59'30"	1485,38
CB60T3HV2	5h26'00"	1453,09

Figure 5.23 UCA test for cement-bentonite grouts

5.5.2.2.2 Isothermal Calorimetry

The tests were done at 23°C. First peak corresponds to the energy liberated immediately after mixing, thus it does not appear completely in the corresponding curves shown in Figure 5.24. The cement-water grout releases less heat than the others since 2,54 water cement ratio is well enough to delay hydration and high bleeding occurs, 70,49%. In its curve the C_3A hydration is not noticeable. In contrast, the bentonite inclusions seem to promote the cement hydration. The acceleration slope and the second peak corresponding to the C_3S hydration in all bentonite additions are higher than CBRef. The contribution of the viscosity of bentonite suspensions and the accumulation of water between the bentonite particles seem to guarantee the cement particle dispersion and provide water uniformly. This effect is improved by increasing bentonite from 20 to 40 kg/m^3 since not only higher bentonite concentration harness better the water amounts but also bleeding is lesser from 4,40% to 1,18%, and higher viscosity guarantees cement particle suspension as well. By adding 60 kg/m^3 of bentonite no better improvements were found at early ages in heat liberation terms.

Bentonite additions also influence on the hydration of C_3A, so a third hydration peak appears, see Figure 5.24. Therefore reactions of ettringite to monosulphate are evident and bentonite may improve the ettringite formation. No great differences were found among the three bentonite additions.

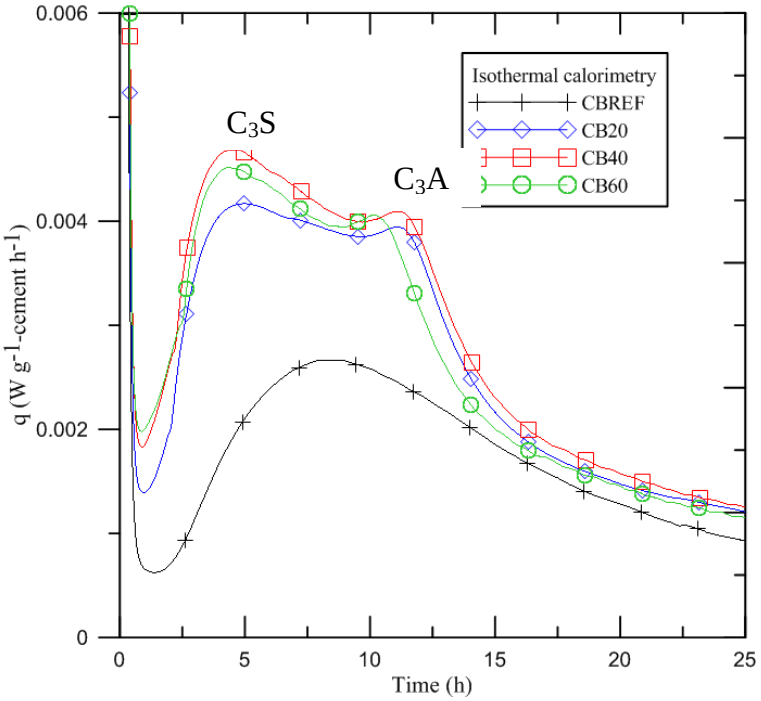

Figure 5.24 Rate of heat development of grouts with bentonite inclusions.

Since better cement dispersion and water uniformly distributed in the grouts, higher cumulative heats were obtained for all bentonite additions in comparison with CBRef. CB20 and CB40 produced more hydration heat release because their bentonite content was enough to help hydration, nevertheless, CB60 might have produced less cumulative heat than these two grouts because of the fact grout mixing may not be as efficient as the others due to its higher bentonite content, see Figure 5.25.

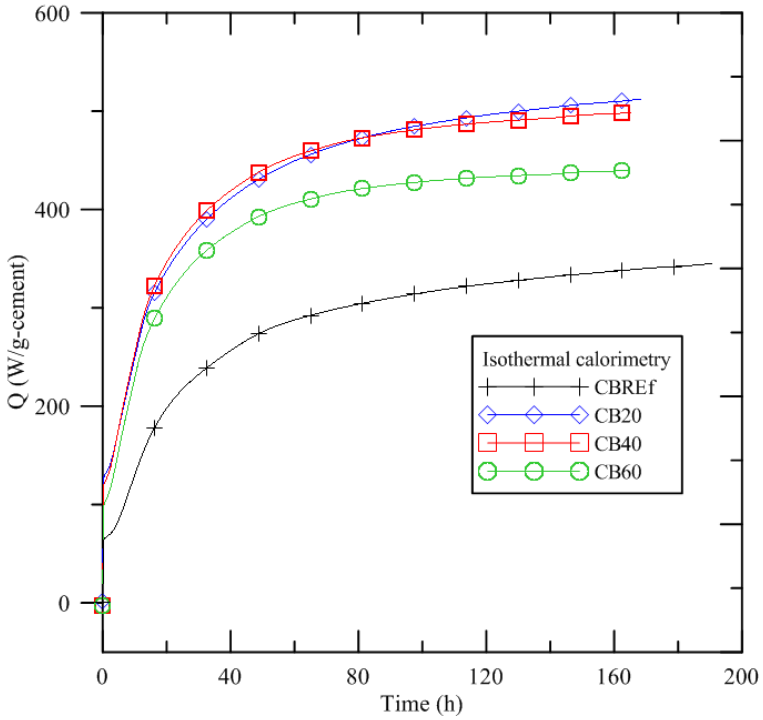

Figure 5.25 Cumulative heat of grouts with bentonite inclusions

5.5.2.2.3 Thermo-gravimetrical Analysis

Samples were taken immediately after mixing from grouts prepared for another tests done in this chapter. A sample for every type of grout was taken and isolated in different plastic bags, Figure 5.30, and delivered to the staff in charge of thermal analysis tests at Labest of COPPE/UFRJ for being tested at 24 hours, 7 and 28 days age. So four samples in total, and tests at different ages were carried out with a 10-20 mg samples.

Thermogravimetry (TG) and derivative thermogravimetry (DTG) were used for analysis. TG results are gathered in Figure 5.26. On the left column, curves show the free water whose amount loss is considered important due to the high water/cement ratios in all grouts. On the right side it was removed for better comparison of the mass losses of the hydration product at higher temperatures. Likewise, DTG analyses are plotted in Figure 5.27, Figure 5.28 and Figure 5.29.

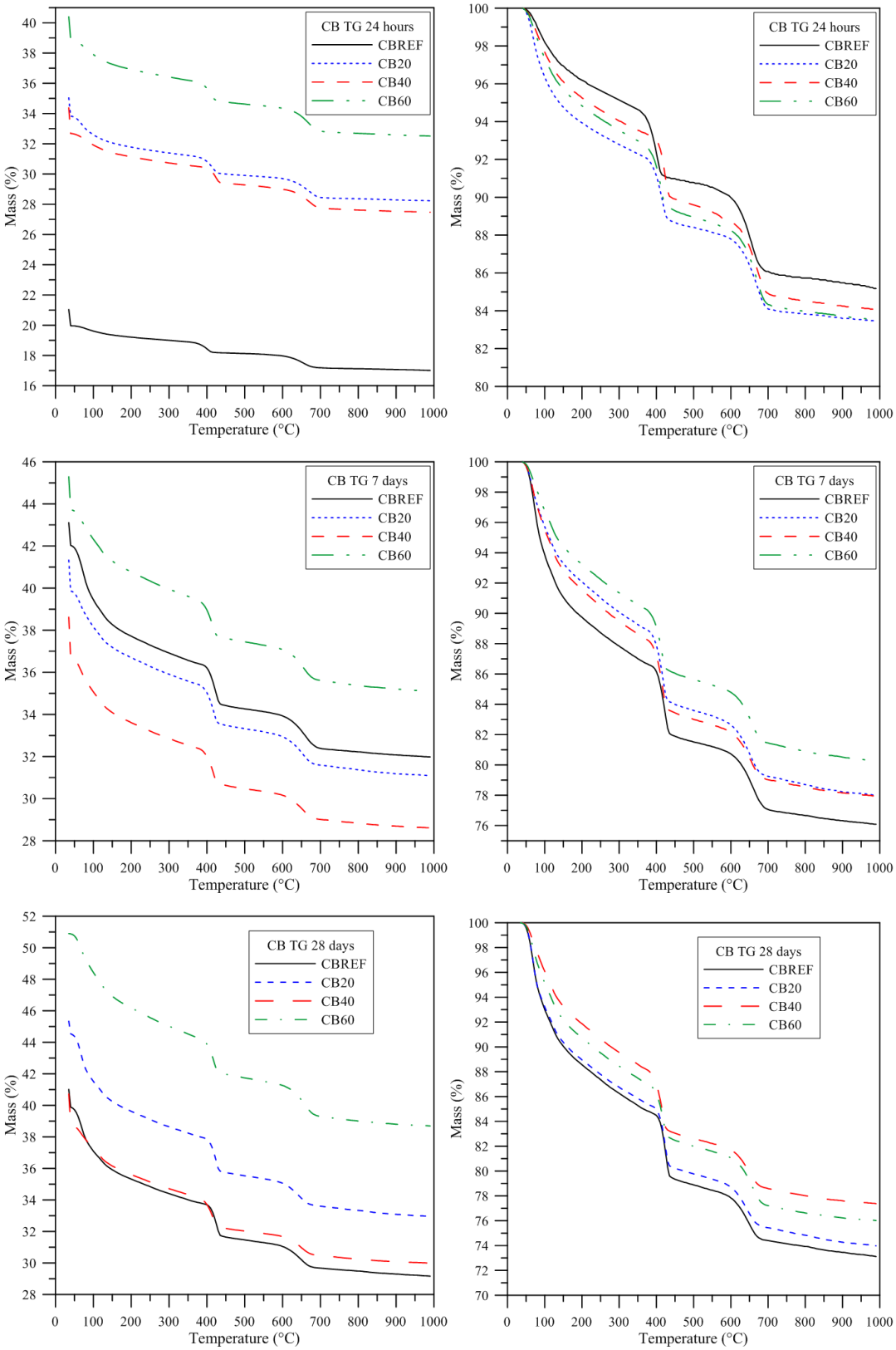

Figure 5.26 TG 24 hours, 7 and 28 days of cement-bentonite grouts

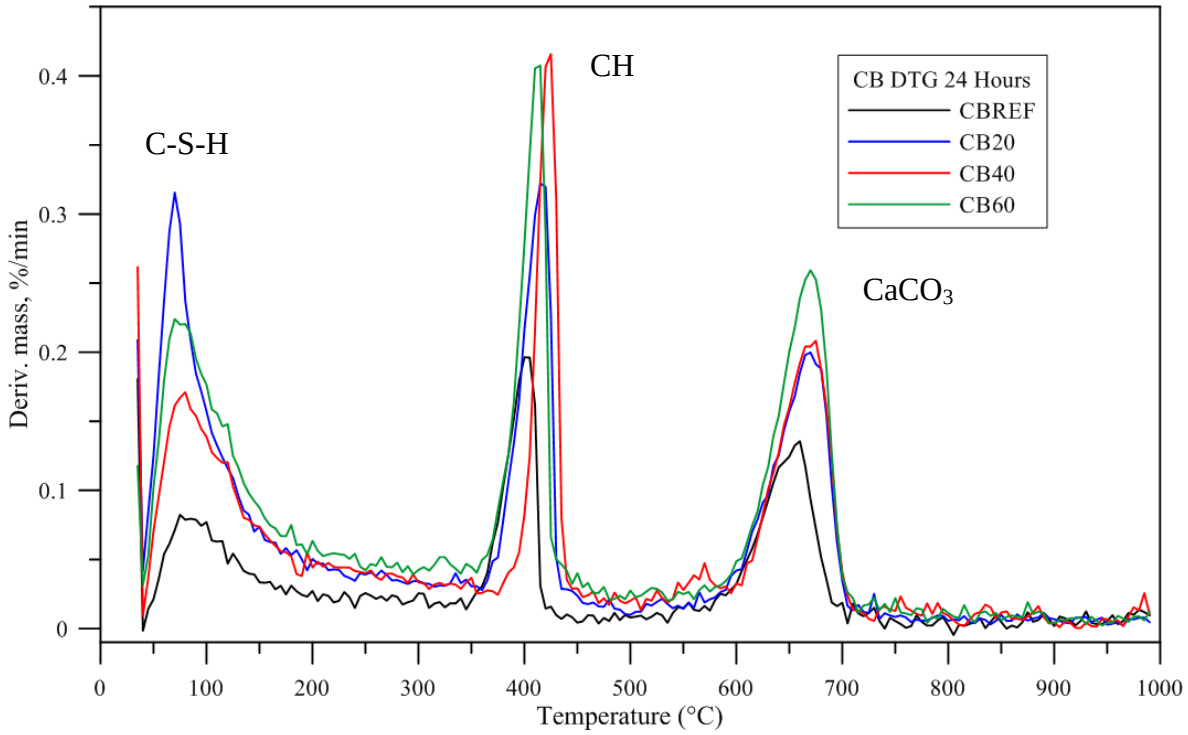

Figure 5.27 DTG at 24 hours of cement-bentonite grouts

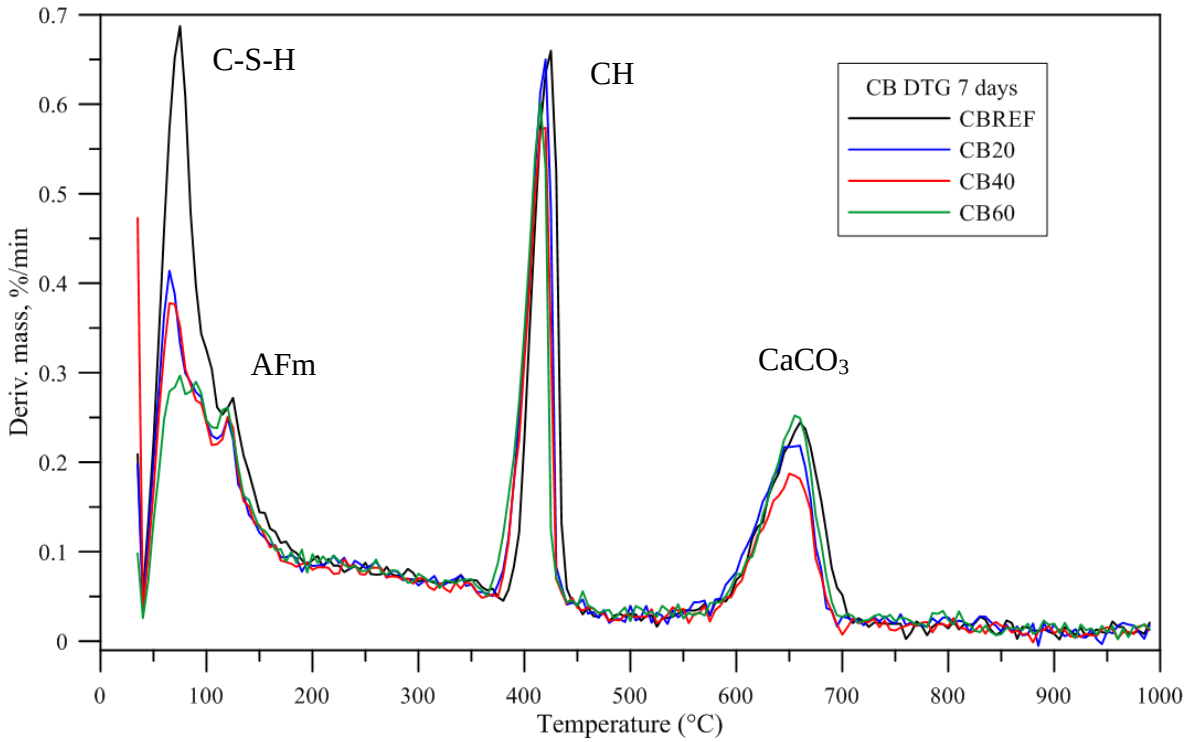

Figure 5.28 DTG at 7 days of cement-bentonite grouts

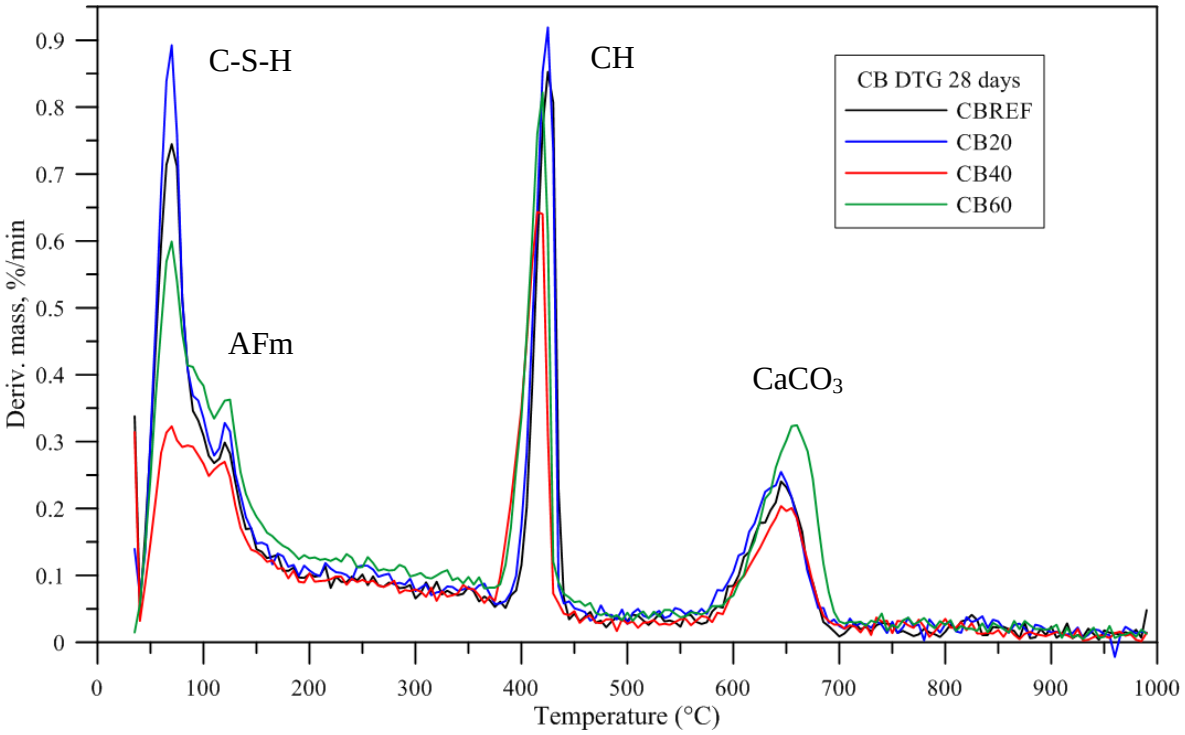

Figure 5.29 DTG 28 days of of cement-bentonite grouts

Calcined cement mass basis was used for comparison the mass losses of the hydration products (DWECK *et al.*, 2009). Consequently, histograms are plotted in Figure 5.31 and used for analysis of the hydration products.

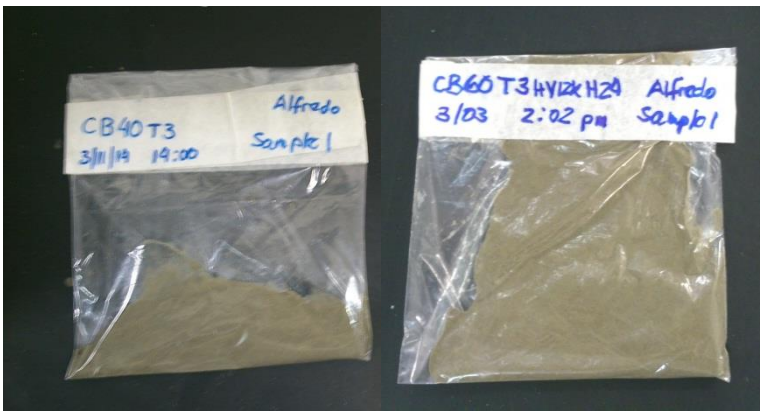

Figure 5.30 Grout sampling for TG analysis

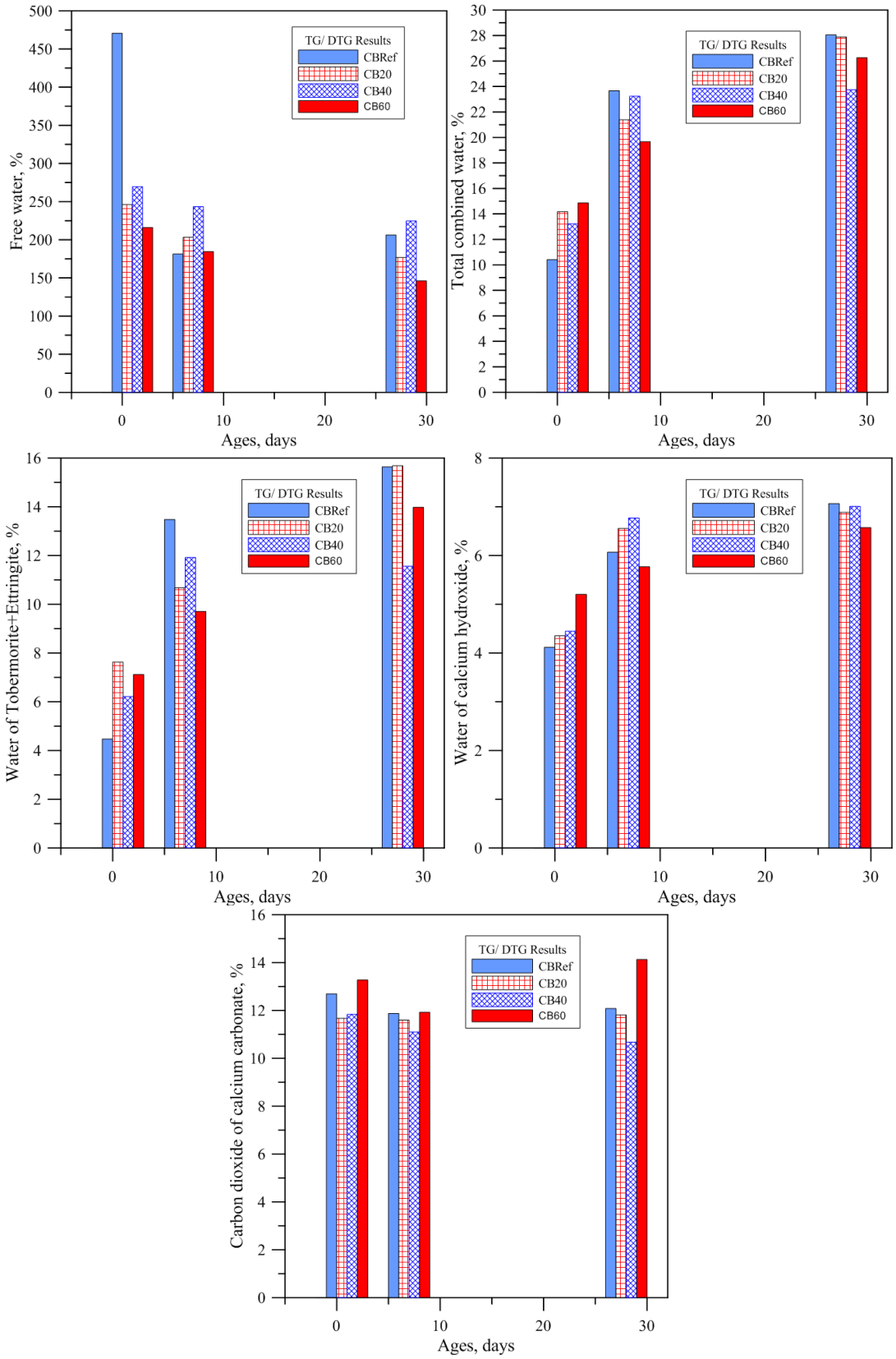

Figure 5.31 Weight losses on calcined cement mass basis at 1, 7 and 28 days of CB grouts

Free water loss is significant due to high w/c ratios in all grouts. It decreases across time, thus it is assumed it converts to combined water as can be seen at 7 and 28 days. It is also important to notice, the more the bentonite, the less free water. CB60 retains better the water between its particles, additionally, it has a lesser w/c ratio, 2,472 .

Grouts with higher water/cement ratios have a retarding effect at early ages but have higher combined water at later stages (NEVES JUNIOR *et al*., 2012). Those are CBREF, CB20 and CB40 which respectively have 2,541, 2,518 and 2,495 w/c ratios. As shown in Figure 5.31, they possess less combined water than CB60 until 24 hours. This means less hydration products are formed at the beginning but the opposite is presented at later ages. The more availability of water produced more combined water at 7 days and beyond.

At early ages the calcium hydroxide formation is higher in low w/c ratios, CB60, than the others. On the contrary, it happens the opposite at later stages. So at early ages ettringite formation consumes more water, then, calcium hydroxide and tobermorite are responsible for more water consumption later. This is consistent since corresponding water loss bars in Figure 5.31 show higher water loss of calcium hydroxide and tobermorite+ettringite.

CO_2 mass loss of $CaCO_3$ remains almost constant however it is relatively higher in CB60. Bentonite was sodium activated, i.e., it reacted with Na_2CO_3 in previous industrial process. Thus calcium carbonate is formed after this chemical reaction. Losses occur almost at the same temperature interval and no second peak at lower temperature was found, see Figure 5.27, Figure 5.28 and Figure 5.29. Therefore non-crystalline form of $CaCO_3$ was not found (DWECK *et al*., 2000).

5.5.2.3 Shrinkage

Shrinkage of CB40 is presented in Figure 5.32. The shrinkage shown was done in quase-adiabatic conditions, which means thermal changes due to heat of hydration has not been discounted. The first point of shrinkage rounds up 12 hours after the

cement+water mix. In the graph positive strains stand for shrinkage. Behavior can be described in the following way

- A first expansion due reabsorption of bleeding. CB40 was proven to have 1,178% bleeding from previous results.
- Then bleeding water might be depleted and continuous shrinkage slope is found until 100 hours approximately. This stage might be known as the stiffening phase where grout is building a solid structure capable of resisting water pore pressure due to self-desiccation.
- Then a hardening phase occurs where less shrinkage occurs. Later than 200 hours, a shrinkage reduction was found after reaching less than 60 microstrains peak approximately.

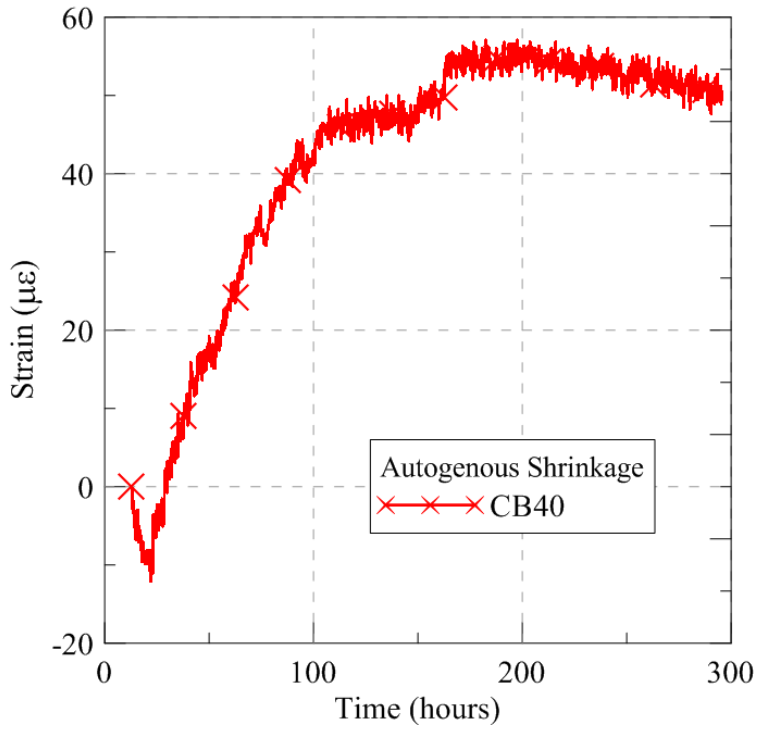

Figure 5.32 Autogenous shrinkage of CB40 grout

On the drying shrinkage case, time 0 stands for the first time the measurements were made, that is 48 hours after batching. Water loss is significant, microstructural cracks occur then they achieve macrostructural size. Therefore it has been measured as representative drying shrinkage 67 microstrains at 48 hours, then bending occurs due to water loss and multiple cracking.

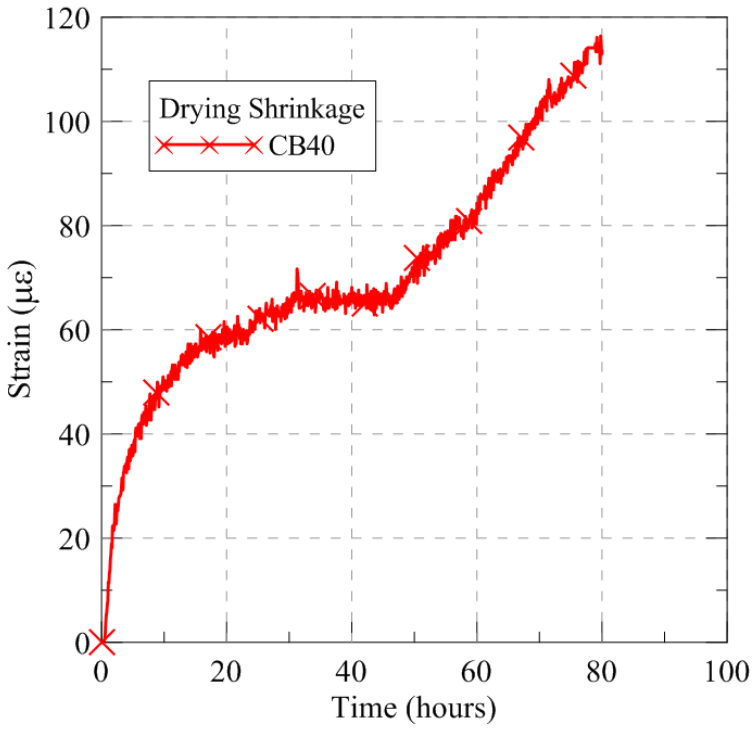

Figure 5.33 Drying shrinkage of CB40 grout

5.5.3 CONCLUSIONS

Rheology tests indicate reliable rheological responses are found for CB20 and CB40, however, because of higher viscoelastic properties of CB60, the rheogram curve falls for this case and does not show higher viscosity in CB60. UCA results reported that by augmenting the clay content from 20 to 60 kg of cubic meter of grout, percolation threshold does not change significantly. Isothermal calorimetry reports hydrated bentonite maintains cement particles in suspension and provides enough water. Therefore, the C_3S and C_3A hydration occurs in all bentonite contents and heat release was found. Also, thermal analyses show some delaying changes due to higher water/cement ratios in CBRef, CB20 and CB40 in the hydration process at early ages, and then more hydration products are formed at later ages. On the shrinkage case, 60 microstrains peaks is reached in autogenous shrinkage and multiple cracking is found on the drying case,

By also gathering conclusion from the preliminary stage, it was proven T3 mixing shall be the mixing procedure and CB40 at high shear conditions is selected as reference for further sections.

6 THE EFFECT OF FLY ASH INCLUSION ON THE CEMENT BENTONITE SYSTEM

6.1 INTRODUCTION

This chapter seeks for improving the cement-bentonite grout behavior. CB40 is chosen as the reference grout and fly ash was added as partial replacement of Portland cement.

6.2 RESULTS AND DISCUSSION

6.2.1 PROPERTIES OF FRESH CEMENTITOUS GROUT

6.2.1.1 VISCOMETRY

Figure 6.1 and Figure 6.2 show the rheological behavior of fly ash additions as cement partial replacement by the following contents, 10%, 30% and 50%. Figures consist of an entire rheogram on the left side and the right one presents a closer view for better understanding. First, 10% fly ash produces changes in rheology at shear rates higher 200 s^{-1}. Fly Ash cement-bentonite thyxotropy is still dominant, but hysteresis loops is slightly diminished (refer to Figure 6.1). Second, by using a 30% replacement, rheological behavior at shear rate less than 200 s^{-1} is less viscous and increasing and decreasing curves get closer. Third, 50% replacement gets the grout more fluid and shear stresses are considerable lesser than reference (see Figure 6.2).

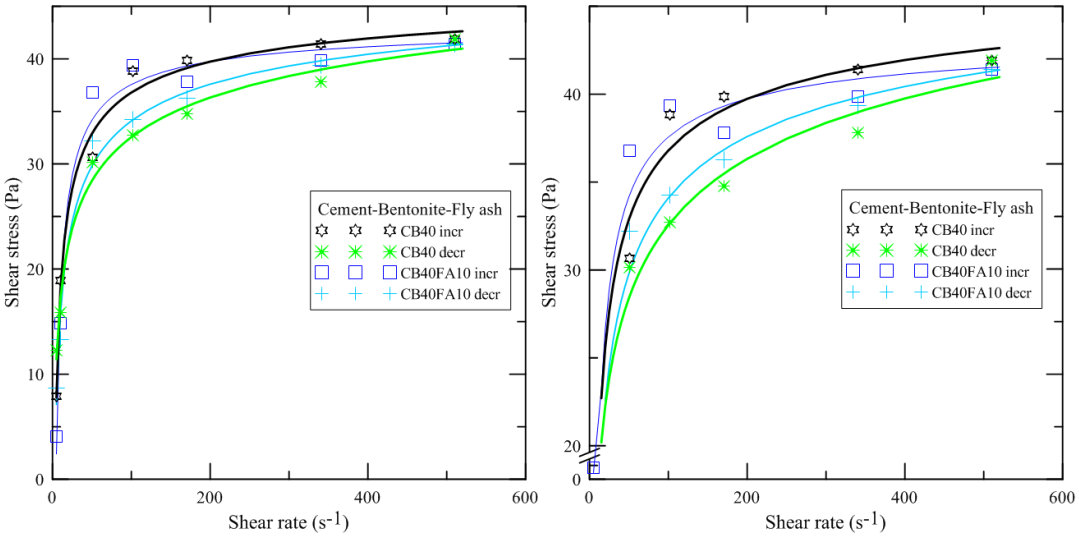

Figure 6.1 Rheogram of CB40 and CB40FA10. Left, entire curves and right, a close-up view

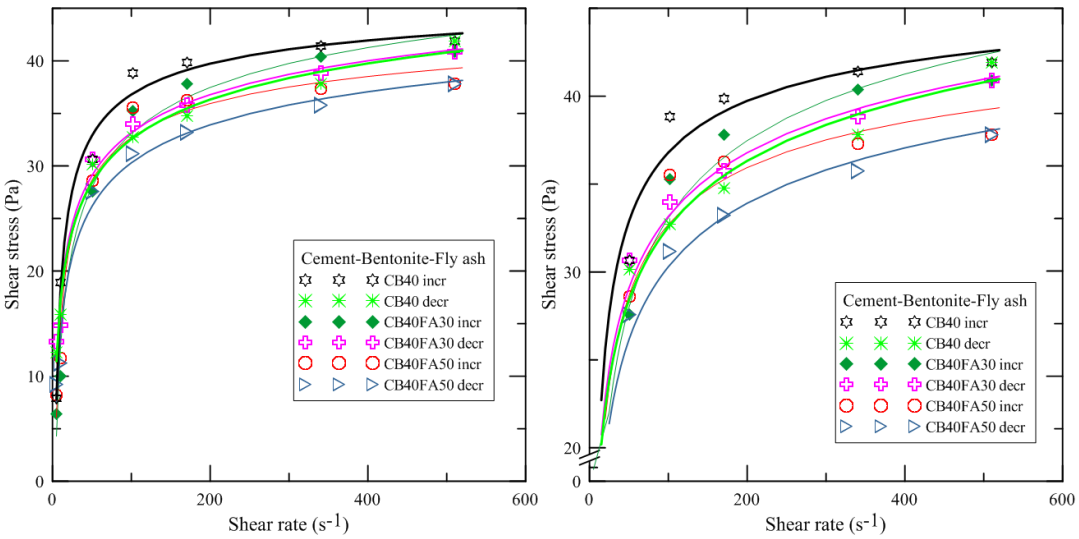

Figure 6.2 Rheogram of CB40 and CB40FA30 CB40FA50. Left, entire curves and right, a close-up view

There are great differences between yield stresses obtained by the numerical approach (MULLINEUX, 2008) and shear stresses at 5,1 s^{-1} (3 rpm). By comparison, the former seem not to correlate physically to experimental points at low shear rates. Because of this fact, apparent viscosity, yo app, is obtained once again (BESQ *et al.*, 2003). The latter seem to fit better, see Table 6.1.

Table 6.1 Herschel-Bulkley parameters obtained by the Mullineux approach, yo, and Apparent yield stress, yo app, by Besq. Cement-bentonite-fly ash behavior.

Grout	CB40		CB40FA10		CB40FA30		CB40FA50	
Shear rate	Incr	Decr	Incr	Decr	Incr	Decr	Incr	Decr
n	-0.42	-0.14	-0.64	-0.30	-0.22	-0.17	-0.33	-0.20
y_0	48.56	74.21	43.69	52.90	64.71	65.78	48.56	58.23
k	-79.55	-78.29	-115.08	-73.82	-85.53	-71.37	-72.14	-70.16
$y_{0\ app}$	9.97	11.14	4.29	7.15	4.69	11.14	6.61	7.15
Experimental Shear stress at 3 rpm	35.77	33.22	35.77	33.22	33.22	32.82	25.04	23.55

6.2.1.2 MUD BALANCE TEST

Apparent densities were determined for the CB40, CB40FA10 and CB40FA30 grouts and are presented in Table 6.4.

Table 6.2 Apparent densities through mud balance use

Grout	Apparent density (g/cm^3)
CB40	1.22
CB40FA10	1.22
CB40FA30	1.22

Figure 6.3 CBFA grout sample before test

Even though fly ash replaced partially Portland cement at different proportions, variations could not be observed in mud balance beam during visual readings.

6.2.2 HYDRATION KINETICS

6.2.2.1 ULTRASONIC CEMENT ANALIZER

As can be seen in Table 4.10 and Table 6.3, the fly ash inclusion delays hydration. By comparing percolation thresholds, they are displaced to the right. After this point, all grouts have higher wave velocities which are consistent with the structure formation due to hydration products. If CB40 set point is considered as a reference, CB40FA10 and CB40FA30 have set point displacements of 1h38’ and 2h4’ later, respectively.

Table 6.3 UCA for cement-bentonite-fly ash grouts

Grout	Set point	Minimum wave velocity (m/s)
CB40	5h59'30'	1485.38
CB40FA10	7h37'30"	1470.76
CB40FA30	8h03'30"	1476.74

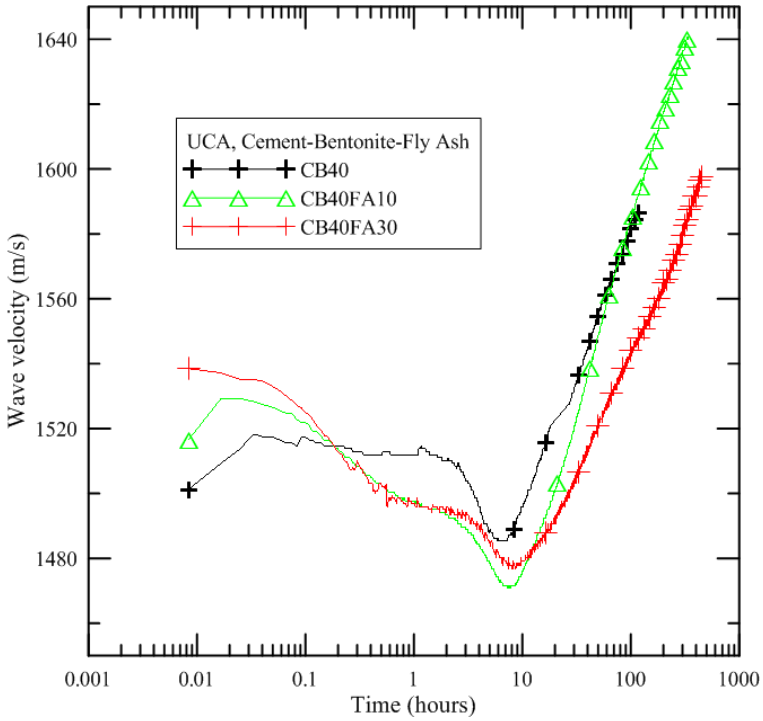

Figure 6.4 UCA fly ash inclusions

6.2.2.2 ISOTHERMAL CALORIMETRY

Although the fly ash inclusions did not cause significant modifications as the ones observed by bentonite in previous chapter, particular modifications across the curves are observed and are detailed below.

The dormant period, the acceleration slope, the second and third peak have slight changes among the grouts. First, the dormant period is very similar in CB40 and 10% and 30% partial replacements but it might be shorter for 50% substitution because of more availability of water for the rest of cement and a subsequent quicker hydration. Second, the acceleration slope, before second hydration peak, is slightly slower for CB40FA50. The dilution effect of the fly ash addition starts to be evident. Similar behavior occurs at a second peak. In addition, the third peak is slightly higher for CB40FA30. It might occur because fly ash promotes the ettringite formation by offering nucleation sites (BAERT, et al., 2008). CB40FA10 shows more similar behavior to the reference grout since its amount of fly ash inclusion is not high enough to produce higher hydration changes in the heat release evolution.

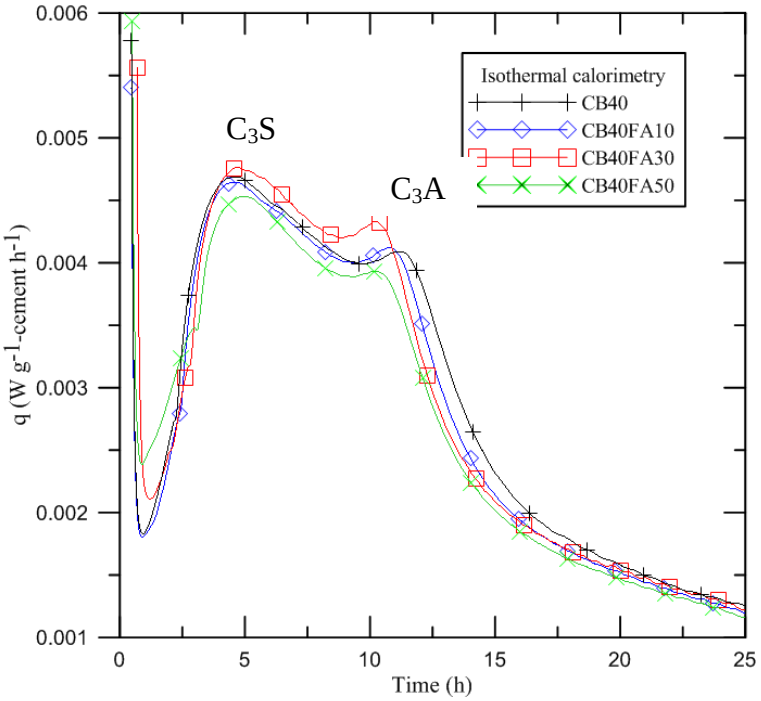

Figure 6.5 Rate of heat development of grouts with fly ash inclusions

Similarly to the first 25-hour hydration heat shown in Figure 6.5, cumulative heat is presented in Figure 6.6. Heat released by CB40 and 10% partial replacement is very similar. CB40FA10 has more cumulative heat than reference since hydration reactions occur with calcium hydroxide forming C-S-H after early ages. Since fly ash offers more nucleation sites and more available water for hydration, CB40FA30 and CB40FA50 produce higher heat released in the long term (BAERT *et al*., 2008). The fact the 50% cement partial replacement grout possesses lesser hydration heat than CB40FA30 is related to its less amount of cement.

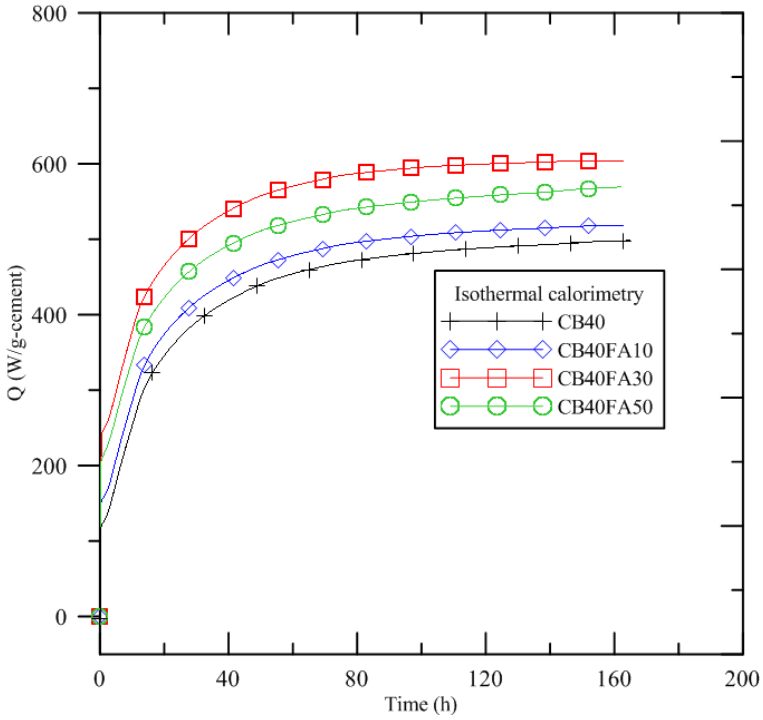

Figure 6.6 Cumulative heat of grouts with fly inclusions

6.2.2.3 THERMO-GRAVIMETRICAL ANALYSIS

Samples were prepared as done in previous chapter and test ages correspond to 24 hours, 7 and 28 days. Thermogravimetry (TG) and derivative thermogravimetry (DTG) were used for analysis. TG results are shown in Figure 6.7. On the left column, curves show the free water due to the high water/cement ratios in all grouts. On the right side it was removed for better comparison of the mass losses at higher temperatures. Likewise, DTG analyses are plotted in Figure 6.8, Figure 6.9 and Figure 6.10.

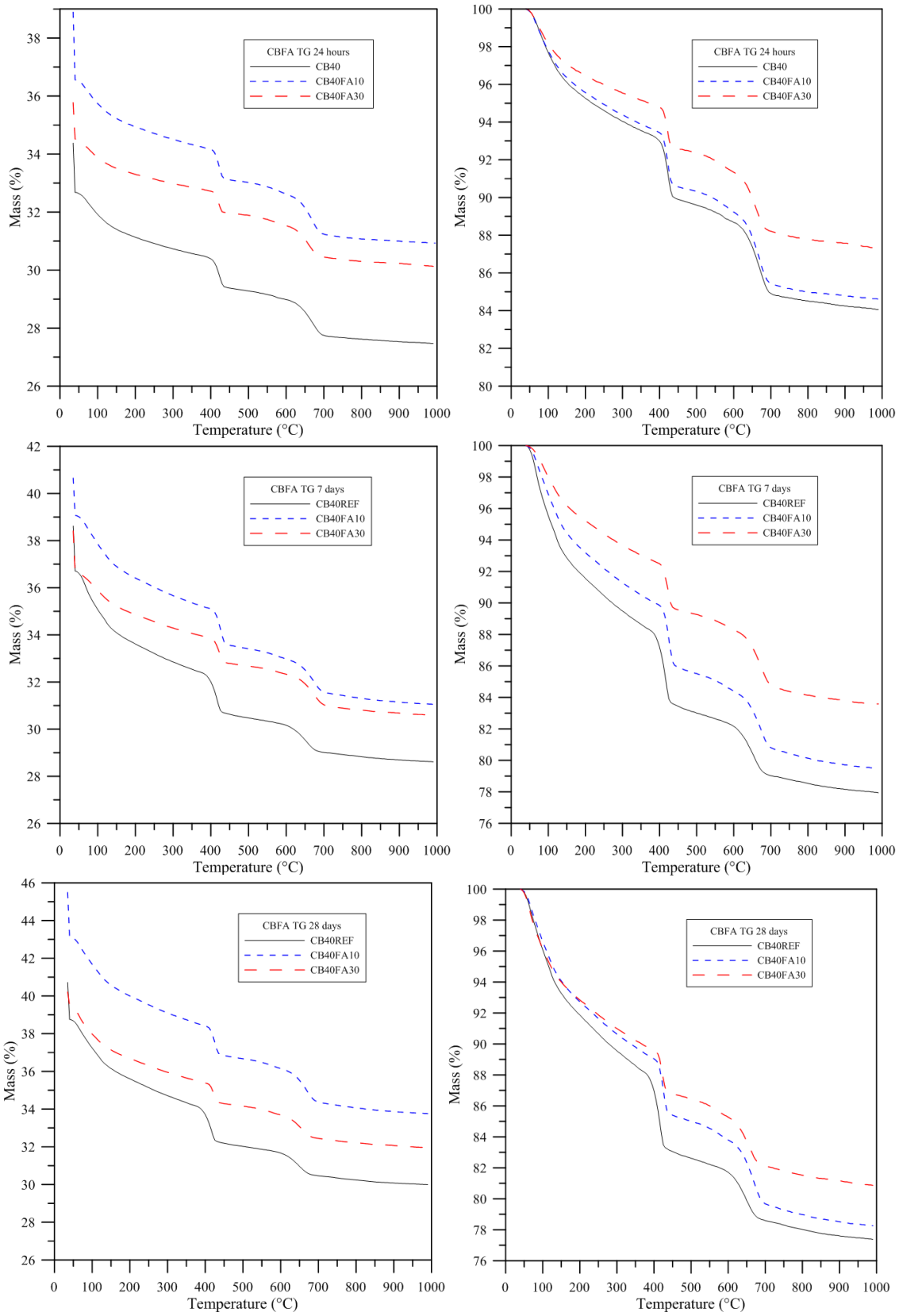

Figure 6.7 TG 24 hours, 7 and 28 days of cement-bentonite-fly ash grouts

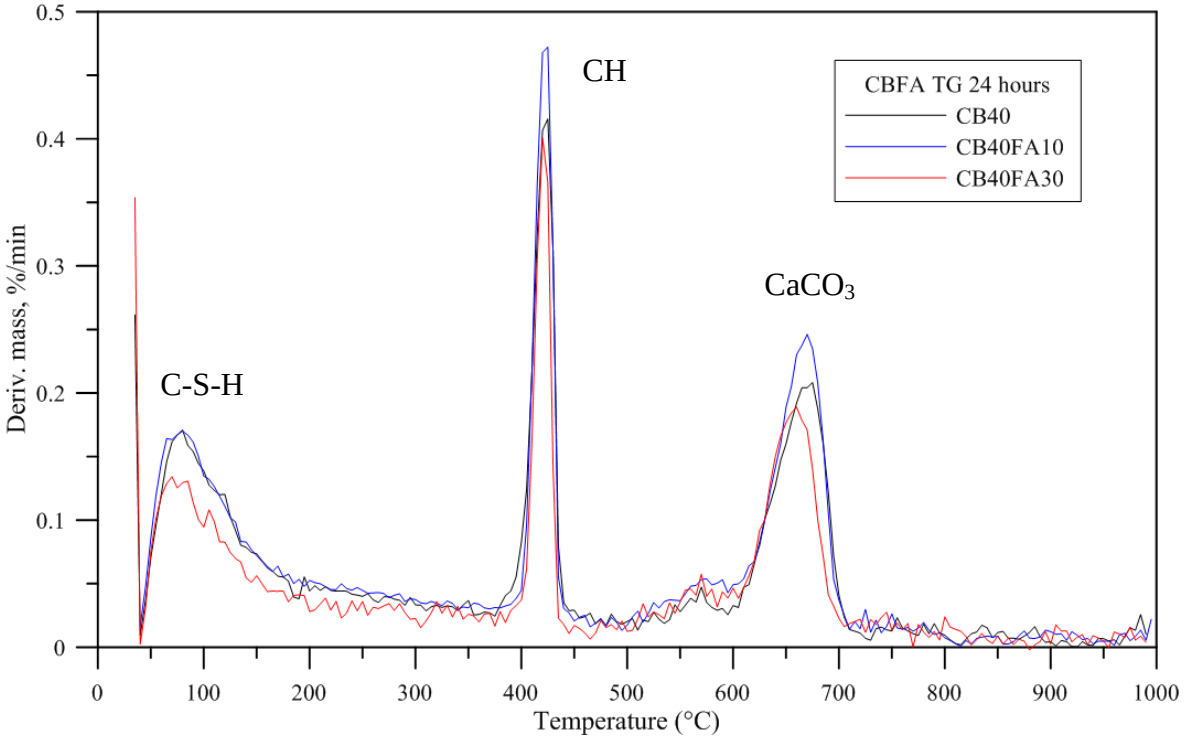

Figure 6.8 DTG 24 hours of cement-bentonite-fly ash grouts

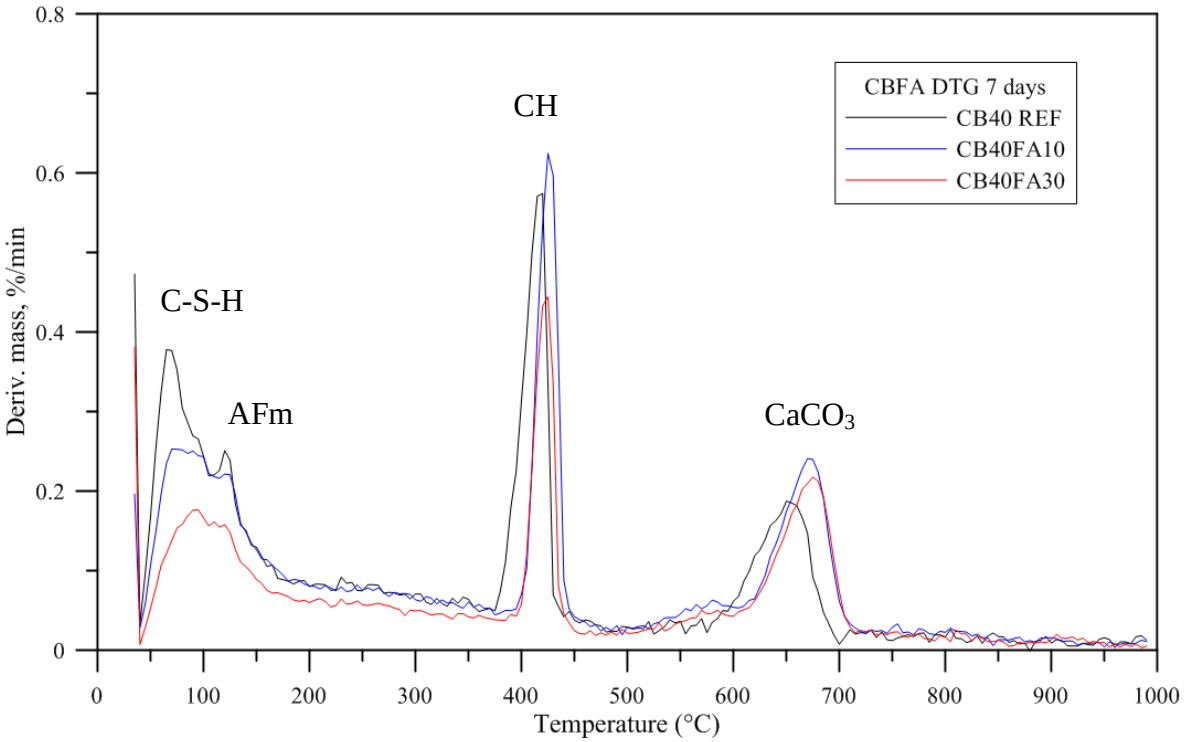

Figure 6.9 DTG 7 days of cement-bentonite-fly ash grouts

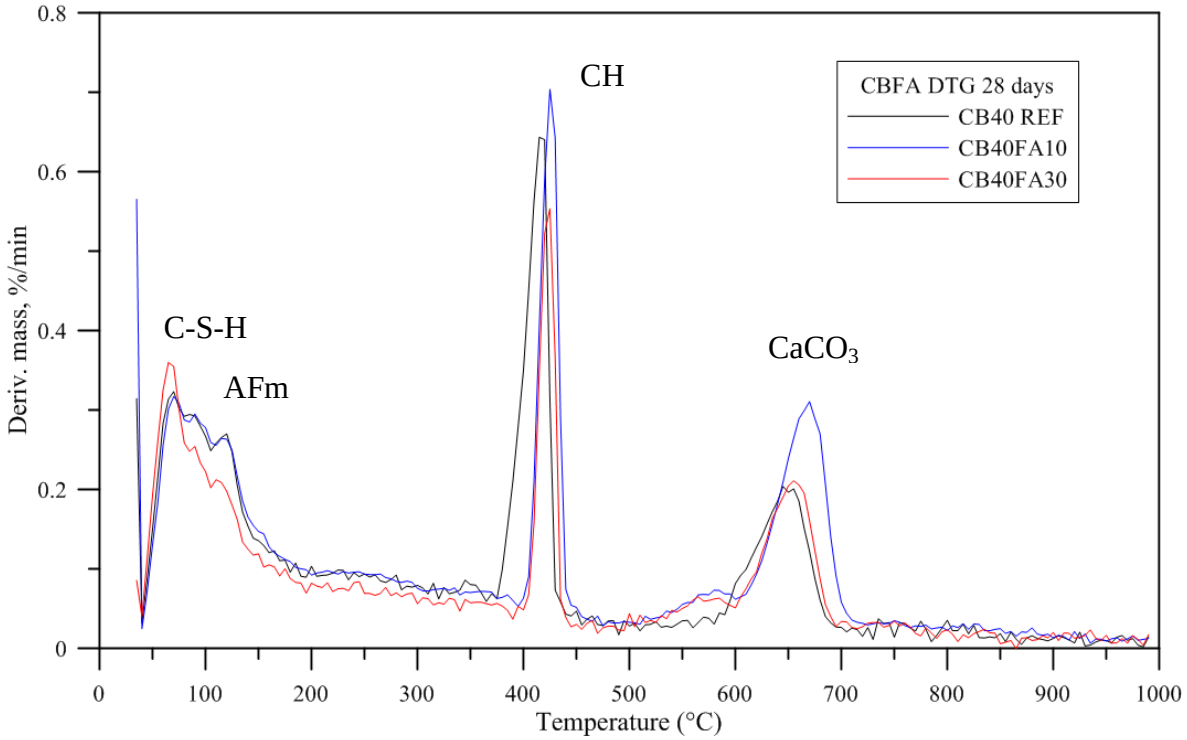

Figure 6.10 DTG 28 days of of cement-bentonite-fly ash grouts

Calcined cement mass basis was used for comparing the hydration products (DWECK *et al.*, 2009). Therefore, histograms in Figure 6.11 were used for analysis of the hydration products.

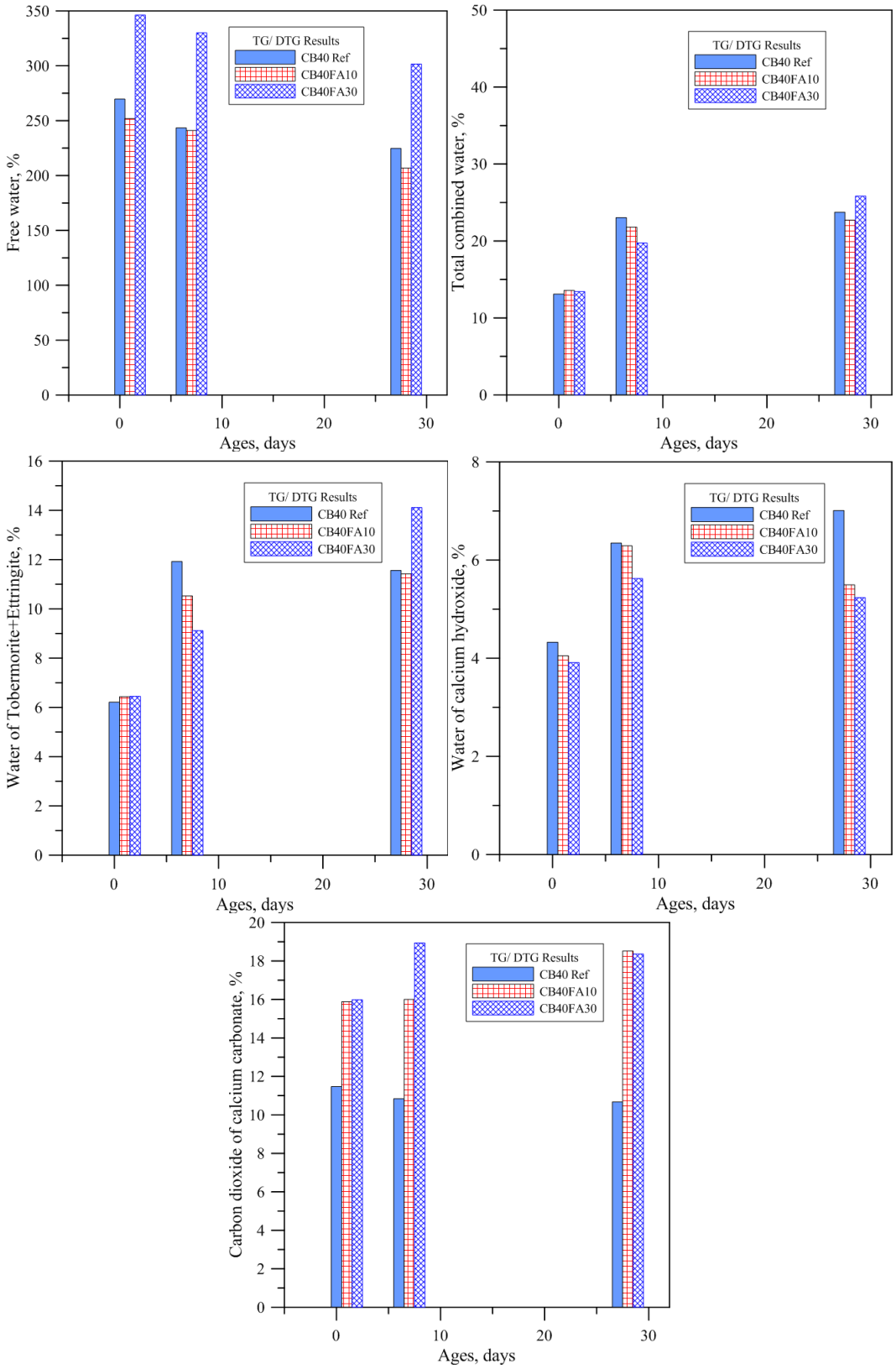

Figure 6.11 Weight losses on calcined cement mass basis at 1, 7 and 28 days of fly-ash-added grouts

Free water diminishes across time in all grouts and the 30% cement partial replacement grout shows a higher loss. Less free water diminishes when the time passes because hydration consumes available water continuously. In case of CB40FA30, the hydration is delayed and more available water is present, especially at 1 day age. Nevertheless the trend to diminish is also consistent with the hydration evolution.

At the same time, combined water increases along time and the effect of fly ash is evident. At 1 day the total combined water is not so different in all grouts since the water consumption is dependent on cement-water reactions only. At 28 days, the 30% fly ash grout starts consuming more water because of the fly-ash- calcium-hydroxide reactions.

The fly ash effect is clearly noticed in the tobermorite+ettringite bars and the calcium hydroxide ones as well. At 1 and 7 days, fly ash presence is negligible in the tobermorite production as show in Figure 6.11, but it is observed at later ages by reacting with calcium hydroxide. Besides that it offers nucleation sites for producing hydration products. In the end, calcium hydroxide falls for both fly-ash-added grouts as presented in the histograms.

6.2.3 MECHANICAL PROPERTIES

6.2.3.1 COMPRESSION BEHAVIOR

Compression tests were done at 28 and 92 days after batching. Table 6.4, Table 6.5 gather results along average characteristics and standard deviations (SD) for 28-day age. Likewise stress-strain behavior can be found in Figure 6.12. Analysis of results was done by plotting comparative curves in Figure 6.13, Figure 6.14 and Figure 6.15. Similar figures and tables were elaborated for 92-day age.

Table 6.4 Compression behavior at 28 days, Fly ash additions

Grout	Fmax (kN)	σ max (MPa)	ε rupture (m/m)	E (MPa)
CB40FA101	1.28	0.65	0.004645	370
CB40FA102	1.43	0.73	0.005621	369
CB40FA103	1.31	0.67	0.004126	383
CB40FA108	1.56	0.79	0.006400	486
Average	1.39	0.71	0.005198	402
SD	0.13	0.07	0.001013	56
CB40FA301	1.14	0.58	0.005346	492
CB40FA302	0.75	0.38	0.008466	184
CB40FA303	0.93	0.48	0.005574	246
CB40FA3010	1.05	0.53	0.007521	284
Average	0.97	0.49	0.006727	301
SD	0.17	0.09	0.001515	134
CB40FA502	0.67	0.34	0.007824	196
CB40FA504	0.61	0.31	0.008319	112
CB40FA505	0.56	0.29	0.004109	171
CB40FA507	0.57	0.29	0.008081	137
CB40FA509	0.67	0.34	0.008194	158
Average	0.62	0.31	0.007305	155
SD	0.05	0.03	0.001796	32

Table 6.5 Summary of compression behavior at 28 days, reference and fly-ash-added grouts

Grout		Fmax (kN)	σ max (MPa)	ε rupture (m/m)	E (MPa)
CB40	Average	1.37	0.70	0.008613	360
	SD	0.05	0.02	0.001545	49
CB40FA10	Average	1.39	0.71	0.005198	402
	SD	0.13	0.07	0.001013	56
CB40FA30	Average	0.97	0.49	0.006727	301
	SD	0.17	0.09	0.001515	134
CB40FA50	Average	0.62	0.31	0.007305	155
	SD	0.05	0.03	0.001796	32

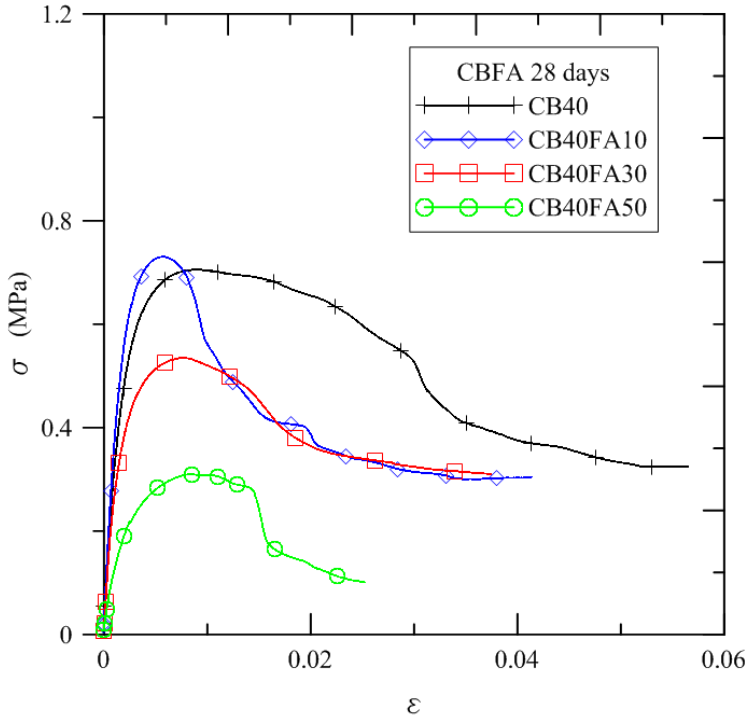

Figure 6.12 Compression behavior of CBFAx at 28 days

CB40FA10 presented 1.9% higher strength and the other grouts had less strength than CB40 because of retarding effect of fly ash. CB40FA30 and CB40FA50 had 70.7 % and 45.1% of CB40 strength. These results and the comparisons are presented in Figure 6.13 where CB40 is used as reference. In the same way modulus of elasticity of CB40FA10 is 11,6higher than reference grout but the others stand for 83,7% and 43% of the CB40 case.

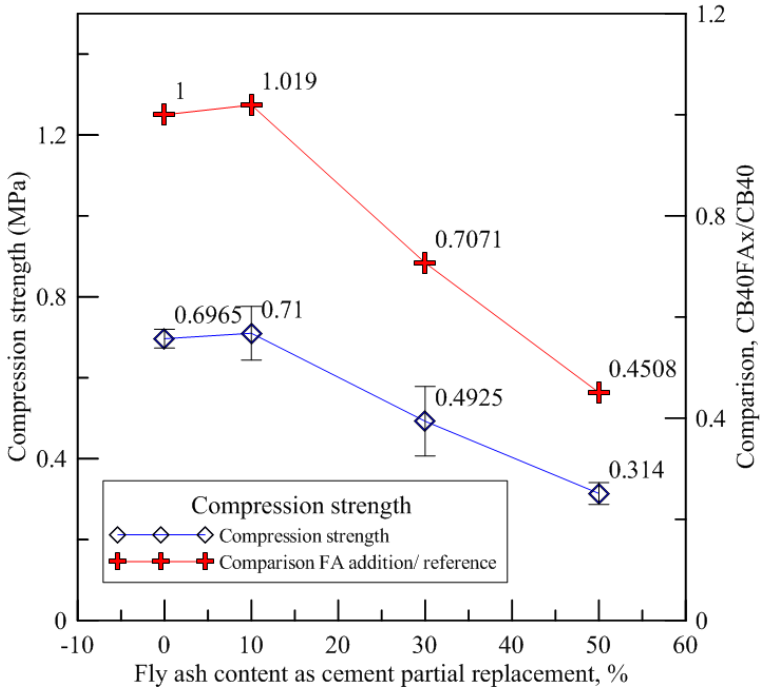

Figure 6.13 Comparison of compression strength of fly ash-added grouts at 28 days

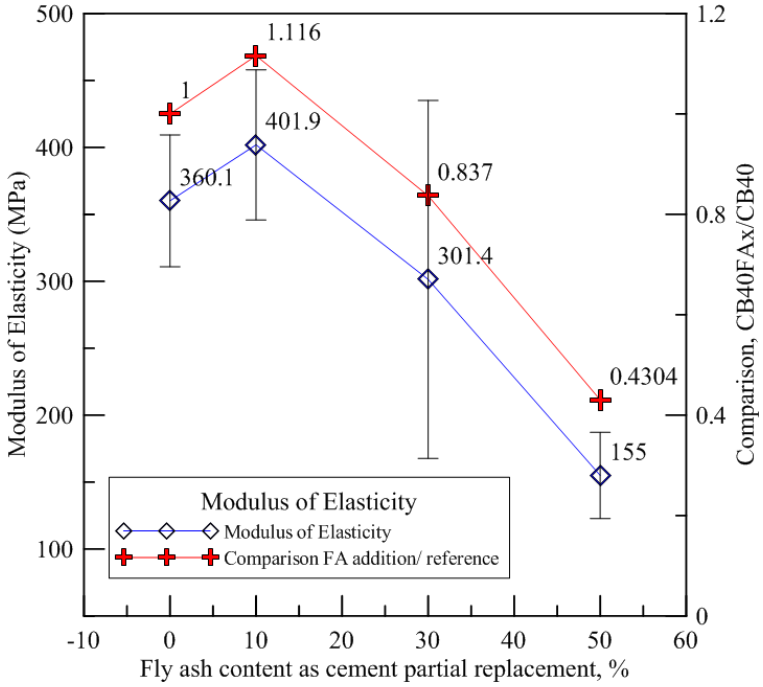

Figure 6.14 Comparison of modulus of elasticity of fly ash-added grouts at 28 days

In case of strain at rupture, grouts with fly ash additions presented more brittle behavior as experimental points show in Figure 6.15. The 10% partial replacement case presents the lowest strain which stands for 60.35% of the CB40 grout. The 30% and 50% case represent the 78.1% and 84.8% of reference, respectively.

Specimens after being tested are shown in Figure 6.16.

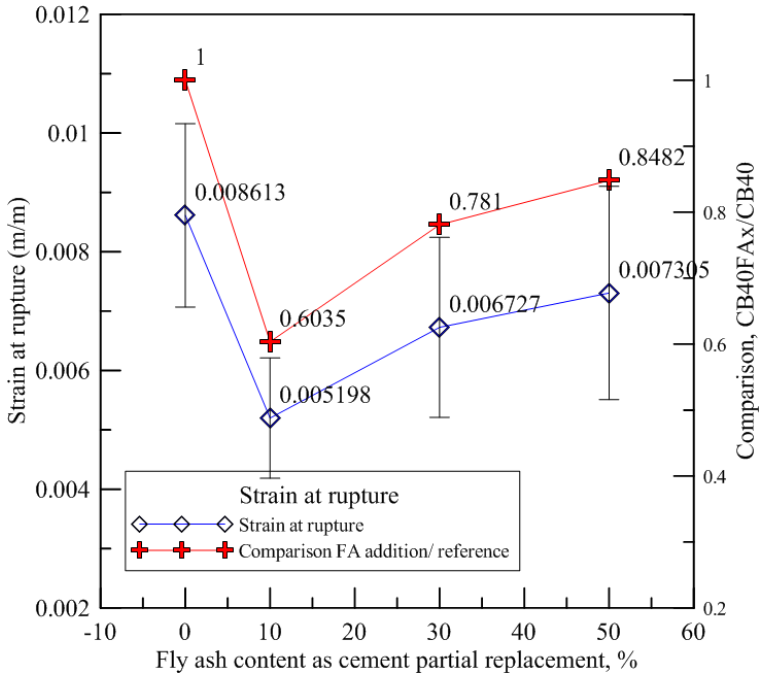

Figure 6.15 Comparison of strain at rupture of fly ash-added grouts at 28 days

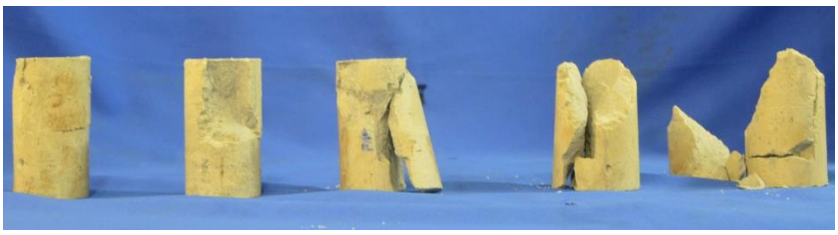

CB40FA10

CB40FA30

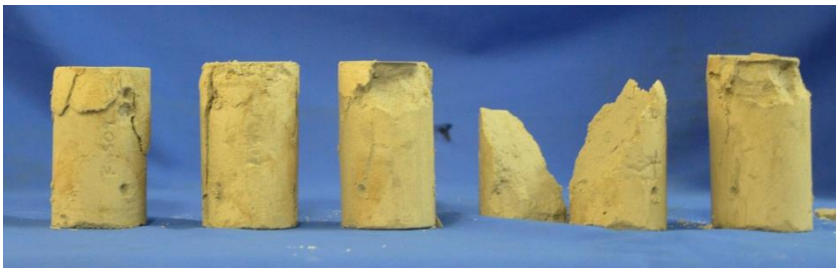

CB40FA50

Figure 6.16 Mechanical compression of CB40FAx specimens at 28 days.

Consequently, grouts were studied at 92 days as well. Figure 6.17 presents the stress-strain behavior and Table 6.6 gathers the experimental parameters which characterize every grout. Comparisons among them will be done in Table 6.6, Figure 6.18, Figure 6.19 and Figure 6.20. Figure 6.17 clearly shows a more brittle behavior and higher strengths than 28-day age.

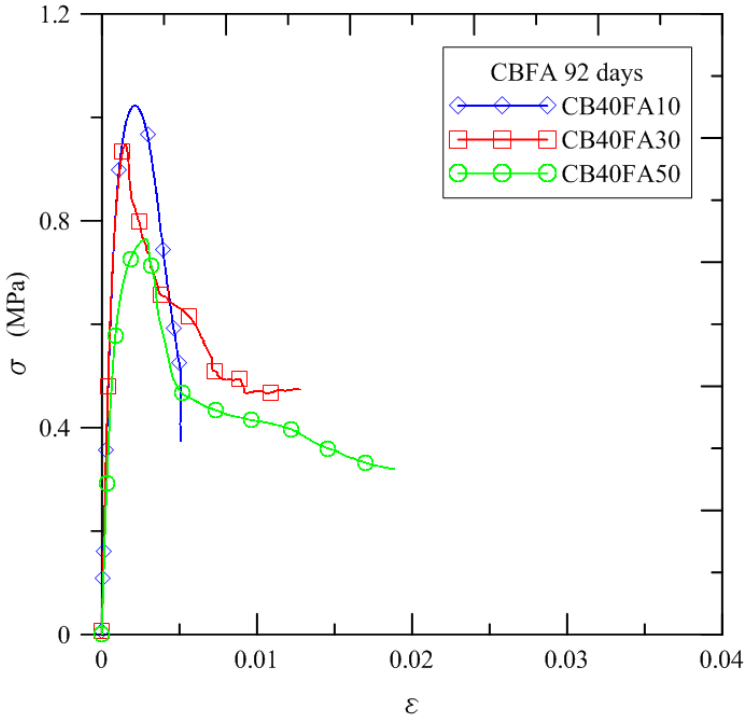

Figure 6.17 Mechanical compression of CB40FAx specimens at 92 days.

Table 6.6 Compression behavior at 92 days, Fly ash additions.

Grout	Fmax (kN)	σ max (MPa)	ε rupture (m/m)	E (MPa)
CB40FA104	1.91	0.97	0.002303	1207
CB40FA105	2.01	1.02	0.002095	1151
CB40FA107	2.27	1.16	0.002205	1341
Average	2.06	1.05	0.002201	1233
SD	0.19	0.10	0.000104	98
CB40FA303	1.57	0.80	0.001141	1144
CB40FA304	1.86	0.95	0.001533	1283
CB40FA305	1.42	0.72	0.001222	1078
Average	1.62	0.82	0.001299	1168
SD	0.22	0.11	0.000207	105
CB40FA506	1.56	0.79	0.003442	761
CB40FA508	1.38	0.70	0.003110	810
CB40FA5011	1.50	0.76	0.002806	888
Average	1.48	0.75	0.003119	820
SD	0.09	0.04	0.000318	64

Strengths achieved 1.05, 0.82 and 0.75 MPa for CB40FA10, CB40FA30 and CB40FA50, respectively. They stand for 48% 67.3% and 75.4% increases based on their 28-day strength, respectively. See Figure 6.18.

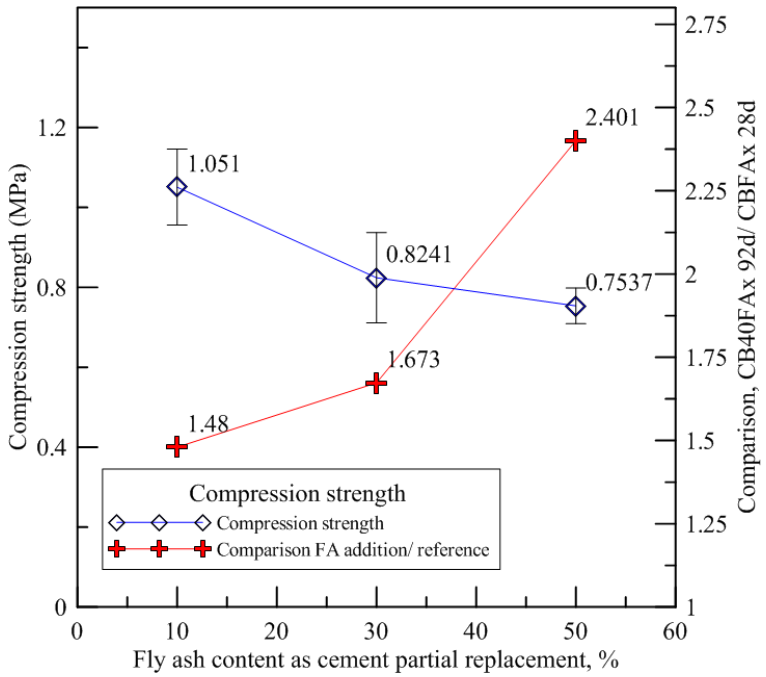

Figure 6.18 Comparison of compression strength of fly ash-added grouts at 92 days

Modulus of elasticity increased several times which indicates the hydration products by fly ash reaction. Accordingly, it increased 3.07, 3.88 and 5.29 times for CB40FA10, CB40FA30 AND CB40FA50. In the same way, because of the stiffening of all grouts, rupture train correlates with the former results by achieving 42.3%, 19.3% and 42.7% of previous strains at 28 days. Figure 6.21 show pictures of the specimens after being tested.

Therefore, fly ash improves mechanical properties by reacting with calcium hydroxide and forming, as a consequence, C-S-H. Based on results it was chosen the 10% fly ash addition grout as the grout with better performance than their counterparts. CB40FA10 presents the best behavior at both ages. At 28 days, it has 0.71 MPa of compressive strength, a 401.9 MPa modulus of elasticity, and 5198 microstrains of strain at rupture. At 92 days, it has 1.05 MPa of compressive strength, a 1233 MPa modulus of elasticity, and 2201 microstrains of strain at rupture. The latter correspond to 1.48 , 3.067 and 0.42 times the corresponding values at 28 days. All this results emphasize the pozzolanic properties of fly ash again.

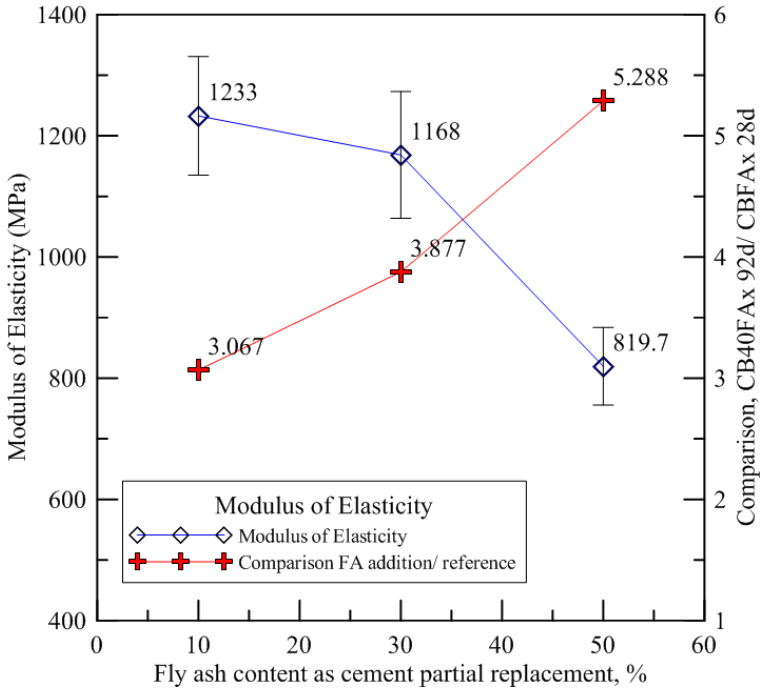

Figure 6.19 Comparison of modulus of elasticity of fly ash-added grouts at 92 days

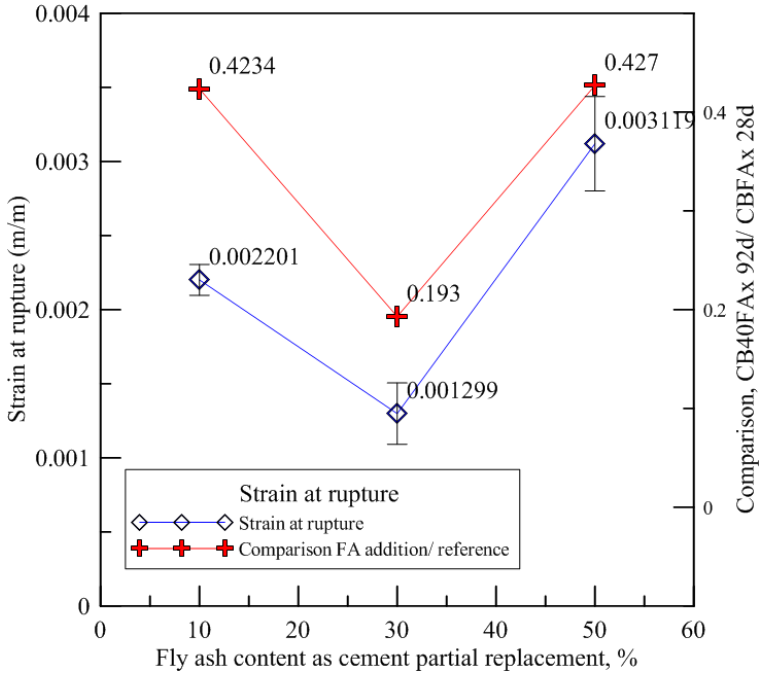

Figure 6.20 Comparison of strain at rupture of fly ash-added grouts at 92 days

Figure 6.21 Mechanical compression of CB40FAx specimens at 92 days

6.2.4 DIMENSIONAL CHANGES

6.2.4.1 Shrinkage

Autogenous shrinkage of CB40, CB40FA10 and CB40FA30 is presented in Figure 6.22. The shrinkage shown was done in quase-adiabatic conditions, The starting point rounds up 12 hours after the cement+water mix. It was tried to start measuring before based on UCA results but axial bolts could not be releasing without damaging the grout. In the graph positive strains stand for shrinkage. Fly ash increase the shrinkage proportionally to its content 158 and 221 microstrains for CB40FA10 and CB40FA30, respectively.

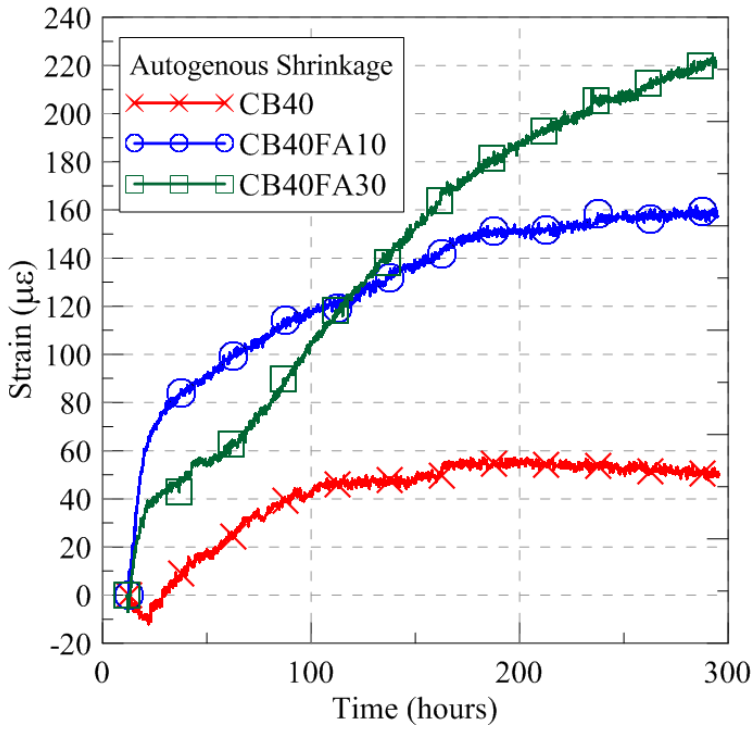

Figure 6.22 Autogenous Shrinkage of fly ash addtions

On the drying case, multiple cracking and non-uniform water loss occurs. Microcraks propagate forming macrocracks. Therefore, strains at 48 hours are considered representative since later ages are influenced by cracking and considerable bending of the specimen. They are 135, 394 and 7334 microstrains for 10%, 30% and 50% partial replacements of cement by fly ash. Water loss and cracking is highly significant in the last case, 50%. Figure 6.23 and Figure 6.24 show the behavior.

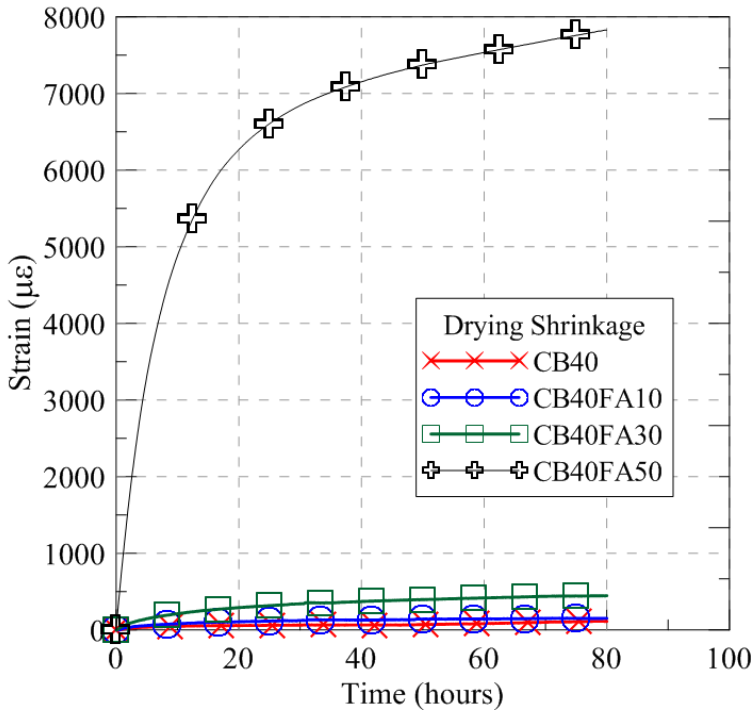

Figure 6.23 Drying shrinkage of CB40, and 10%, 30% and 50% FA contents

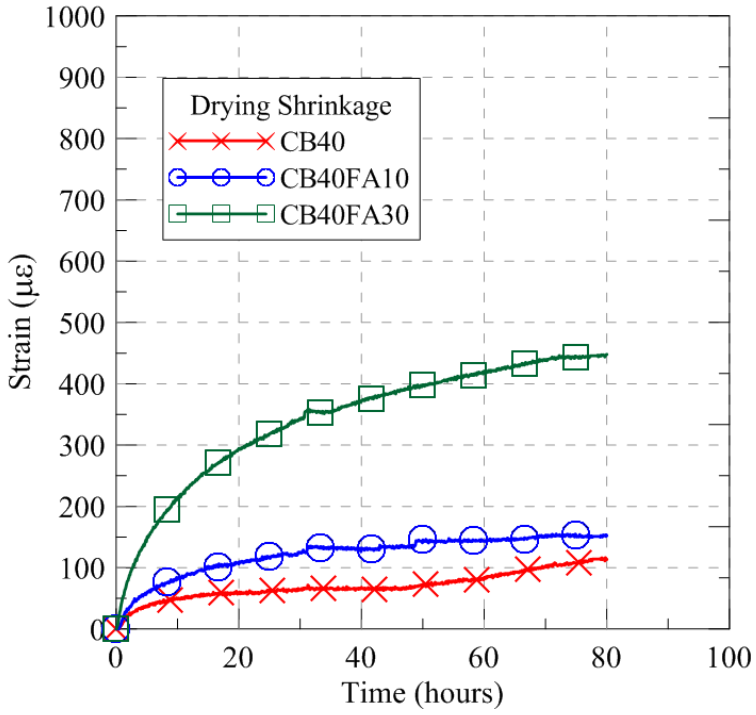

Figure 6.24 Drying shrinkage of CB40, and 10% and 30% FA contents

6.3 CONCLUSIONS

It is concluded that

- Fly ash can reduce hysteresis loops of grouts by augmenting the partial substitutions. By increasing fly ash, a reduction in viscosity and shear stresses is found at shear rates higher than 100 s^{-1}. Higher additions improve the rheology at shear rates less than 100 s^{-1} as well.
- In hydration terms, fly ash produced delaying in percolation threshold. No major changes in heat release at early ages but cumulative heat is higher due its reactions with calcium hydroxide. Thermal analysis reported a reduction in calcium hydroxide at later ages as well.
- Mechanical tests proved fly ash produces more brittle grouts at 28 days and the improvement in strength is not significant yet. However at 92 days the strength gain was significant.
- Fly ash proved to increase autogenous and drying shrinkage. Cracking and bending of the specimens occurs and influence measurements after 48 hours of the test initial time.
- Therefore due to mechanical strength, low autogenous shrinkage, an improving in rheology, CB40FA10 is chosen to be used as reference for the accelerator addition.

7 THE EFFECT OF AN ACCELERATOR ADMIXTURE ON THE CEMENT BENTONITE SYSTEM

7.1 INTRODUCTION

Because of conclusions, in section 6.3, CB40FA10 was selected as reference grout.

7.2 RESULTS AND DISCUSSION

7.2.1 HYDRATION KINETICS

7.2.1.1 ULTRASONIC CEMENT ANALYZER

Because of the quick stiffening experienced during tests, either the specimens could not fit the precise height required for the ultrasound wave get through the grout or the specimen lost contact with the superior surface of the steel chamber. So hydration evolution records stopped continuously. Since all tests were done under normal pressure in this study, no additional pressure was imposed in tests.

7.2.1.2 ISOTHERMAL CALORIMETRY

Because of the fact mixing of the cement-based grout and the accelerator was done outside the calorimeter, the first peak which occurs immediately after mixing could not be registered completely. As it is observed in Figure 7.1, the hydration heat release was modified significantly and will be described in the next paragraphs.

Even though first peak could not be registered completely, its slope indicates a proportional relation between accelerator content and rate of heat. The sodium-silicate-based accelerator reacts immediately after contact with the fresh grout and quick stiffening occurs, immediate sedimentation of the reaction products is observed. So first reactions are accelerated and it can be noticed by the slope changes of first peak. However, it has other effects in the dormancy period and posterior peaks. More heat is produced during the dormancy period by comparison with the reference CB40FA10. It

goes up proportionally to the accelerator content used. Then, the next acceleration slope is decreased which means accelerator delays hydration in the 2,5-5 hour period. Not only hydration is delayed but also less C_3S reacts as can be seen in the progressive fall of the second peak in the 5-6,5 hour period. This event is important for mechanical behavior since C_3S hydration defines the C-S-H production and consequently affects the mechanical strength. In addition, third peak is compromised. Therefore the effect of bentonite and fly ash on C_3A hydration is suppressed and this peak disappears almost completely by using 30% of accelerator.

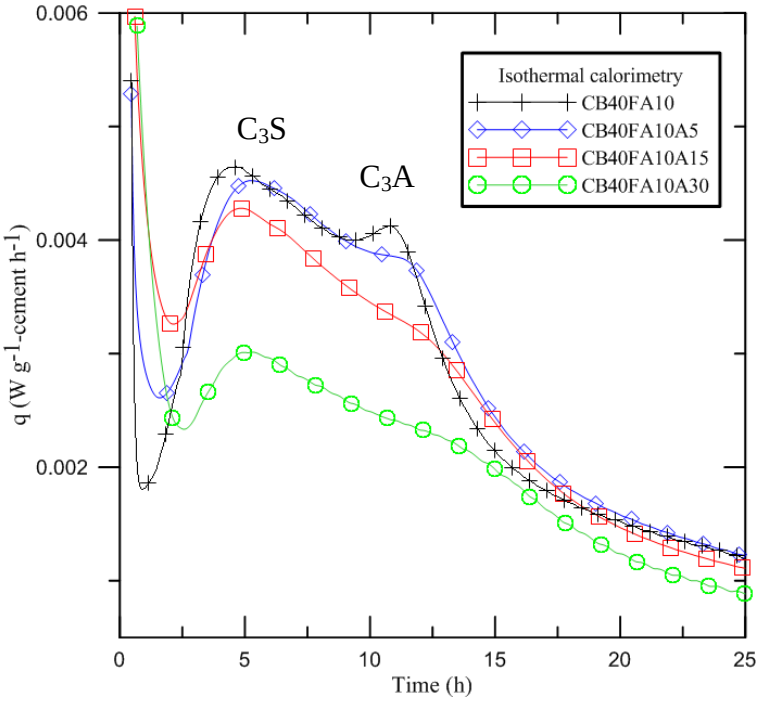

Figure 7.1 Rate of heat development of two-component grout

Cumulative heat along the first 200 hydration hours show less total heat produced for all accelerator contents. By observing Figure 7.2, significant heat decay occurs after the first 20 hours for the FA10A30 since the hydration rate is well diminished. Until approximately 100 hours, the grout with 30% of accelerator still releases consistent with hydration reaction happening. However, after that time the hydration decays continuously.

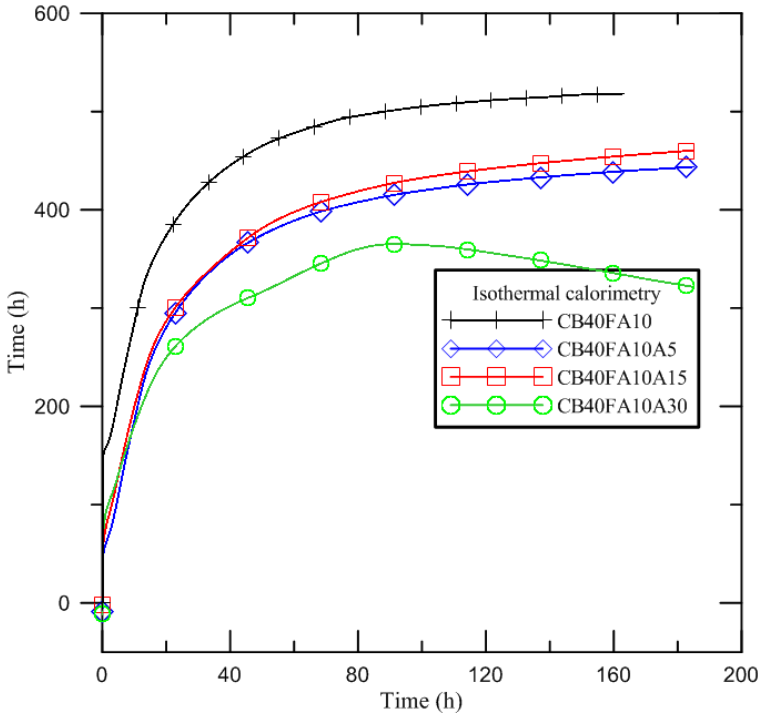

Figure 7.2 Cumulative heat of a two-component grout

7.2.1.3 THERMO-GRAVIMETRICAL ANALYSIS

Similar procedure for preparing samples and delivery were carried out as in previous chapter. Thermogravimetry (TG) and derivative thermogravimetry (DTG) results are presented in Figure 7.3, Figure 7.4, Figure 7.5 and Figure 7.6. They correspond to 1, 24 hour and 48 hours of the CB40FA10 and the CB40FA10A30.. It acquires major interest to understand the products formed at early ages since reviewed references do no mention what really happens after mixing both components of the final grout. On the left column, curves show the free water loss which is considered important due to the high water/cement ratios in all grouts. On the right side it was removed for better comparison of the mass losses of the hydration product at higher temperatures.

The mass losses which correspond to free water, total combined water, tobermorite+ettingite, calcium hydroxide and calcium carbonate are plotted in Figure 7.7. A further analysis is presented after the figures.

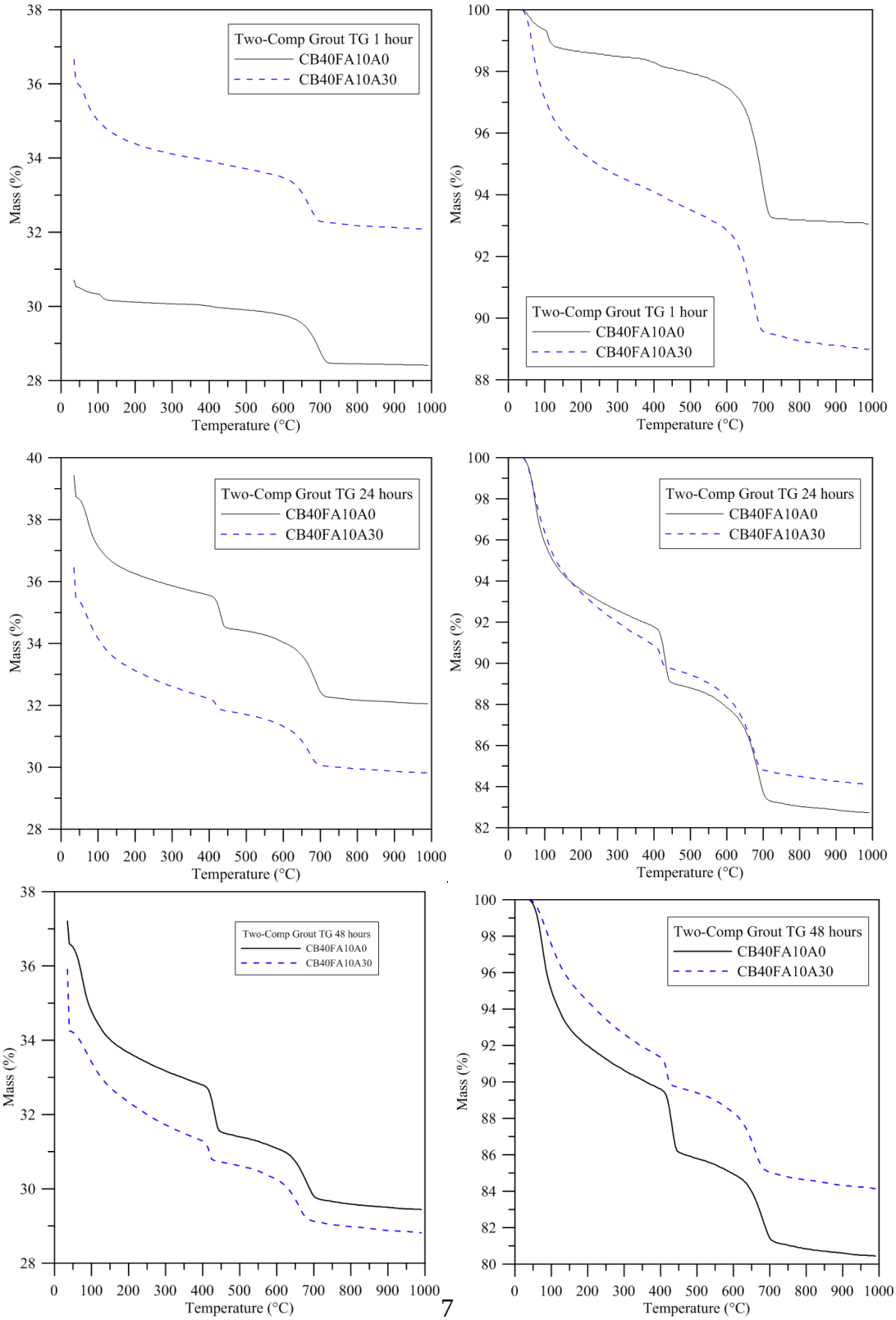

7

Figure 7.3 TG 48 hours of two-component grouts

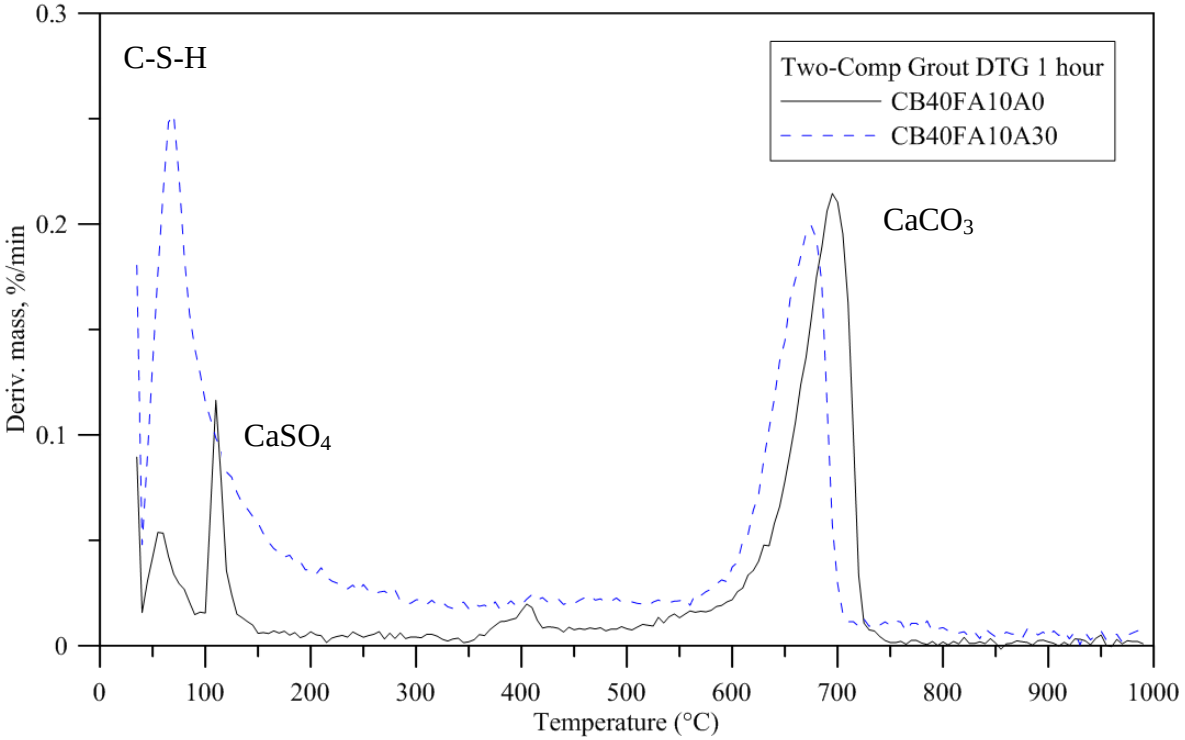

Figure 7.4 DTG 1 hour of two-component grouts

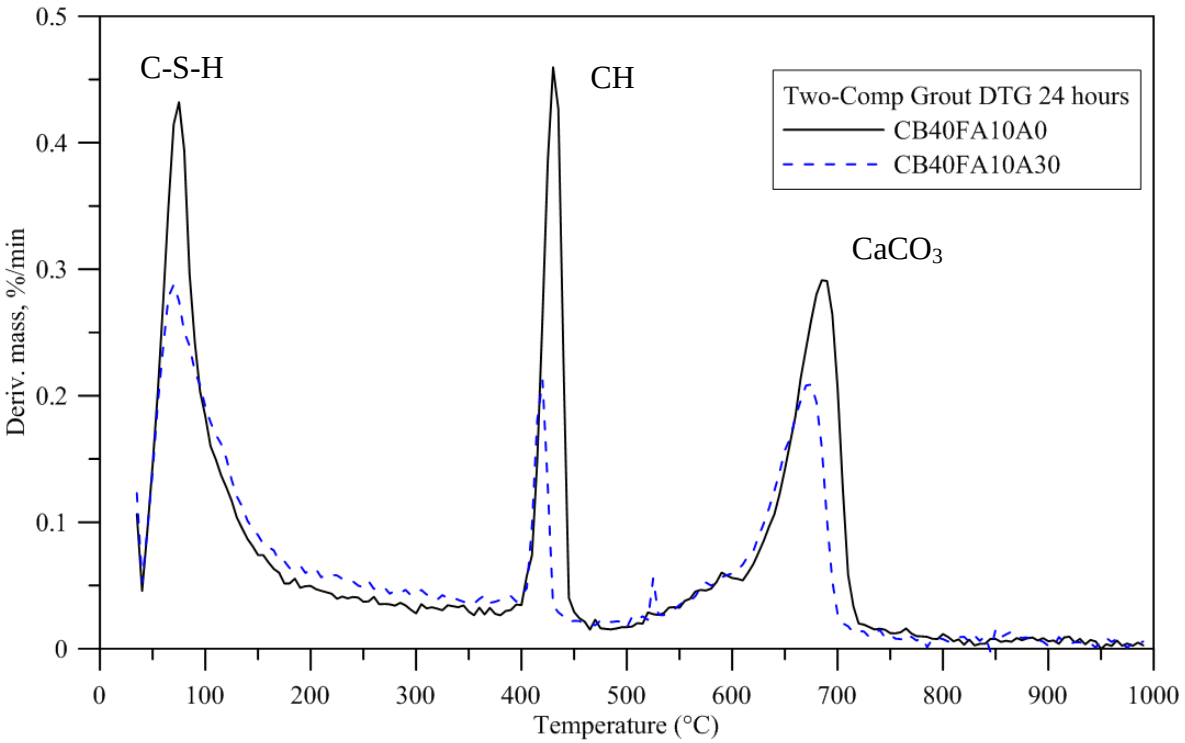

Figure 7.5 DTG 24 hours of two-component grouts

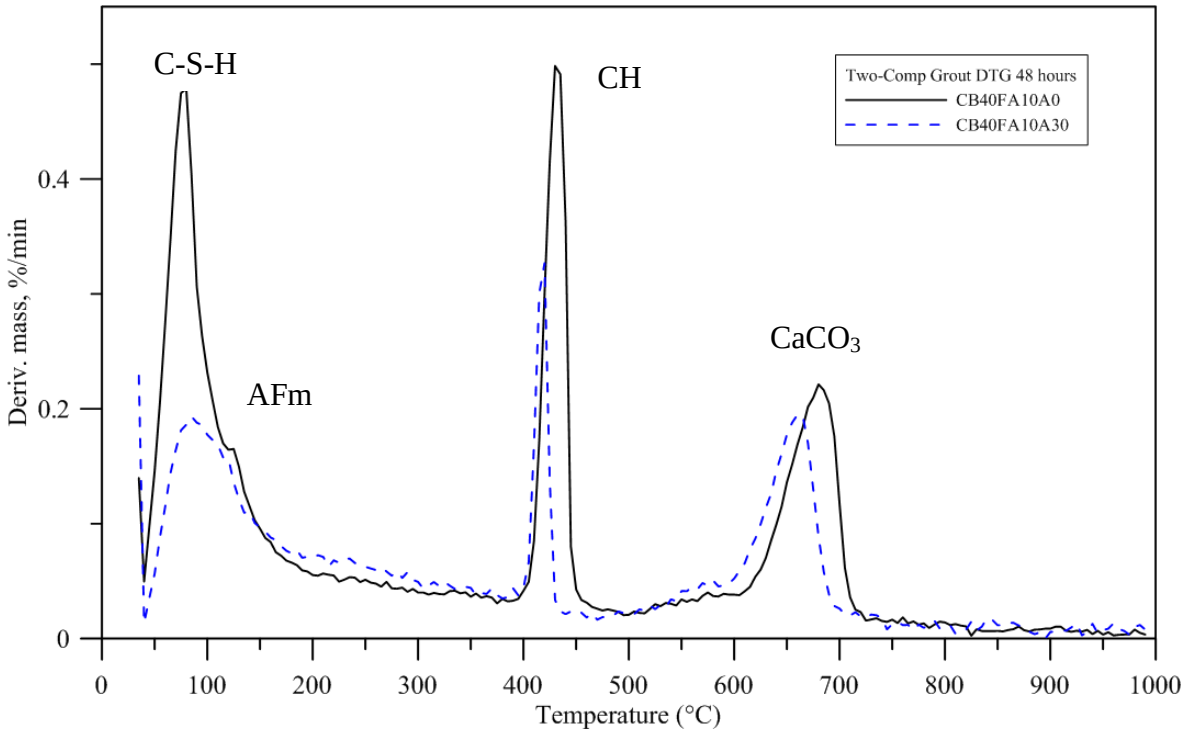

Figure 7.6 DTG 48 hours of of two-component grouts

TG and DTG plots at 1 hour show less calcium hydroxide production than the reference grout. At the same time DTG shows an abrupt hydration products rise between 35° and 200° which might indicate an immediate production of C-S-H and calcium sulphate reaction after components get into contact. A unique peak gathers the hydration products at 1 hour. Although it is still low, the reference grout shows a small peak corresponding to calcium hydroxide production. Calcined cement mass basis was used for comparing the hydration products (DWECK, et al., 2009).

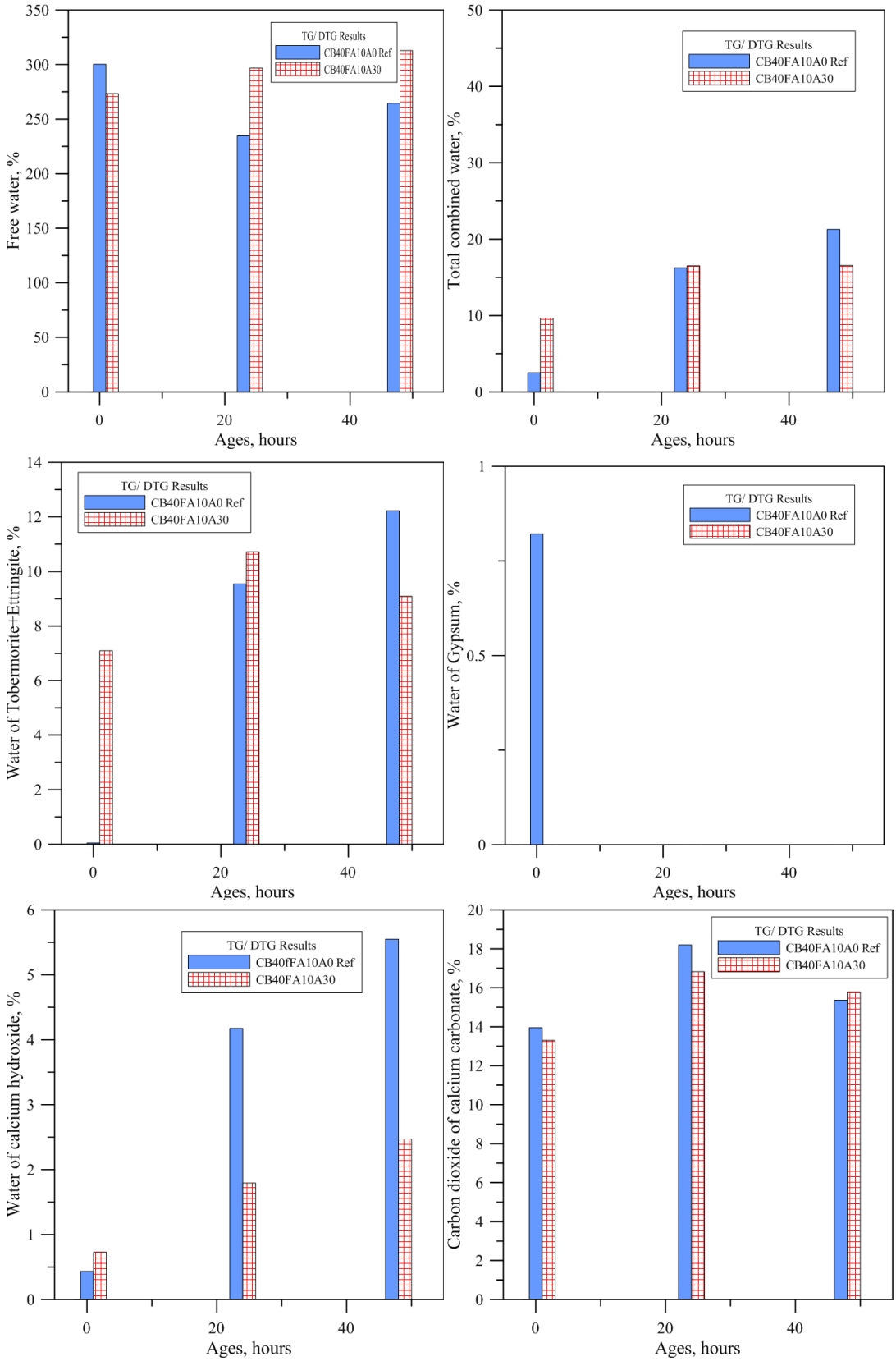

Figure 7.7 Weight losses on calcined cement mass basis at 1, 24 and 48 hours of two-component grouts

The accelerator consumes more water than reference grout at 1 hour as can be seen. This is proved by the total combined water used. When the time passes, total combined water of the accelerator sample does not increase in the same proportion as the reference one, see bars at 48 hours. Therefore, the grout with accelerator has less hydration products.

The analysis of the tobermorite+ettringite formation peak and calcium sulphate dehydration are described as follow. At 1 hour the reference grout shows both peaks. The calcium sulphate peak disappears in less than 24 hours as can be seen in the water of gypsum histogram (Figure 7.7). This means that in the 50-200°C range, the peak corresponds entirely to tobermorite+ettringite after calcium sulphate depletion. It can be seen, that the C-S-H formation of the CB40FA10A30 grout is less than the reference grout. Thus it is expected it has less compressive strength. Since calcium hydroxide is used as a hydration rate factor, it can be seen that the accelerator tends not only to accelerate the hydration after immediate contact with the grout but also diminishes the hydration after. The calcium hydroxide formation is much less than the reference. Those results are consistent with isothermal calorimetry results.

About the calcium carbonate peak, the CO_2 mass losses represent a crystallized $CaCO_3$ which remains similarly constant in both grouts.

7.2.1.4 VICAT NEEDLE TEST

The test does not offer reliable results because there were dispersion of setting across the small volume of grout and quick stiffening of grout can also deviate results. The hydration is not uniform across the exposed surface of the grout. Various measurements were done at the same age and dispersion of results was found. Despite an isolation, plastic bag, covered the test setup, evaporation occurred and hydration did not occur uniformly. On the other hand, since the water glass accelerator stiffens the sample at the simple contact of both grout components, vacuums can occur as during placement in the mold. After unmolding, some small holes were found, Figure 7.8. Although it was not mention, previous research indicated not suitability of the test for this kind of material (PRUDÊNCIO, 1998).

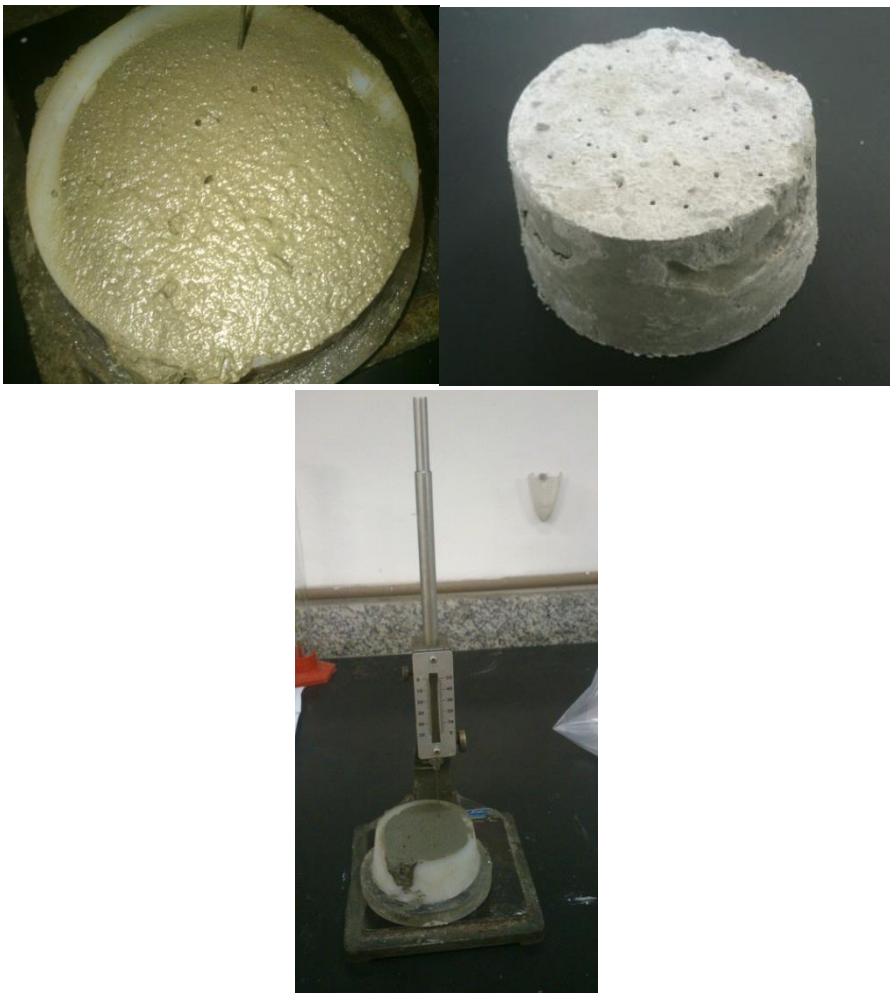

Figure 7.8 Vicat test of a two-component grout

7.2.2 COMPRESSION TESTS

It is the intent of this section to establish compression behavior of two-component grouts at early ages by using three accelerator admixture contents: 5, 15 and 30%. It was used as component A, CB40FA10 grout by following T3 mixing procedure. Component B, refers to the sodium-silicate-based accelerator admixture. Material amounts are presented in Table 4.11. During mixing both components, two procedures were used. The first procedure was used for 5 and 15% contents. It consists on mixing both components outside the molds, then immediately pouring the two-component grout on molds (see

Figure 7.12). The action of component B was immediate, it stiffened component A in a few seconds and effect was directly proportional on its content. When 15%

accelerator specimens were unmolded, the grout left some spaces because of the component B action. Stiffening was higher than gravity forces, Figure 7.13. Consequently, a second procedure was used for 30% accelerator admixture. Since stiffening was sudden, this method consists on mixing both components inside the molds (see Figure 7.14). On the other hand, Figure 7.9,

Table 7.1 and Table 7.3 summarize results at 24 and 72 hours. Since component B has immediate effect after getting contact with component A, it gets special attention to know its mechanical behavior at early ages. During tunnel construction advancement, it is needed to transfer stresses between soil and tunnel lining from short times after being placed in the empty annular ring.

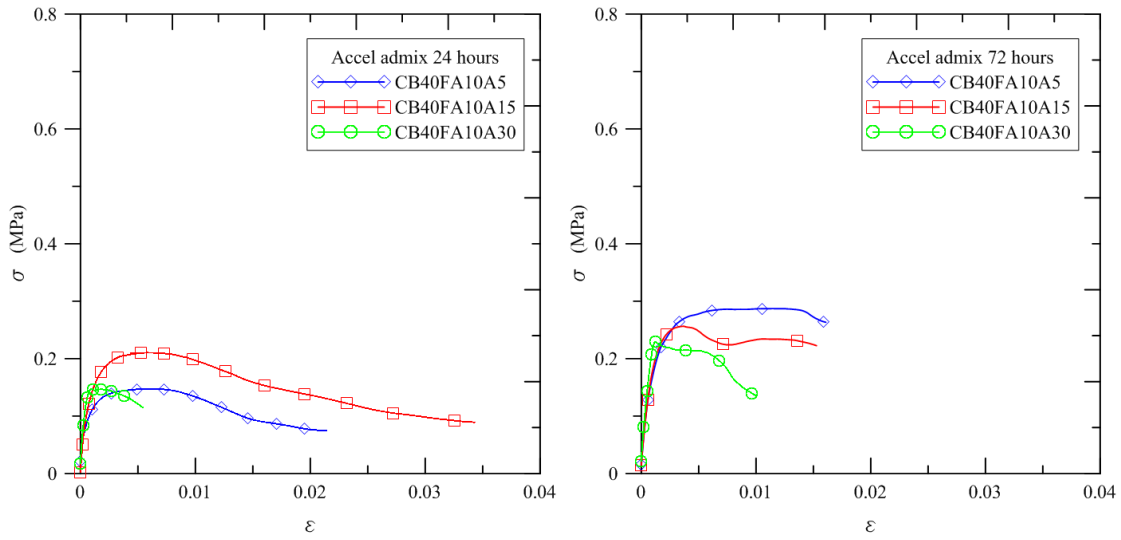

Figure 7.9 Compression behavior at 24 and 72 hours of two-component-grouts

Table 7.1 Compression behavior at 24 hours of two-component grouts.

Grout	Fmax (kN)	σ max (MPa)	ε rupture (m/m)	E (MPa)
A0	-	-	-	-
A5	0.28	0.14	0.0077538	163
A15	0.34	0.17	0.0058502	202
A30	0.30	0.15	0.0018128	211

Table 7.2 Compression behavior at 72 hours of two-component grouts.

Grout	Fmax (kN)	σ max (Mpa)	ε rupture (mm/mm)	E (Mpa)
A5	0.56	0.29	0.004054	198
A15	0.50	0.26	0.003669	207
A30	0.45	0.23	0.001290	260

Figure 7.9 shows a 24-hour less brittle behavior than at 72 hours. By analyzing Figure 7.10, we observe at 24 hours FA10A15 possess a higher strength. But at 72 hours after mixing, the higher the content, the lesser the strength. In spite of the fact a higher content can accelerate hydration products immediately, it does not improve the strength gain in further ages. The compressive strength diminishes. In addition, Young modulus increases in all grouts when the accelerator augments. In case of the strain at rupture, the higher the content, the more brittle the grout is. Figure 7.15 shows specimens after being tested.

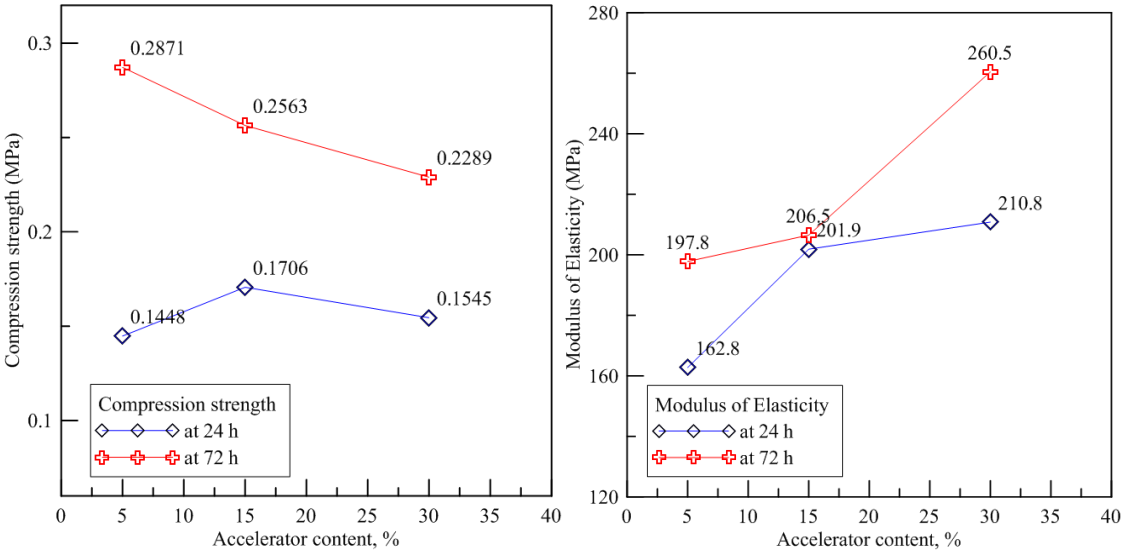

Figure 7.10 Compression and modulus of elasticity of two-component grouts

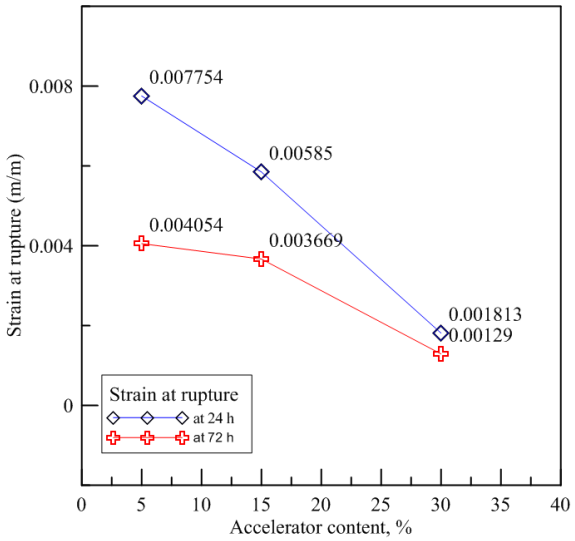

Figure 7.11 Strain at ruptures of two-component grouts

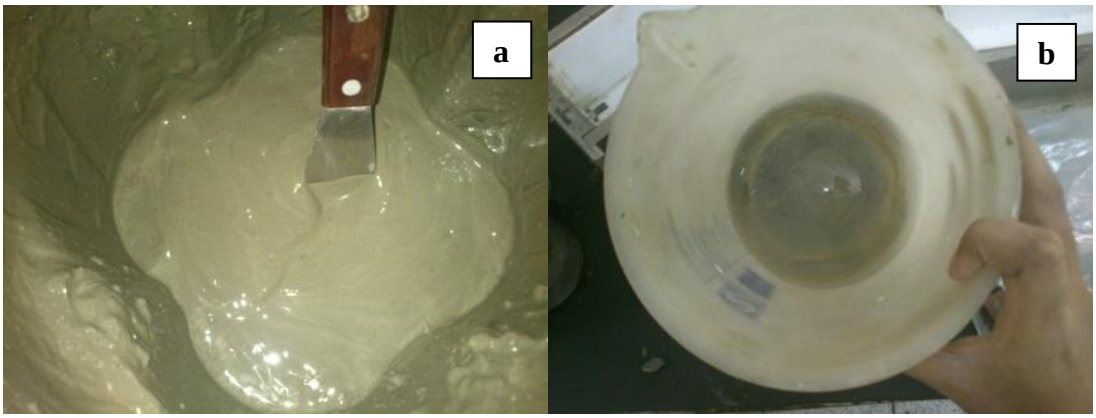

Figure 7.12 Batching components

a) grout, component A; b) accelerator, component B

Figure 7.13 Specimens after moulding.

Figure 7.14 Moulding and unmoulding of A30 grout.

Figure 7.15Two-component grout specimens after being tested

7.2.3 DIMENSIONAL CHANGES

7.2.3.1 Shrinkage

Shrinkage of CB40FA10A15 and CB40FA10A30 and the reference grout are presented in Figure 7.16. The shrinkages shown are in quase-adiabatic conditions, The starting point of the 15% of accelerator has been displaced in order to show better the curves. When axial bolts of CB40FA10A15 were tried to be released a softer grout than 30% accelerator grout was found. In the graph positive strains stand for shrinkage. CB40FA10A30 produced higher shrinkage than CB40FA10A15 at the beginning but both of them tended to diminish. First, the stiffening phase where a high shrinkage slope is found. Second, hardening phase occurs and shrinkage remains stable and reduction tendency of shrinkage occurs for both grouts.

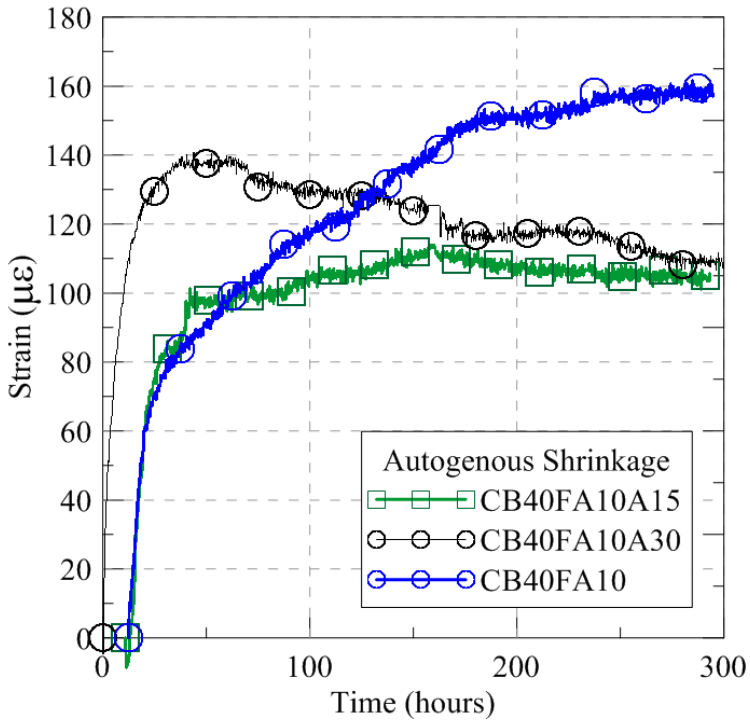

Figure 7.16 Autogenous shrinkage of two- component grouts

7.3 CONCLUSIONS

It is concluded from results that:

- The accelerator use produces a reduction in hydration peaks of C3S and C3A in Isothermal Calorimetry. By using 30%, the peaks are really low which means it affects the hydration process.
- Thermal analysis are consistent with calorimetry results since an immediate hydration occurs when CBFA grout gets contact the accelerator but later hydration reactions are affected according to tests done at 24 and 48 hours. Less hydration products are produced
- Accelerator use might turn the grout more brittle and less resistant when the chemical admixture increases.
- Autogenous shrinkage increased by the accelerator admixture at early ages and reduction was found later.

8 CONCLUSIONS AND SUGGESTIONS

8.1 CONCLUSIONS

After carrying out the experimental tests and proper analysis, conclusions follow the same order of the thesis.

Rheology of bentonite suspensions described a thixotropic behavior with hysteresis loops. Both of them influenced by previous treatment for sodium activation, clay content, hydration time and mixing energy. It has been noticed not only high shear mixing increases viscosity of suspensions but also rheology is time-dependent. The more the hydration time, the more the bentonite-water structuration during the swelling process. Special attention needs to be paid for the yield stress determination since differences were found among the apparent yield stress, shear stresses at low shear rates and the parameter obtained by numerical approach. Moreover, appearance of bubbles after mixing might be a result of cavitation during the high shear mixing process.

From evaluation of two mixing procedures, pre-dispersion of cement (T3) was found to be better than addition of dry cement to pre-hydrated bentonite (T2). The former produced a more homogenous grout and eliminates the likelihood of appearance of cement nodules which can cause crack propagation and might turn the grout more permeable. T2 produced a 5,6% higher strength and 10,1% higher modulus of elasticity. However, 13.2% higher strains at rupture could confirm crack propagation on this grout. In addition, dispersion was found in T2 stress-strain curves. Therefore, T3 mixing procedure was employed for other tests.

Low and high shear mixing was evaluated with better results for the latter. It was proven that low shear produces more bleeding and less internal cohesion. Low shear neither can break all the clumps formed nor can disperse homogenously the bentonite. On the contrary, high shear does so and offers a more efficient use of bentonite hydration properties, thus a better cement-bentonite system. Although high shear has these advantages, the bentonite content also influences the final performance. The use of 40 kg/m^3 of bentonite had the lowest bleeding at high shear mixing. However, 60

kg/m^3 of bentonite use became difficult to mix and a higher viscosity was found. Therefore, high shear mixing was employed for the experimental plan.

Hydration tests of CB grouts allowed us to understand that the cement particles receive water more uniformly in cement-bentonite grouts but they were dispersed in the specimen volume. Bentonite content variants did not produce significant changes in percolation threshold among them. A more uniform and enough supply of water for cement hydration allowed simultaneous hydration of more cement particles. As a result, the heat released is increased with 20 and 40 kg/m^3 of bentonite. The use of 60 kg/m^3 of bentonite did not produce more heat changes. In addition, C_3A hydration was clearly noticed in cement-bentonite grouts. Moreover, TG and DTG tests allowed to establish the influence of w/c ratios on hydration of the four grouts and the significant free water available in all of them. Although w/c ratios are not significantly different, they are a factor in minor hydration products of tobermorite+ettringite and calcium hydroxide at 24 hours. Then the effect is reversed at 7 and 28 days.

CB grouts presented: thixotropic behavior, two different behaviors according to shear rate. High apparent viscosities are presented at shear rates less than 100 s^{-1} and can fit well for a Bingham model. At higher shear rates than 100 s^{-1}, small increases in shear stresses correspond to high shear rate increases. CB60 grout presented a more elastic behavior. Additional attention is necessary for determining yield stresses. CB40 was selected as the best CB mixture because it has the lowest bleeding, less gel strength than CB60. The use of 40 kg/m^3 of bentonite is high enough to harness water amounts without jeopardizing the workability and the efficiency of mixing. Autogenous shrinkage was not found high after 300 hours and cracking occurs on drying shrinkage. The mix CB40 reached 0,696 ±0,023 (MPa) compressive strength at 28-day age,

Fly ash additions to CB40 caused modifications in hydration. Percolation threshold was delayed and occurred at 1h38’ and 2h4’ later than reference. About the heat release there are not significant changes. Dilution effect is more evident in CB40FA50 in the acceleration slope after dormancy period. Higher third peak in 10% and 30% fly ash additions are consistent with C_3A hydration and the nucleation sites the mineral admixture offers. Conversely, cumulative heat show more heat release at later

ages due to pozzolanic characteristics. TG results confirmed calcium hydroxide consumption at 28 days.

CBFA rheology showed the effects of including 10, 30, 50 of fly as partial replacement of Portland cement. The use of 10% 30% and 50% fly ash as cement replacements allowed diminishing shear stresses and reductions of hysteresis loops as well. On the other hand, improvements were obtained in mechanical compression behavior. CB40FA10, CB40FA30 and CB40FA50 allowed to determine that 10% of fly ash can improve the strength in 1,9% at 28 days and the others diminished the strength. The mix CB40FA10 produced a more brittle grout with 11,6% higher modulus of elasticity and a strain at rupture standing for 60,35% of the reference grout. As expected, considerable improvements were found when specimens were tested at 92 days. Increments are achieved in the three CBFA grout compositions but the 10% fly ash grout reaches 1,05 MPa, a 48% increment based on its 28-day age value. Similarly modulus of elasticity is higher more than three times for all grouts and less strain at rupture is found as well. Fly ash increased autogenous shrinkage and during drying shrinkage, severe cracking and bending was found, especially in the 50% FA case. In the end, CB40FA10 was chosen to be used as reference in a two-component grout.

The two-component grout responded with the following characteristics. After immediate contact between components, an abrupt hydration occurs shown in the isothermal calorimetry plots. Then, the dormancy period gets shortened and the acceleration slope is diminished. When the accelerator content rises, the acceleration slope is diminished and the C_3S peak diminishes too, this is important, since C-S-H production is affected. A similar lowering happens with the C_3A peak. Therefore the accelerator produces a sudden hydration immediately after contact but changes the hydration evolution later. The thermal analyses support this. For example, the hydration products and total combined water in thermal analysis report similar behavior and its rate diminishes in studies from 1 hour to 48 hours. Calcium hydroxide content, used as hydration factor in other studies, is considerably lower than the reference case at 24 and 48 hours after the beginning of chemical reactions. In the same way, mechanical compression tests proved the strength diminishes when the accelerator content increases. On the autogenous shrinkage case, accelerator increased the shrinkage at the

beginning but reduction was found later. Finally, hydration rate is not maintained and consequent products are less than the produced by the reference grout.

8.2 SUGGESTIONS

The following suggestions are done:

- Inclusion of a delaying chemical admixture. Possible improvement of rheology for pumping easiness.

- Study drying shrinkage of CB, CBFA and two-component grouts

- Deepen the rheological studies. Increase the analysis of rheological parameters, especial attention on determination of yield stresses

- Study mechanical behavior at later ages.

REFERENCES

ABNT NBR 10908, 1990, *Aditivos para argamassa e concreto- Ensaios de uniformidade.* Associação Brasileira de Normas Técnicas, Rio de Janeiro.

ABNT NBR 11578, 1991, *Cimento Portland Composto – Especificação.* Associação Brasileira de Normas Técnicas, Rio de Janeiro.

ABNT NBR 5739. 2007, *Concreto - Ensaio de Compressão de corpos de prova cilindricos.* Associação Brasileira de Normas Técnicas, Rio de Janeiro.

AFZAL, S., SHAHZADA, K., FAHAD, M., et al., 2014, "Assessment of early-age autogenous shrinkage strains in concrete using bentonite clay as internal curing techinique", *Construction and Building Material* , v. 66, pp. 403-409.

ANNETT, M. F., 1994, *Structural Grouts.*: Chapman and Hall.

ASTM C125-13a, 2013, *Standard terminology relating to concrete and concrete aggregates.* American Society for Testing and Materials International.

ASTM C191-13, 2013, *Standard Test Methods forTime of Setting of Hydraulic Cement by Vicat Needle.* American Society for Testing and Materials International, Pennsylvania.

ASTM C940-10a, 2010, *Standard Test Method for Expansion and Bleeding of Freshly Mixed Grouts for Preplaced-aggregate Concrete in the Laboratory.* American Society for Testing and Materials International, Pennsylvania.

BAERT, G., HOSTE, S., DE SCHUTTER , G., et al., 2008, "Reactivity of fly ash in cement paste studied by means of thermogravimetry and isothermal calorimetry", *Journal of Thermal Analysis and Calorimetry*, v. 94, pp. 485-492.

BÄPPLER, K., 2008, "Entwicklung eines Zweikomponenten-Verpresssystems für Ringspaltverpressung beim", *Taschenbuch für den Tunnelbau.*, pp. 263-304.

BARCELO, L., 2002, *Early Age Cracking in Cementitious Systems - Section 3.2 Chemical Shrinkage.* In: Report 25 TC 181-EAS, RILEM.

BEKKOUR, K., LEYAMA, M., BENCHABANE, A., et al., 2005. "Time-dependent rheological behavior of bentonite suspensions: An experimental study". *Journal of Rheology.*

BENTUR, A., 2002, *Early age cracking in Cementitious Systems - Terminology and Definitions.* In Report 25 TC 181-EAS, RILEM.

BESQ, A., MALFOY, C., PANTET, A., et al., 2003, "Physicochemical characterisation and flow properties of some bentonite muds", *Applied Clay Science*, v. 23, pp. 275-286.

BESQ, A., PANTET, A., MONNET, P., 2002, "Caractérisation des fluides de forage: boues propres et chargées". *Actes des Journées nationales de géotechnique et de géologie de l'Ingeniue á Nancy.*

BURATTI, N., FERRACUTI, B., SAVOIA, M., 2013, "Concrete crack reduction in tunnel linings by steel fibre-reinforced concretes", *Construction and Building Materials.* 2013, v. 44, pp. 249-259.

CHIAIA, B., FANTILLI, A., VALLINI , P., 2009, "Combining fiber-reinforced concrete with traditional reinforcement in tunnel linings", *Enginnering Structures*, v. 31, pp. 1600-1606.

COATS, W., REDFERN, J. P., 1963, "Thermogravimetric analysis. A review". *Analyst. v*. 88, 1053, pp. 906-924.

COPPETEC-PEC, 2014, *Influência da fração volumétrica e tipo de macro fibra polimérica na tenacidade à flexão do concreto pré-moldado a ser utilizado na obra da Linha 4 do Metro do Rio de Janeiro,17928. Relatório preliminar. Parte 1: Análise do Graute e "Slurry".* Rio de Janeiro .

DWECK, J., BUCHLER, P.M., COELHO, A.C.V., et al. 2000. "Hydration of a Portland cement blended with calcium carbonate". *Thermochimica Acta*, v. 346, pp. 105-113.

DWECK, J., CHEREM DA CUNHA, A.L., PINTO, C.A., et al., 2009, "Thermogravimetry on calcined massa basis- Hydrated cement phases and pozzolanic acitivy quantitative analysis". *Journal of Thermal Analysis and Calorimetry. v*. 97, pp. 85-89.

DWECK, J., FERREIRA DA SILVA, P.F., BUCHLER, P.M., et al., 2002, "Study by thermogravimetry of the evolution of ettringite phase during type II Portland cement hydration", *Journal of Thermal Analysis and Calorimetry, v*. 69, pp. 179-186.

EFNARC, 2005. Specification *and Guidelines for the use of specialist products for Mechanized Tunneling (TBM) in Soft Ground and Hard Rock.* European Federation of Producers and Contractors of Specialist Products for Structures, United Kingdom.

HANSEN, W., 1987**, "**Drying Shrinkage Mechanisms in Portland Cement Paste", *American Ceramic Society*, v. 70, pp. 323-328.

HARRISON, D. M., 2013, *The grouting handbook* .2 ed. Massachusetts, Elsevier.

HERRENKNECHT, AG. 2015, *Herrenknecht Tunneling Systems*. Online: https://www.herrenknecht.com/en/products/core-products/tunnelling/epb-shield.html. Accessed on 1 de October de 2015.

HOBART, MFG. CO., 2015, *Hobart N50 5-quart mixer. Hobart.* Online: http://www.hobartcorp.com/Products/Food-Prep/Mixers/N50-5-Quart-Mixer/. Accessed on 18 de September de 2015.

HOFMANN, U., ENDELL, K. WILM, D., 1933, "Kristalstruktur und Quellung von Montomorrillonit. Das Tonmineral der Bentonittone", *Z Kristallogr*, v. 86, pp. 340-348.

JCI, 1999, *Autogenous Shrinkage of Concrete.* In: Proceedings of the International Workshop organized by Japan Concrete Institute, edited by Ei-ichi Tazawa, pp 1-62, Hiroshima, June 1998.

JEFFERIS, S. "Cement-Bentonite Slurry Systems",In *Grouting and Deep Mixing, American Society of Civil Engineers*. 2012.

JEFFERIS, S., 1982, "Effects of mixing on bentonite slurries and grouts". In *Proceeding Conference on Grouting in Geotechnical engineering.*

JEFFERIS, S., 1982, *Private communications*.

LUCKHAM, P. F., ROSSI, S., 1999, "The coloidal and rheological properties of bentonite suspensions". *Advances in Colloid and Interface Science*, v. 82, pp. 43-92.

MAILVAGANAM, N. RIXOM, R., 1999, *Chemical Admixtures for Concrete. 3 ed. London,* Taylor and Francis e-Library.

MIRZA, J., SALEH, K., LANGEVIN, M. A., et al., 2013, "Properties of microfine cement grouts at 4 °C, 10°C and 20 °C". *Construction and Building Materials.* 2013, v. 47, pp. 1145-1153.

MULLINEUX, G., 2008, "Non-linear least squares fitting of coeficients in the Herschel-Bulkley model". *Applied Mathematical Modeling.* 2008, v. 32, pp. 2538-2551.

NEVES JUNIOR, A., TOLEDO FILHO, R. D., FAIRBAIRN, E.M.R., et al., 2012, "Early stages hydration of high initial strength Portland Cement". *Journal of Thermal Analysis and Calorimetry.* 2012, v. 108, '725-731.

NEVILLE , A. M., 1995. *Properties of Concrete.* 4 ed, E. Longman.

ORNAU, N., MOLINS, C., BLOM, C. B.M., et al., 2012, "Longitudinal time-dependent response of segmental tunnel linings". *Tunnelling and Underground Space Technology.* 2012, v. 28.

PEILA, D., BORIO, L., PELIZZA, S., 2011, "The behavior of a two-component back-filling grout used in a tunnel boring machine". *ACTA Geotechnica Slovenica.* 2011.

PETROBRAS, 2005, *Procedimentos e Métodos de Laboratório destinados à Cimentação de Poços Petrolíferos.* Rio de Janeiro, Petrobras-Schlumberger-Halliburton-BJ Service.

PRUDÊNCIO, L.R., 1998, "Accelerating Admixtures for Shotcrete". *Cement and Concrete Composites*, v. 20, pp. 213-219.

RAMOS-TEJADA, M. M., DE VICENTE, J, ONTIVEROS, A., et al., 2001, "Scaling behavior of the rheological properties of montmorrillonite suspensions: Correlation between interparticle interaction and degree of floculation". *Journal Colloid Interface Science*, v. 235, pp. 251-259.

REJEB, S. K., 1995, "Technique of multi-step concrete mxing", *Materials and Structures*, v. 28, pp. 230-234.

TERMKHAJORNKIT, P., NAWA , T., NAKAI, M., et al., 2005, "Effect of fly ash on autogenous shrinkage". *Cement and Concrete Research*, v. 35, pp. 473-482.

THEWES, M., BUDACH, CH., 2009, Grouting of the annular gap in shield tunnelling– an important factor for minimisation of Settlements and production performance. *ITA-AITE World Tunnel Congress - Safe tunneling for the city and the enviroment*, Budapest.

TIBERTI, G., MINELLI, F., PLIZZARI, G,. 2014, "Reinforcement optimization of fiber reinforced concrete linings for conventional tunnels". *Composites: Part B.*, v. 58, pp. 199-207.

UNFPA, 2011, *The State of World Population 2011*. United Nations Fund for Population Activities,

WORLDOMETERS, 2015, *World Population Clock.* Online: http://www.worldometers.info/. Accessed on 24 de July de 2015.